

AN ABSTRACT OF THE THESIS OF

Robert Irvin Scherpelz for the degree of Master of Science
in Nuclear Engineering presented on June 2, 1978

Title: THE MEASUREMENT OF URANIUM CONCENTRATIONS
BY THE DELAYED NEUTRON COUNTING TECHNIQUE

Redacted for Privacy

Abstract approved: _____

Dr. Stephen E. Binney

The counting of delayed neutrons emitted by fission is presented as a valuable technique for the measurement of uranium concentrations in a variety of matrices. The concentrations successfully analyzed can vary from well under one part per million to the high concentrations found in uranium ores. In a sample analysis, fission is induced in the uranium in the sample by irradiation in a thermal neutron flux, then the sample is rapidly transferred to a counting assembly capable of detecting delayed neutrons. In the system described, irradiation is performed in a TRIGA reactor, and counting is done in a paraffin-moderated assembly of BF_3 gas-filled detectors. All equipment needed for the analysis and the necessary procedures are discussed.

The delayed fission neutron (DFN) counting technique is compared to other methods of analysis for uranium, and the experiences of other researchers using the DFN technique are summarized. When compared to many other methods, DFN counting is relatively free of

interferences. The interferences which may occur, such as high energy gammas, unknown neutron-emitting nuclides or strong neutron absorbers in the sample, are discussed. Any uncertainties associated with a DFN measurement are also analyzed.

DFN counting has been used in many applications, such as the measurement of uranium in geological samples, phosphate products and seawater adsorbers. It can also be used for the measurement of thorium in many samples. These applications are presented, and the results of many different analyses are listed.

Experience gained at Oregon State University is examined in detail, and several improvements are suggested.

The Measurement of Uranium Concentrations
by the Delayed Neutron Counting Technique

by

Robert Irvin Scherpelz

A THESIS

submitted to

Oregon State University

in partial fulfillment of
the requirements for the
degree of

Master of Science

Completed June 2, 1978

Commencement June 1979

APPROVED:

Redacted for Privacy

Assistant Professor of Nuclear Engineering
in charge of major

Redacted for Privacy

Head of Department of Nuclear Engineering

Redacted for Privacy

Dean of Graduate School

Date thesis is presented June 2, 1978

Typed by Opal Grossnicklaus for Robert Irvin Scherpelz

ACKNOWLEDGEMENTS

First of all, thanks must be extended to the Exxon Nuclear Company, Inc. Exxon's funding of the Uranium in Seawater project made the research possible, and without their funding of my graduate assistantship, this paper could not have been written.

Special appreciation is extended to my Major Professor, Dr. Binney. His leadership of the seawater project, guidance of my graduate program, and many hours spent in helping me with my many questions and crises have been invaluable. Thanks also to the other members of my graduate committee, and especially to Dr. Hornyik for reading through the first draft of this thesis and offering good suggestions. Acknowledgement must also be made of the help and advice from so many people around the Radiation Center: faculty, staff and students, friends and colleagues--listing them all would require another long appendix. Special mention should be made of the help of T. J. Trapp, who had a plotting routine on the Cyber computer to make my graphs, a ready answer for all my questions, and the misfortune of occupying an office next to mine.

This paper could never have been in an acceptable form without the able typing of Mrs. Opal Grossnicklaus: her extra effort at a busy time is truly appreciated. Thanks also go to Deb E. Trapp for her fine job of illustrating.

Finally I am grateful to my wife, Joy. Her understanding of the problems of a DFN counter is truly amazing for a person who claims to be "non-technical." Her support in so many ways and at so many times has been crucial to my work.

Thanks to all!

TABLE OF CONTENTS

	<u>Page</u>
I. INTRODUCTION	1
II. THEORY OF DELAYED FISSION NEUTRON COUNTING	4
III. ANALYTICAL METHODS FOR URANIUM DETERMINATION	16
IV. DESCRIPTION OF THE DELAYED FISSION NEUTRON SYSTEM	35
V. UNCERTAINTIES	68
VI. APPLICATIONS	102
VII. RESULTS	111
VIII. IMPROVEMENTS	123
BIBLIOGRAPHY	131
APPENDICES	137
Appendix A. Total Counts for a DFN Measurement	137
Appendix B. The Production of ^{16}N in a Rabbit Capsule	143
Appendix C. Derivation of the Detection Limit	146

LIST OF FIGURES

<u>Figure</u>		<u>Page</u>
4-1	OSTR Core Configuration	36
4-2	Variation of Neutron Flux in the Rabbit Irradiation Position	38
4-3	DFN Counting Assembly-Cross Section	42
4-4	Overhead View of the DFN Test Assembly	45
4-5	C*N vs Detector Position	47
4-6	Neutron Flux Distribution in a Water-Moderated Assembly	49
4-7	DFN Counting Assembly--Overhead View	50
4-8	Block Diagram of DFN Electronics	52
4-9	Discrimination against Gamma Rays in a DFN System	54
4-10	Decay of Delayed Neutron Activities	58
4-11	Net Counts and Background vs Counting and Irradiation Times	60
4-12	Uncertainty vs Counting and Irradiation Times	63
5-1	Thorium-to-Uranium Mass Ratio to Cause Interference	84
5-2	Variation of Position in Rabbit Capsule and in Counting Assembly	89
5-3	Counts vs Reactor Power Level for a Single Sample	95
7-1	Uranium Calibration Curve for 100 kW	112
7-2	Thorium Calibration Curve for 100 kW	120
8-1	Uncertainty vs Number of Cycles for a 300 Second Total Experiment	128

LIST OF TABLES

<u>Table</u>		<u>Page</u>
2-1	Important delayed neutron precursors from ^{235}U thermal fission	8
2-2	Delayed neutron properties for thermal fission	9
2-3	Delayed neutron properties for fast fission	10
3-1	Description of DFN systems	26
4-1	Counts due to varying irradiation and counting times	65
5-1	Variation of counts with reactor power level	96
5-2	Uranium standards results	97
7-1	Seawater-uranium adsorbers	115
7-2	Porcelain dentures	116
7-3	Phosphates	117
7-4	Uranium ore samples	118
7-5	Miscellaneous geological samples	118

THE MEASUREMENT OF URANIUM CONCENTRATIONS BY THE DELAYED NEUTRON COUNTING TECHNIQUE

I. INTRODUCTION

The increasing importance of the nuclear industry as a supplier of energy has resulted in an increased need for the measurement of uranium concentrations in a wide variety of materials. The most obvious example is the analysis of uranium ore: the profitability of mining any ore deposit clearly depends on the concentration of uranium in that ore, and accurate analysis is vital for determining that profitability. The United States Department of Energy's current National Uranium Resources Evaluation program, an intensive effort to identify the amount of uranium which this country could supply, is an indication of the need for an accurate analytical system capable of handling a large number of samples. Such an analytical tool can also be used by suppliers of material which must be free of uranium contamination. This type of impurity must be especially avoided in material to be used in nuclear reactors, such as zirconium, which is used in fuel pin cladding and for other applications requiring a low neutron absorber.

Various techniques utilize neutron activation analysis (NAA) to measure small concentrations of uranium, but neutron activation can be followed by delayed fission neutron (DFN) counting to provide

an excellent analytical tool. The uranium in a sample being irradiated in a neutron flux will experience a number of fission reactions. A certain small percentage of these fissions will result in delayed neutrons which are emitted as long as a minute or more after the fission events. The DFN technique involves removing the sample from the irradiating flux and rapidly transferring it to a counting facility in time to detect some of the delayed neutrons. The number of delayed neutrons counted will correspond to the amount of uranium present in the sample.

The DFN system described in this paper was developed in response to a specific need. The Departments of Chemical and Nuclear Engineering at Oregon State University (OSU) have been studying the extraction of uranium from seawater. Seawater contains uranium at a concentration of about three parts per billion, and since this concentration is nearly constant in all the oceans' water, the oceans contain a tremendous supply of uranium. The OSU project has been using various adsorbers to collect some of these uranium atoms. The project's goal is to analyze the effectiveness of the various adsorbers by determining each adsorber's uranium concentration before and after exposure to the seawater. The analysis requires a technique for measuring concentrations of less than one part per million (ppm) uranium, and the technique must be able to routinely and quickly handle a large number of samples.

The DFN technique proved to be well suited to the analysis of such small concentrations of uranium. Sample preparation is neither difficult nor time-consuming, requiring only three to five minutes per sample and involving no chemical preparation. The irradiation and instrumental analysis itself takes only two minutes per sample, and the mass of uranium can be determined with an uncertainty of less than five percent in the one microgram range. The few interferences in the analysis can be easily avoided, and any solid or liquid sample can be analyzed. The method is insensitive to any nuclide which does not undergo fission reactions. These qualities make the DFN technique an excellent one for measuring uranium and other fissionable nuclides as well.

II. THEORY OF DELAYED FISSION NEUTRON COUNTING

Measurement of uranium by the DFN technique is based on counting delayed neutrons from the fission reactions of the ^{235}U or ^{238}U in the sample. When ^{235}U is exposed to a neutron flux, some of the neutrons will be captured to induce fission reactions. Each fission reaction results in the emission of two or three additional neutrons, the vast majority of which are "prompt neutrons," emitted essentially immediately. A small fraction of the emitted neutrons are not emitted immediately, however, and these are the delayed neutrons. Counting the neutrons emitted by fission reactions is a good method of determining the mass of material which can undergo fission, but counting the prompt neutrons is extremely difficult due to the problem of discriminating between the neutrons emitted by fission reactions and the source neutrons needed to initiate the fission. A good alternative to counting prompt neutrons is to count delayed fission neutrons. It is possible to use a pneumatic sample transfer system (a "rabbit system") to quickly remove the sample from the irradiating neutron flux and deposit it in a counting system while the sample is still emitting delayed neutrons. Even trace concentrations of uranium will result in the emission of a sufficient number of delayed neutrons during the counting time interval to give an accurate determination of the mass of uranium present in the

sample.

The two major isotopes of uranium are quite different in the dependency of their fission reaction rates on the energy of the incident neutrons. For ^{235}U exposed to thermal neutrons the probability of a capture reaction occurring which results in fission is very high, as indicated by the microscopic fission cross section of 582 barns (1) for an incident neutron energy of 0.025 eV. This fission cross section can be characterized by a $\frac{1}{v}$ energy dependence through the thermal neutron energy range, up to about 1 eV. Above 1 eV this cross section experiences a number of resonances, and above about 1 keV the resonances are too close together to be resolved (1). The ^{235}U fission cross section for fast neutrons varies smoothly, but is quite low, about 1.2 b at 1.0 MeV (1), and fast fission of ^{235}U is seldom a very important effect. ^{238}U has a much different fission behavior, experiencing no fission below a theoretical threshold energy of about 0.6 MeV (1). The microscopic fission cross section for ^{238}U is quite small, less than 0.1 b at 1 MeV, but increasing to 0.5 b at 2 MeV (1). Fast fission of ^{238}U is usually a more important effect than fast fission of ^{235}U , however, due to the differences in natural abundance of the two isotopes. ^{235}U usually comprises 0.71% of the natural uranium's mass, while the other 99.29% is ^{238}U .

When a neutron is absorbed by a uranium nucleus to induce a fission reaction, it forms a highly unstable compound nucleus

which quickly decays. The vast majority of the mass of the compound nucleus is then divided into two fission fragments and usually two or three free neutrons. A "fission fragment" is a new nuclide, having [very] roughly half the atomic mass of the original uranium atom. Fission reactions are not all identical, and a large number of different nuclides may be fission fragments. The frequency of production of the various nuclides by fission has been carefully observed and recorded by several researchers. A ^{235}U nucleus contains 92 protons and 143 neutrons, which is a very high neutron-to-proton ratio. Such a high ratio is necessary to overcome the large coulomb repulsion of the 92 protons, but this ratio is much higher than that needed to stabilize the 40- or 50-proton nucleus of a fission fragment. Thus fission fragments are generally neutron-rich, and nearly always transform to a more stable nuclear configuration by the emission of a β^- particle. This decay increases the atomic number of the nuclide by one without changing the mass number, and thus decreases the number of neutrons by one. The daughter therefore has a more stable neutron-to-proton ratio.

In a very small number of fissions, a fission product atom (either the atom whose nucleus is a fission fragment or one of its daughters) will decay by the emission of a neutron. Neutrons emitted by these fission products are the delayed neutrons, and the nuclides which emit them are the delayed neutron precursors. Precursors are

characterized by half lives of less than 60 seconds, and for any given mode of fission (e. g. , fast fission of ^{238}U , thermal fission of ^{235}U), one or more precursors form a delayed-neutron group (see Table 2-1). Each group is characterized by a group half life and a group fraction. The group fraction indicates the fraction of fission neutrons that are actually delayed neutrons from that group. Each mode of fission has six delayed neutron groups, ranging in half life from about 0.2 to 55 seconds. Although it is fairly certain that not all delayed neutron precursors have been identified, the six-group division of delayed neutrons is an accurate representation. The six groups for fast and thermal fission of ^{235}U and fast ^{238}U fission are listed in Tables 2-2 and 2-3. For comparison the tables also include the common fissionable nuclides ^{233}U , ^{239}Pu , and ^{232}Th .

The detection of neutrons presents special problems, since radiation detection is usually based on the radiation's ionizing properties. Since neutrons have no charge and normally do not engage in such ion-producing reactions as pair production or the photoelectric effect, they do not normally produce ionization in conventional detection media. The neutron detectors most commonly used are basically gas-filled proportional counters. The detectors either have a special coating or are filled with gases which contain nuclides having high neutron capture cross sections for absorption reactions which emit a charged particle. This charged particle creates ions in the gas as

Table 2-1. Important delayed neutron precursors from ^{235}U thermal fission (2).

Group Number	Group Half-Life (sec)	Precursor	Precursor Half-Life (sec)
1	55.72	^{87}Br	54.5
2	22.72	^{88}Br	16.3
		^{137}I	24.4
		^{136}Te	20
		^{141}Cs	24.9
3	6.22	^{87}Se	5.9
		^{89}Br	4.4
		^{93}Rb	6.2
		^{138}I	6.3
		^{137}Te	3.5
4	2.30	^{85}As	2.03
		^{88}Se	1.7
		^{90}Br	1.6
		^{93}Kr	1.3
		^{94}Rb	2.3
		^{98}Y	2.3
		^{135}Sb	1.7
		^{139}I	2.0
		^{142}Cs	1.94
5 & 6	0.61 &	^{91}Br	0.5
	0.23	^{95}Rb	0.36
		^{96}Rb	0.23
		^{97}Rb	0.14
		^{99}Y	0.8
		^{140}I	0.8
		^{141}I	0.4

Table 2-2. Delayed neutron properties for thermal fission (3).

Group	²³³ U		²³⁵ U		²³⁹ Pu	
	Half Life (sec)	Fraction β_i	Half Life (sec)	Fraction β_i	Half Life (sec)	Fraction β_i
1	55.00 ± 0.54	0.000224 ±0.000008	55.72 ± 1.28	0.000215 ±0.000020	54.28 ± 2.34	0.000074 ±0.000019
2	20.57 ± 0.38	0.000777 ±0.000010	22.72 ± 0.71	0.001424 ±0.000059	23.04 ± 1.67	0.000626 ±0.000074
3	5.00 ± 0.21	0.000655 ±0.000104	6.22 ± 0.23	0.001274 ±0.000143	5.60 ± 0.40	0.000443 ±0.000101
4	2.13 ± 0.20	0.000723 ±0.000052	2.30 ± 0.09	0.002568 ±0.000072	2.13 ± 0.24	0.000685 ±0.000069
5	0.615 ± 0.242	0.000133 ±0.000062	0.610 ± 0.083	0.000748 ±0.000059	0.618 ± 0.213	0.000181 ±0.000061
6	0.277 ± 0.047	0.000088 ±0.000036	0.230 ± 0.025	0.000273 ±0.000052	0.257 ± 0.045	0.000092 ±0.000034
Total Delayed Fraction β		0.0026		0.0065		0.0021

Table 2-3. Delayed neutron properties for fast fission (3).

Group	²³² Th		²³³ U		²³⁵ U		²³⁸ U		²³⁹ Pu	
	Half Life (sec)	Fraction β_i								
1	56.03 ± 0.95	0.000690 ±0.000041	55.11 ± 1.86	0.000224 ±0.000008	54.51 ± 0.94	0.000243 ±0.000019	52.38 ± 1.29	0.000192 ±0.000015	53.75 ± 0.95	0.000076 ±0.000006
2	20.75 ± 0.66	0.003045 ±0.000102	20.74 ± 0.86	0.000712 ±0.000013	21.84 ± 0.54	0.001363 ±0.000032	21.58 ± 0.39	0.002028 ±0.000030	22.29 ± 0.36	0.000560 ±0.000008
3	5.74 ± 0.24	0.003147 ±0.000305	5.30 ± 0.19	0.000590 ±0.000091	6.00 ± 0.17	0.001203 ±0.000102	5.00 ± 0.19	0.002398 ±0.000296	5.19 ± 0.12	0.000432 ±0.000036
4	2.16 ± 0.08	0.009054 ±0.000305	2.29 ± 0.18	0.000824 ±0.000029	2.23 ± 0.06	0.002605 ±0.000045	1.93 ± 0.07	0.005742 ±0.000178	2.09 ± 0.08	0.000656 ±0.000020
5	0.571 ± 0.042	0.003492 ±0.000264	0.546 ± 0.108	0.000190 ±0.000036	0.496 ± 0.029	0.000819 ±0.000051	0.490 ± 0.023	0.003330 ±0.000192	0.549 ± 0.049	0.000206 ±0.000018
6	0.211 ± 0.019	0.000873 ±0.000122	0.221 ± 0.042	0.000060 ±0.000018	0.179 ± 0.017	0.000166 ±0.000019	0.172 ± 0.009	0.001110 ±0.000074	0.216 ± 0.017	0.000070 ±0.000010
Total Delayed Fraction β		0.0203	0.0026		0.0064		0.0148		0.0020	

it slows down, and these ions are collected by a potential difference between the detector wall and a central wire electrode. The resulting current pulse then can be routed through standard NIM-bin compatible electronics and recorded.

A common neutron detector is the fission chamber, which has a sensitive coating containing a fissionable material. Neutrons absorbed in the coating will cause fission reactions, and kinetic energy from either the fission fragments or the radioactive fission product decays will be deposited in the fill gas to produce counts. One advantage of the fission chamber is that the coating can be selected to suit the energy of the neutrons being detected. If it is to be used in a thermal neutron flux, ^{235}U or ^{239}Pu would be a good choice for the coating. For measurement of a fast neutron flux, a cutoff energy for the minimum energy detected could be achieved by using a fissionable nuclide with the desired threshold for fission. Thus ^{238}U in a detector would limit the detectable neutrons to those having energies greater than 0.6 MeV. Fission chambers also have the advantage of being relatively insensitive to gammas, and are often used to measure neutron fluxes in reactor cores. Fission chambers have the disadvantage of having a high background due to the fact that most fissionable nuclides are also alpha emitters. This ultimately limits the amount of fissionable coating which can be included in the detector and restricts the

detector's sensitivity.

A more sensitive coating for a gas-filled neutron detector is a coating containing ^{10}B . ^{10}B has a very high thermal cross section, 3837 b at 0.025 eV (1). Upon neutron capture, the nuclide experiences a $^{10}\text{B}(n, \alpha)^7\text{Li}$ reaction, and the emitted alpha produces ionization in the chamber. The ^{10}B can also be incorporated into the detector in the form of BF_3 , a gas in which the boron is enriched in ^{10}B , usually to 96%. Another common fill gas is ^3He , which has a higher neutron capture cross section than ^{10}B . The $^3\text{He}(n, p)^3\text{H}$ reaction has a 0.025 eV cross section of 5400 b (1). ^3He has a disadvantage of a very high elastic scattering cross section, which is even higher than the (n, p) cross section. Aside from this difference and the much higher cost of ^3He , ^3He and BF_3 have many similarities.

Several characteristics give BF_3 and ^3He detectors unique characteristics for neutron detection. Since the detector tube is usually made of aluminum or stainless steel, ionizing radiation such as alpha and beta particles are not able to penetrate into the detector, and the detectors are thus insensitive to α and β radiation. High energy photons, however, are able to penetrate into the detector walls, and may produce a current pulse similar to that of a neutron, although this is not usually a problem. Since the sensitive material is in gaseous form the probability of a neutron-nucleus interaction is smaller than in a higher-density solid. Although ^{10}B and ^3He have high capture

cross sections for neutrons of thermal energies, the cross sections decrease by factors of greater than one thousand for the capture of fast neutrons. This means that neutrons emitted at fast energies must be slowed down to thermal energies to be efficiently counted.

Several researchers have done studies of the energies at which delayed neutrons are emitted and found distributions lower than prompt fission neutron energies, but much greater than thermal (4, 5). There is not a smooth distribution of delayed neutron production as a function of energy, as with prompt neutrons, primarily due to the fact that neutrons in each group are emitted at energies characteristic of the precursors in that group, and a number of different precursors introduce a complicating factor into the determination of the spectrum. Energy distributions for most of the groups have been compiled, and an example of the results is indicated in the following list from Batchelor and Hyder(5):

<u>Group</u>	<u>Mean Energy (keV)</u>
1	250±20
2	460±10
3	405±20
4	450±20
5	--
6	--

Since the mean energy of delayed neutron emission is around several hundred keV, the delayed neutron counting assembly must include a moderator between the neutron-emitting sample and the detector to slow the neutrons to well under 1 eV and thus take advantage of the high thermal cross section of ^{10}B or ^3He . Materials typically used for neutron moderation include D_2O , graphite, and H_2O (or other materials rich in ^1H). H_2O has the advantage of requiring fewer collisions between the neutron and a moderator molecule (or atom) to slow it from a given high energy to a given low energy. D_2O and graphite, however, have lower capture cross sections, which means that more neutrons can arrive at the detector without being absorbed. The best parameter for comparing moderating abilities is the moderating ratio, $\xi \Sigma_s / \Sigma_a$, where Σ_a is the macroscopic absorption cross section, Σ_s is the scattering cross section, and ξ is the average lethargy gain (logarithmic energy loss) per collision. The moderating ratios can be summarized (6):

Moderator	Moderating Ratio
H_2O	71
D_2O	5670
C	192

By this criterion, D_2O is obviously the superior moderator, and graphite is much better than water. Graphite and D_2O , however,

both have the disadvantage of high cost, and water (or some other material with a high concentration of ^1H) is frequently chosen.

III. ANALYTICAL METHODS FOR URANIUM DETERMINATION

Several traditional chemical techniques have been applied to the analytical determination of uranium. Many variations of these techniques were developed or refined during the Manhattan Project in the early 1940's and are still used in many laboratories. These chemical techniques include colorimetry, fluorimetry, and polarography.

In a colorimetric determination (7, 8) the uranium is in an aqueous solution which has a distinctive yellow coloring. The amount of uranium present in solution will determine how deep the yellow coloring is. When the method was first developed, the determination depended on the analyst's judgment in comparing the color of the tested solution to the colors of standard solutions, but now a spectrophotometer is usually used to measure the solution's transmittancy to light with a wavelength of 400 nm. This instrumental comparison to a standard is more accurate. The success of a colorimetric determination depends on the quality of the tested solution, and several different reagents have been used for the preparation of the solutions. These reagents include ammonium thiocyanate, ascorbic acid, hydrogen peroxide, and others. The chemical procedures necessary to arrive at the test solution also depend on the matrix in which the uranium occurs, and a number of different analyses could require a number of different sets of procedures to prepare the solutions.

Colorimetric determinations are most useful for uranium concentrations near 200 ppm, although it has been used for solutions as dilute as 0.2 ppm (9).

When uranium, fused in a pellet with NaF, is irradiated in long-wavelength ultraviolet light (365 nm), it fluoresces with a bright yellow-green color (554.6 nm), where the amount of fluorescence is proportional to the mass of uranium present (10). This is the basis of the fluorimetric method of analysis (11, 12), which can be used to determine uranium masses as small as 10^{-10} grams. Such a low level of detection, however, requires careful, time-consuming sample preparation, since any elements in the matrix which might cause interference or quenching of the emitted fluorescence must be separated out, and the remaining uranium-bearing material must be fused with the NaF flux into a pellet. The separation procedures to remove the interferences and quenchers depend, of course, on which elements are present in the matrix, and again each type of material to be analyzed must be treated as an individual case. The fluorescence was originally measured by visual or photographic techniques, but this is also now done more accurately by instrumental methods, using photoelectric measurements.

Polarographic techniques (8) determine the amount of uranium present in a solution by measuring the current which can flow through the solution when an electric potential is applied. The potential is

applied between a stationary reference electrode and a dropping mercury electrode (DME). The DME ejects tiny drops of mercury into the solution. Since each drop is charged, it becomes an electrode, and the current which flows between it and the reference electrode is an indication of how much uranium is in the solution. Several variations, such as pulse polarography, have also been successfully applied to uranium determination. Careful chemical procedures are again required to extract the uranium from its original matrix and put it into solution without contaminants which could alter the current flow. With care, however, the polarographic techniques can measure as little as 0.2 ppm uranium, and it has been applied to the measurement of uranium in seawater (13).

Mass spectrometry, which is capable of accurately determining the isotopic ratio in a sample, has been used for uranium determination by the method of isotopic dilution (14, 15). In this technique, the ratio of ^{235}U to ^{238}U in the sample is first determined (if it is not already known, as in samples containing natural uranium). Then a spike containing an isotopic ratio much different from that in the sample is prepared, and its ratio is similarly determined. A known quantity of the spike is then added to the uranium-bearing sample, and the isotopic ratios are once again measured. Knowing the isotopic ratios of the sample, spike, and spiked sample, and the quantity of spike added in the spiked sample, the analyst can calculate

the concentration of uranium in the original sample. A drawback of this method is the need to perform some type of preconcentration in samples of low concentration before the determination. The preconcentration step is time-consuming and offers opportunities for errors to be made.

In the previously discussed methods, the chemical state of the uranium atoms was an important consideration, and the chemical state of the uranium is determined by the states of the outermost electrons in the uranium atoms. X ray fluorescence (16), on the other hand, involves interactions with only the inner electrons, and their states are determined only by the nuclear charge. The analyst is thus relieved, somewhat, from chemical considerations. When the uranium-containing sample is irradiated by a beam of polychromatic x rays, the inner electrons will be excited to higher energy levels in the atom, or perhaps will be given enough energy to become free electrons. The resulting vacancy in a low energy state will quickly be filled by an electron from a higher energy state, and this transition will result in the emission of an x ray whose energy is determined by the electron energy levels involved. Since these x rays are characteristic of the atom emitting them, the amount of uranium in a sample can be measured by measuring the intensity of the proper wavelength x-ray emission. With care, low concentrations of uranium can be accurately determined, and x-ray

fluorescence has successfully determined the concentrations of uranium solutions (17). For low concentrations, preconcentration may be helpful. Also, care must be taken to avoid matrix contaminants which can quench the emitted x rays.

Since ^{238}U is a natural emitter of alpha particles, the concentration of uranium in a sample can be determined by counting the alphas being emitted by the uranium in the sample (18). It is best to use a detector and multichannel analyzer arranged to count alphas as a function of their energy, thus ensuring that only alphas of the proper energy will be used for the uranium determination. The count rate can be converted to a mass of uranium by comparison with a standard, or by using the detector's absolute efficiency. Since ^{238}U has a long half life (4.47×10^9 years), its specific activity is very low, and count times must be long to get measurements with low statistical uncertainties. In one experiment, the ratio of ^{234}U to ^{238}U was being measured in seawater (^{234}U is a daughter isotope of ^{238}U , so the two are usually found together). In order to obtain enough counts to measure about 30 micrograms of uranium, more than 50 hours of counting were needed (19).

The natural radioactivity of uranium can also be used for the measurement of uranium by passive gamma spectrometry. ^{235}U decays by alpha emission to ^{231}Th , and this decay is accompanied by the emission of a 185.7-keV gamma. Although the half life of ^{235}U

is very long (7.04×10^8 years), one gram of ^{235}U will emit 4.3×10^4 γ /s. Thus the 185.7-keV gammas can be counted on either a NaI or Ge(Li) detector whenever sufficient ^{235}U is present. This method can be especially useful for determining uranium enrichments in fuel material or for measuring fissile uranium concentrations in spent fuel rods. Counting the 185.7-keV gamma is subject to problems due to high attenuation of the low energy gammas, especially in material which is very dense or is composed of atoms with high atomic number. Thus slight physical variations among the samples and standards could result in large errors in measurements (20, 21).

Recently a method has been devised which depends on examining some direct effects of fission. The sample is placed in close contact with a thin detector sheet, made of lexan, muscovite, mica, or some other suitable material. It is then irradiated in a flux of thermal neutrons to induce fission in the ^{235}U in the sample. The fission products which pass through the detector sheet will leave faint tracks, and after irradiation, the sheet is etched with acid to expose these tracks. The density of the fission tracks is then carefully determined and compared to a standard to determine the mass of ^{235}U in the sample. Fission track counting can be extremely sensitive, but it requires laborious procedures for sample preparation, etching, and counting each sample (22, 23).

Neutron activation analysis, usually using neutrons from a

reactor, is now widely used in the determination of uranium in a wide variety of matrices. If the uranium's isotopic abundance of ^{235}U is known, as in natural uranium, gamma or beta radiation from one of the fission products can be counted. ^{140}Ba and its daughter nuclide, ^{140}La , are frequent choices (24, 25). With its relatively high cumulative fission yield, 6.29%, ^{140}Ba is abundantly produced, and its 12.8-day half life, and ^{140}La 's 40.2-hour half life, result in an activity which is high enough for a good count rate. In early studies, betas were counted after chemically extracting the barium from the sample, but ^{140}Ba 's 537-keV gamma, and ^{140}La 's 1596-keV gamma are easily counted by gamma spectrometry. Similarly, ^{103}Ru and ^{106}Ru (26) and ^{131}I and ^{133}I are also fission products counted by gamma spectrometry for the determination of uranium. Fission product counting in the case of small uranium concentrations often necessitates removing the particular fission product from the irradiated sample to avoid interference from nuclides emitting gammas of similar or interfering energies. Sometimes the interference will die away with long decay times, but if not, removal is necessary. Such removal from a sample requires time-consuming chemical procedures, and sometimes a tracer must also be used to determine the extent of recovery of the particular fission product.

Other methods of gamma spectrometry use the following chain of reactions: $^{238}\text{U}(n, \gamma) \xrightarrow[23.5 \text{ m}]{\beta^-} ^{239}\text{Np} \xrightarrow[2.35 \text{ d}]{\beta^-} ^{239}\text{Pu}$. The decay

of ^{239}Np proves to be convenient for gamma spectrometry. The sample is allowed to decay for several hours before counting, which allows the ^{239}Np concentration to build up and interfering nuclides to decay. Then the 278-keV gamma, which accompanies the beta decay of Np into ^{239}Pu , can be counted on a high-resolution Ge(Li) detector (27). There are problems involved in counting low-energy gammas, since they occur in the Compton scattering distribution from higher-energy gammas, which increases the background. This problem can be avoided by counting the 74-keV gammas from the decay of ^{239}U on a Si(Li) detector, which is insensitive to higher-energy gammas. Several researchers report that both ^{239}U and ^{239}Np counting can be improved by irradiating the sample with epithermal neutrons, which can be done by covering the sample with a cadmium shield in the irradiation facility. A cadmium shield will prevent activation by low energy neutrons, leaving only higher energy neutrons for activation, and these produce far fewer competing nuclides. Since ^{238}U has a fairly high resonance capture cross section, epithermal activation will still produce sufficient ^{239}U and ^{239}Np activity (28).

Echo and Turk were the first researchers to report on developing a DFN system for measuring uranium (29). Their system consisted of six BF_3 detectors imbedded in a paraffin moderator. The source of irradiating neutrons was a reactor with a flux of 1×10^{13} n/cm²-s. A 4-minute, 15-second, 3-minute irradiation, decay,

count cycle resulted in 480 counts per microgram of natural uranium. This cycle gave 64 background counts, and the authors report that the method is useful for determining uranium masses as low as seven micrograms.

Amiel reported on a similar detector assembly, with six BF_3 tubes in a paraffin moderator (30). He also described shielding to protect the system from counts due to external neutrons. This shielding included a 0.075 cm thick sheet of cadmium around the inside moderator, with a layer of paraffin surrounding the cadmium shielding. Most external neutrons were thermalized in the paraffin and absorbed in the cadmium. Amiel also recognized that long irradiation and count times did not gain many counts. He found that a 60-second, 20-second, 60-second cycle gave good sensitivity: 300 counts per microgram of natural uranium. Since the number of counts can be shown to be directly proportional to the irradiating flux, this is more sensitive per unit flux than Echo and Turk reported, since Amiel used an irradiating thermal neutron flux of 3.75×10^{12} n/cm²-s. The minimum level of detection (MLD--defined in this case as the mass necessary to produce a number of counts equal to three times the standard deviation of the background) was reported to be 0.03 micrograms for this system.

Dyer, Emery and Leddicotte, of the Oak Ridge National Laboratory (ORNL), made a detailed report on DFN counting (31). Their

detector assembly was similar to the two previously described, with the addition of a lead cylinder between the sample position and the detectors to prevent a high gamma radiation field from producing erroneous counts. This system also used detector tubes two inches (5.08 cm) in diameter, compared to the one-inch (2.54-cm) tubes used by Amiel. The sensitivity of the ORNL system was in the same range as the others, about 1210 counts per $\mu\text{g U}$, using a reactor thermal flux of $6 \times 10^{13} \text{ n/cm}^2\text{-s}$. This report investigated applying DFN counting to the routine analyses of samples such as ores, granites, sea sediments, biological tissues, uranium-zirconium alloys, and uranium isotopic ratios.

A number of researchers have reported on variations in the design of DFN systems and on various applications of DFN counting. Table 3-1 is a summary of several of these systems. It presents the available information on system design, performance, and applications.

Table 3-1 shows that nearly all the systems had moderators of either paraffin or polyethylene, two materials which are rich in hydrogen and easy to work with, but the system described by Jewell and Brownlee is a departure from this tendency (32, 44). They wanted a system with the highest possible efficiency (defined as the fraction of delayed neutrons emitted during the counting period which actually produce counts). They eliminated ^1H from consideration because the

Table 3-1. Description of DFN systems.

Citation Number Year Published Country	Neutron Source (R = reactor; power level; flux in n/cm^2-s Cf = ^{252}Cf ; mg of ^{252}Cf)	Detectors (Number; type; size; location)	Moderator (Material; size)	Shielding (Material; size)
(29), 1957 (USA)	R 40 MW 1×10^{13}	6 BF_3	Paraffin	. 5mm Cd plus paraffin
(30), 1962 (38), 1967 (Israel)	R 5 MW 3.75×10^{13} @ 1 MW	6 BF_3 2.5 cm Dx70 cm L on a 5.5 cm radius	Paraffin 40x40x70 cm	. 75 mm Cd plus borated paraffin
(31), 1962 (USA)	R 30 MW 6×10^{13}	6 BF_3 5 cm D on an 18 cm radius	Paraffin 49 cm Dx61 cm H	7.6 cm Pb around sample; none outside paraffin
(39), 1964 (UK)	R 2.5 MW 2.10×10^{12}	5 BF_3	Paraffin	
(40), 1967 (UK)	R 5 MW 5×10^{12}	8 BF_3 5 cm Dx40 cm L on 11 cm radius	Paraffin	. 75 mm Cd plus 10 cm borated paraffin; 6.4 cm Pb around sample
(41), 1967 (42), 1969 (43), 1971 (USA)	R 5 MW 2.5×10^{13}	4 BF_3 2.5 cmD	Paraffin	. 3 cm Pb+. 5 mm Cd; 2.5 cm Pb around sample
(32), 1968 (44), 1969 (USA)	R 1.2×10^{13}	40 BF_3 5 cm Dx61 or 143 cm L in 5 ring hex matrix	Graphite 153 cm D x183 cm H	Water 61 cm

Table 3-1. (Continued)

Citation Number Operation Times (Irradiation/Delay/ Counting Times; Seconds)	Background Counts	Efficiency	Sensitivity, Counts/ μg			Minimum Level of Detection	Applications
			natural U	^{238}U	^{232}Th		
(29), 24/15/80	64		480			7 μgU	Liquids; synthetic ores
(30), 60/20/60 (38)	20 @ 1 MW 11 @ .5 MW 6 @ no power	14.3%	300	13.5	3.8	.03 μgU	U, Th ores; geologic samples; meteorites
(31), 60/20/60	40 to 50 no power	5%	1690	20.2	19.6	.7 μgU	Ore; granites; sea sediment; graphite; biological tissue, Zr-U alloys, U isotopic composition
(39), 60/20/60 60/25/60	27		231 208			.02 μgU	Solutions; urine
(40), 60/20/60	10	17%	430		1.16	.15 μgU	Geological samples
(41), 30/20/60 (42) (43)	113		929 775	36.2			Urine; ore; soil; water; sediments; plants
(32), 30/45/600 (44)	1200	60%					

Table 3-1. (Continued)

Citation Number Year Published Country	Neutron Source (R = reactor; power level; flux in n/cm^2-s Cf = ^{252}Cf ; mg of ^{252}Cf)	Detectors (Number; type; size; location)	Moderator (Material; size)	Shielding (Material; size)
(33), 1969 (USA)	R 250 kW 2.5×10^{12} R (pulsed) 16 MW -sec $1.7 \times 10^{14} n/cm^2$	1 BF_3 5 cm	Polyethylene 30x30x20 cm	
(45), 1971 (UK)	R 5×10^{12}	6 BF_3 2.5 cm Dx30 cm L on a 3.75 cm radius	Polyethylene 30x30x42 cm	.5 mm Cd, 3.5 cm polyethylene
(46), 1972 (Czech)	R 1.2×10^{13}	6 BF_3 1 LiF-ZnS(Ag)	Paraffin Paraffin	
(35), 1973 (47), 1976 (USA)	Cf 0.25 Cf 0.85	30 3He 5 cmx51 cm L, 3 circles		
(48), 1973 (USA)	R 250 W 2.5×10^9	6 BF_3 5 cm Dx30 cm L on 6.35 cm radius		
(49), 1974 (So. Afr.)	R 2×10^{13}	6 BF_3 2.5 cm Dx30 cm L	Water 46 cm D 46 cm H	Cd
(50), 1974 (Canada)	R 5 MW 2.2×10^{13}	8 BF_3 on 10 cm radius	Polyethylene 30x30x30 cm	1 mm Cd, 5 cm polyethylene, 20 cm paraffin; 10 cm Pb around sample
(51), 1974 (Korea)	R 1 MW 1×10^{13}	6 BF_3 2.5 cm Dx51 cm L on 8 cm radius	Paraffin 27 cm Dx60 cm H	.75 mm Cd, 6 cm borated paraffin
(52), 1974 (India)	R 40 MW 6×10^{13}	8 BF_3 5 cm Dx30 cm L on 12 cm radius	Paraffin	1 mm Cd, 10 cm borated paraffin, 2.5 cm Pb around sample

Table 3-1. (Continued)

Citation Number Operation Times (Irradiation/Delay/ Counting Times; Seconds)	Background Counts	Efficiency	Sensitivity, Counts/ μ g			Minimum Level of Detection	Applications
			natural U	^{238}U	^{232}Th		
(33), 30/0/40	<10		34.6		0.40	.58 μ gU	
pulse/0/40	<10		525		10.4	.038 μ gU	
(45), 60/25/60	4 to 6	8%	350			.03 μ gU	Geological samples; water; stream sediments; soil; rock; vegetation
(46), 60/50/120						.05 μ gU .1 μ gU	Lunar soil; rocks
(35), 120/10/200		40%	.0005			2.8 gU	Mixed oxide and carbide fuel beads
(47), 120/10/100			.002				
(48), 45/40/60		7%	.186				HTGR fuel sticks
(49), 40/25/40			330			.25 μ gU	
(50), 40/25/64	1.4		593	21.8	4.9		Meteorites
(51), 60/20/60	48	13%	340	26.6	5.6	.05 μ gU	Geological samples, U, Th ores
(52), 60/30/60	220	15%	4054		3.23	.1 μ gU	Rocks; sediments; soils; archaeological samples; high purity materials, biological samples

Table 3-1. (Continued)

Citation Year Published Country	Neutron Source (R = reactor; power level; flux in n/cm ² -s Cf = ²⁵² Cf; mg of ²⁵² Cf)	Detectors (Number; type; size; location)	Moderator (Material; size)	Shielding (Material; size)
(53), 1975 (Finland)	R 5x10 ¹²	6 BF ₃ 4 cm Dx25 cm L	Polyethylene 36 cm Dx50 cm H	Polyethylene 4 cm; Cd
(54), 1976 (USA)	R 8 MW 1x10 ¹³	20 ³ He 2.5 cm Dx30 cm L on 14.6 and 22.2 cm radii 12 ³ He 2.5 cm Dx30 cm L on 17.8 cm radius	Polyethylene 9 cm ID, 30.5 cm ODx38.1 cm H Polyethylene 11.5 cm ID, 25.4 cm ODx38, 1 cm H	2.5 cm Pb around sample; water 4.8 cm Pb around sample; water
(37), 1976 (USA)	Pulsed 14 MeV 10 ⁸ n/sec	1 ³ He 7 cm Dx10 cm L	Borehole	
(36), 1976 (USA)	Cf . 33	9 ³ He (2 sets)	Borehole	
(55), 1977 (So. Afr.)	R 2x10 ¹⁵	4 BF ₃		
(34), 1977 (USA)	Cf 100 3x10 ⁹	12 BF ₃ 2.5 cmDx46 cm L on 6.4 and 9.6 cm radii	Polyethylene	Cd, borated WEP
(56), 1977 (USA)	R 10 kW 1.4x10 ¹¹ 1 MW	14 BF ₃ 5 cmDx31 cm L	Paraffin	
(57), 1978 (USA)	R 1 MW 1.7x10 ¹³	12 BF ₃ 5 cmDx31 cm L on 6.4 and 11.7 cm radii	Paraffin 38 cm Dx70 cm H	.5 mm Cd, 6 to 12 cm paraffin

Table 3-1. (Continued)

Citation Number Operation Times (Irradiation/Delay/ Counting Times; Seconds)	Background Counts	Efficiency	Sensitivity, Counts/ μ g			Minimum Level of Detection	Applications
			natural U	^{238}U	^{232}Th		
(53), variable			240			.03 μ gU	Commercial unit
(54), 60/20/80	13	40					Water samples
	10	27%					Sediment samples
(37)							Borehole logging
(36), 11/1/11			406 counts per % U_3O_8			100 ppm @ 2.5 cm/sec	Borehole logging
(55), 30/20/50	400		2000			.04 μ gU	Borehole water; seawater
(34), cyclic		12%				7.5 μ gU	
(56), 60/20/60	20		6.8			.04 μ gU	Dental porcelain
(57), 60/20/60	31 @ 1 MW 20 @ 10 kW	22%	1950			.012 μ gU	Phosphate by-products; zirconium impurities; soil; seawater samples

absorption cross section, although quite small, is higher than that of ^{12}C or ^2H . ^2H was eliminated because high energy gammas could produce false counts by producing neutrons by means of (γ, n) reactions with the deuterium nuclei. ^{12}C was thus considered the best moderator; therefore graphite was chosen for their detector assembly. To complete the high efficiency system, they used a large number of detectors, 40 BF_3 's, and most of these were unusually long, 143 cm of active length. This arrangement gave a system efficiency of 60%. The 40 detectors were arranged in five circles, all concentric about the sample tube, and all detectors in each ring were connected to a single set of electronic signal-processing components, so that five sets of counts could be recorded. There was a slight dependence noticed between the energy distribution of the neutrons emitted by the sample and the ratio of counts in the outer to inner detector rings. It is believed that higher energy neutrons, which will require more collisions with moderator atoms to thermalize, will result in relatively more counts in the outer detectors than in the inner ones.

Although most systems used neutron sources which gave steady neutron fluxes, Lukens and Guinn experimented with irradiation in a TRIGA reactor operating in a pulsing mode (33). A 30-second steady state irradiation in a thermal flux of 2.5×10^{12} n/cm²-s gave a sensitivity of 34.6 counts/ μg U, while a pulse with an integrated fluence (the total flux integrated over the irradiation time) of 1.7×10^{14} n/cm²

resulted in a sensitivity of 525 counts/ μg U. The fluence of the pulse was slightly more than twice the fluence of the steady state irradiation, but the sensitivity was better by a factor of 15. In the longer irradiation many of the short-lived precursors decayed while the sample was still in the reactor, but the pulse was so brief (full width at half maximum of 16 msec) that very few precursors decayed during the irradiation. Thus irradiation in a pulsing mode appears to be a promising way to improve sensitivity, at the expense of fewer samples per unit time.

Most of the early researchers used a reactor as a source of irradiating neutrons. Some research facilities, however, do not have access to a reactor, and several researchers have thus looked at californium-252 as an alternate source of neutrons. ^{252}Cf is a practical nuclide for a neutron source, since it has a half life of 2.63 years, which is short enough for a high specific activity, but long enough to have a long useful life. Three percent of the disintegrations are by spontaneous fission, producing an average of 3.76 neutrons per fission. Thus 100 mg of ^{252}Cf will emit 2.31×10^{11} neutrons per second. These neutrons are emitted at energies typically in the low-MeV region and thus must be thermalized by a moderator around the source to obtain slow neutrons. The use of californium-252 sources for DFN counting has been reported by two groups of researchers, MacMurdo (34) and Hagenauer, Zyskowski and Nelson (35). Hagenauer et al. used modest-sized ^{252}Cf sources: 0.25 mg and 0.85. Even

with a very high efficiency counting assembly of 30 ^3He detectors, the minimum level of detection was 20 mg of ^{235}U . Still the system was successfully applied to the analysis of fissile material concentrations in samples of reactor fuel. MacMurdo has used larger quantities of ^{252}Cf , about 100 mg, to get better sensitivities. With 12 BF_3 detectors in the counting assembly, the MLD was 7.5 $\mu\text{g U}$, which is still a factor of 10^2 higher than that obtained using the more intense neutron fluxes obtained in a reactor.

An interesting application of the DFN technique is borehole logging: the analysis of uranium ores within the borehole itself. Steinman used a 3.35 mg ^{252}Cf source and ^3He detectors in a sonde which was lowered down the borehole (36). After a brief irradiation by the californium source, the equipment was quickly repositioned so that the detectors could count the delayed neutrons being emitted from the uranium in the rock around it. Uranium concentrations in ores are high enough, and the size of the "sample" emitting delayed neutrons is large enough, that a milligram-level ^{252}Cf source and counting assembly can give good information. Givens et al. have also developed a successful borehole logging system which uses a pulsed neutron generator giving 10^8 neutrons per second in place of the californium source (37).

IV. DESCRIPTION OF THE DELAYED FISSION NEUTRON SYSTEM

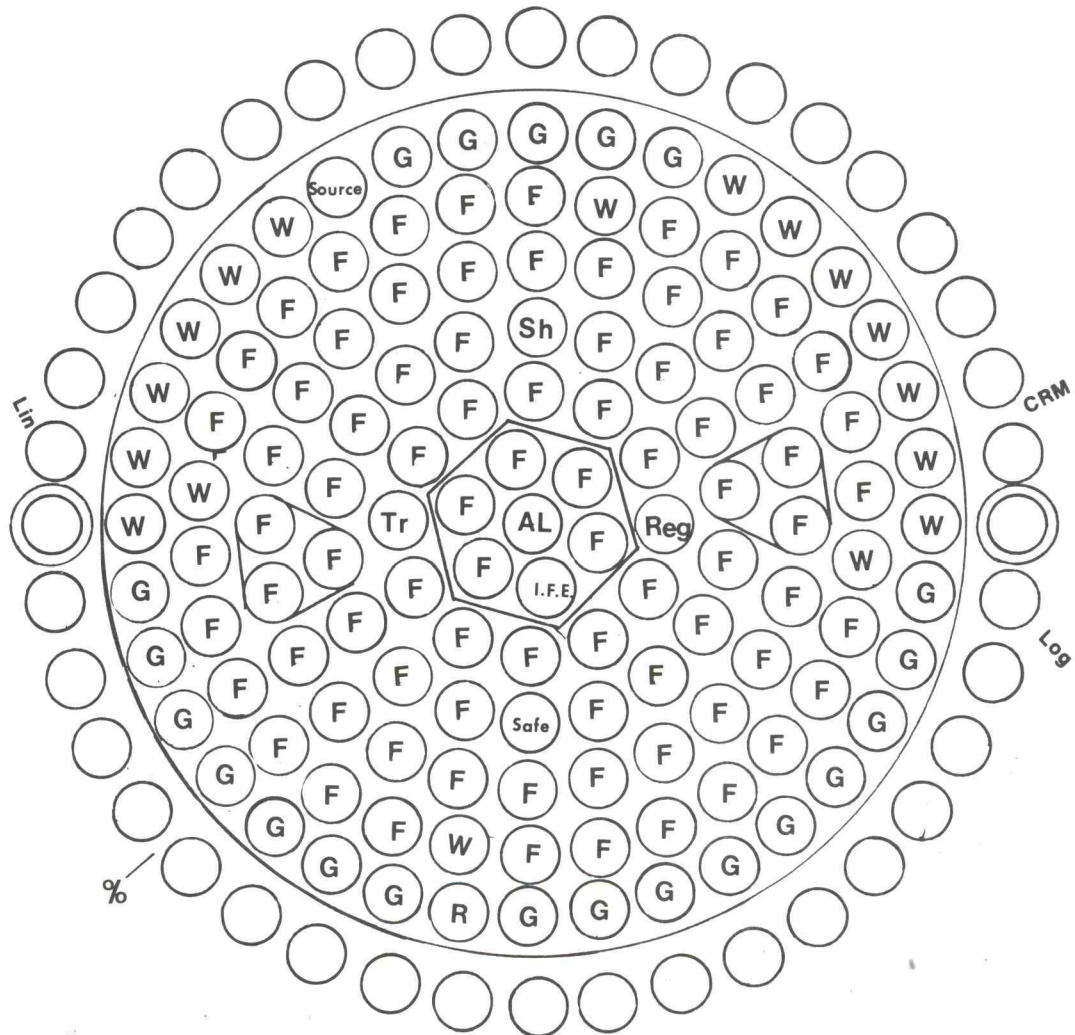
The irradiation source for the OSU DFN system is the Oregon State TRIGA Reactor (OSTR). This reactor is a TRIGA Mark II light water reactor capable of steady state operation at a power level of one megawatt. It is also capable of operation in a pulsing mode, with a typical peak pulse power of 2200 MW and full width at half maximum of ten milliseconds. Irradiations occur in the pneumatic transfer system terminus, which is in the outer ring of fuel elements in the reactor core. Figure 4-1 is a diagram of the current OSTR core configuration.

Several modifications in the original TRIGA core have resulted in a higher thermal flux at the rabbit position, thus increasing the DFN system's sensitivity. In August, 1976 the reactor was refueled with FLIP fuel, which has a higher ^{235}U enrichment than the original TRIGA fuel. In July, 1977 the fuel elements were repositioned so that a position next to the rabbit position, which formerly contained a fuel rod, is now empty (water-filled). The resulting increase in moderator and decrease in absorbing material in the vicinity of the rabbit position increased the thermal flux there by about 17%. Since uranium fission is dominated by thermal fission of ^{235}U , this increase in thermal flux improved the DFN sensitivity by the same factor.

The thermal flux in the rabbit position has been determined by irradiating gold foils. These foils were positioned inside the rabbit capsule, irradiated, and counted on a sodium iodide detector to

Figure 4-1

OSTR CORE CONFIGURATION



F: Fuel Rod

W: Water Channel

G: Graphite Rod

AL: Aluminum Plug

IFE: Instrumented Fuel Element

SOURCE: Neutron Source

R: Rabbit Irradiation Position

OUTER RING: Lazy Susan Irradiation Position

FLUX METER:

CRM: Count Rate Meter

% : Percent Power Channel

LIN: : Linear Power Channel

LOG : Logarithmic Power Channel

Control Rods:

Tr: Transient

Safe: Safe

Sh: Shim

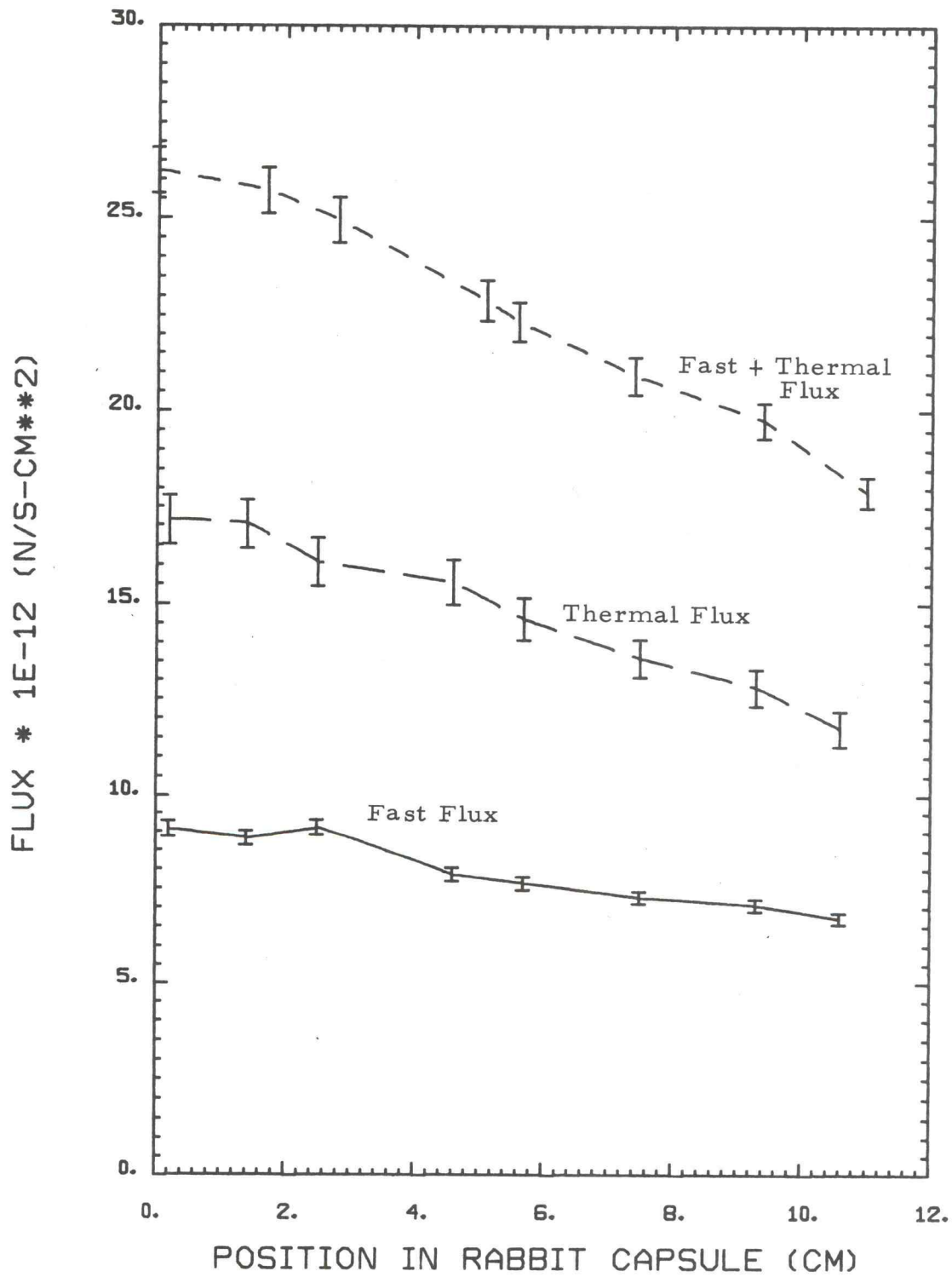
Reg: Regulating

(Safe, Shim and Reg rods all have following fuel rods below them)

determine the count rate of the ^{198}Au , which emits a 412-keV gamma when it decays. Measurement of this count rate allowed the determination of the number of $^{197}\text{Au}(n, \gamma) ^{198}\text{Au}$ reactions which occurred, and hence the neutron flux could be calculated. Two types of gold foil determinations were carried out, one with the foils covered by cadmium shields during irradiation and one with the foils bare during irradiation. The cadmium-covered gold could be activated only by neutrons having an energy higher than the cadmium cutoff energy (about 0.5 eV), and the epithermal (or "fast") flux could be measured. In the bare foil irradiation, the gold could be activated by neutrons of any energy. If the flux is considered to consist of two components, the thermal and the epithermal fluxes, then the thermal flux could be found by subtracting the epithermal flux from the flux found in the bare foil determinations.

Figure 4-2 shows the results of the flux determination performed in October, 1977 for the OSTR rabbit position. The thermal flux values were found using the measured fast and fast-plus-thermal fluxes. Since the fast and fast-plus-thermal measurements were not made at the same positions, the three fast-plus-thermal measurements in the positions closest to a fast position were used in a second order interpolating scheme to evaluate the fast-plus-thermal flux at the appropriate position. The thermal flux at each position was then found as the difference between the fast flux and the interpolated fast-

Figure 4-2

VARIATION OF NEUTRON FLUX
IN THE RABBIT IRRADIATION POSITION

plus thermal flux at the same position. The error bars for the thermal line were determined from the errors in the corresponding fast and fast-plus-thermal flux uncertainties. The 0 cm position is the bottom (inside) of a 2-dram polyvial positioned in the bottom of a rabbit capsule, and the uncertainty in the measurement of these positions was about ± 0.2 cm (this uncertainty is not reflected in the graph).

It is important to note the variation of flux with position inside the rabbit capsule when it is in the irradiation position. The thermal flux at the bottom of the rabbit capsule is about 42% higher than the flux at the top of the capsule, and the flux gradient is about 2.9% per centimeter in the part of the capsule most often used for holding the sample. Since the number of DFN counts is proportional to the thermal flux, the flux gradient can introduce a small uncertainty in the determination of uranium concentrations in two samples which differ in size or in their positioning in the capsule during irradiation.

The facility which transfers the sample into the reactor, and then back to the counting room, is the pneumatic transfer "rabbit" facility. The sample travels through an aluminum tube connecting the reactor and the rabbit terminal room. The operator manually loads the capsule into the tube before irradiation and unloads it at the same place after irradiation. Some DFN systems have a two-station rabbit system which transfers the capsule directly into the counting assembly after irradiation. This type of system has the advantage of allowing

short decay times, since no operator manipulation is required, and samples returning from the reactor with high beta and gamma activities would not pose a hazard to the operator. It also has a major disadvantage. The rabbit capsule itself has been determined to be responsible for a high number of background counts (about 300 in 60 seconds, with a decay time of 20 seconds). Removing the sample from the rabbit capsule can reduce the background. Thus it has been advantageous to manually unload the rabbit capsule from the rabbit terminal in order to take the sample out of the capsule for counting.

The DFN counting assembly is located in the rabbit terminal room, which is located next to the reactor bay, about ten meters from the reactor itself. The rabbit tube is about 34 meters long, and the sample travels from one position to the other in about five seconds. The rabbit system can be operated in either a manual or an automatic mode. In the automatic mode, a timer controls the time between launching the rabbit and the start of its return trip.

Since the rabbit capsule is travelling fairly fast, it stops suddenly at the end position, and care must be taken to seal the irradiation vials so that the sample does not leak. It is thus a policy of the OSTR reactor operations staff that any sample in powdered or liquid form must be doubly encapsulated and sealed to prevent leaks which possibly could contaminate parts of the rabbit system. This restriction often imposes a constraint on the amount of a powdered or liquid

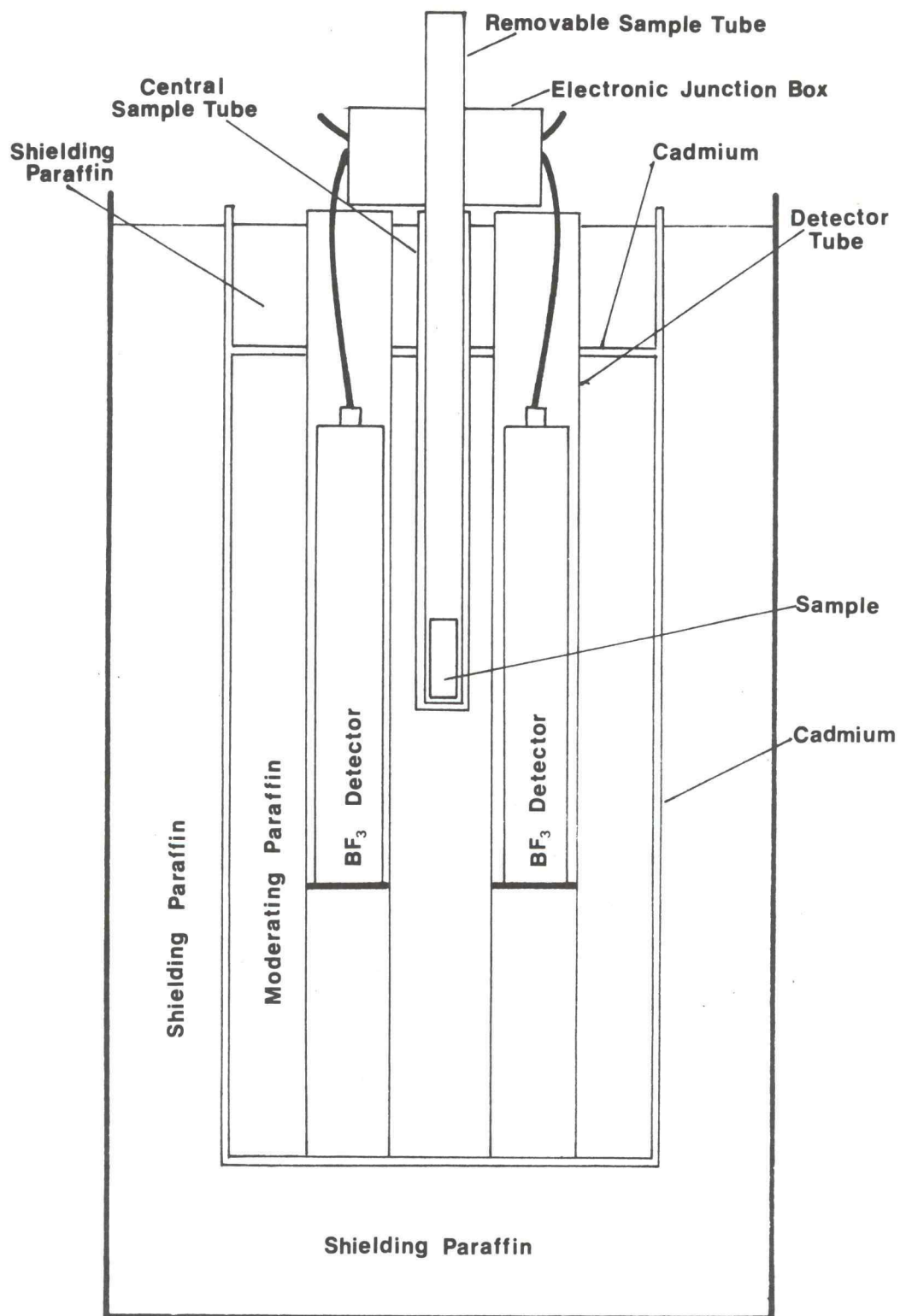
sample which can be analyzed in one irradiation.

The rabbit capsules which carry the sample in the rabbit system are made of high-density polyethylene with screw-on lids. The sample is never placed directly in the rabbit capsule, since the rabbit capsules are reused until the cumulative radiation exposure makes them too brittle for reliable service. The sample is always placed inside a two-dram polyethylene "polyvial," which is then heat sealed. The two-dram polyvial will hold a little over 7 cm^3 of sample, and two can be stacked one on top of the other inside a rabbit capsule. In samples which must be doubly encapsulated, two 2/5-dram polyvials will fit inside a two-dram vial, and one 2/5-dram vial will hold about $1 \frac{1}{2} \text{ cm}^3$ of sample. The 2/5-dram vial is the one most commonly used for sample analysis. In some situations a vial must be used which will fit inside the 2/5-dram vial. For these situations a 2/27-dram vial is used, which holds only about $1/4 \text{ cm}^3$.

Figure 4-3 is a cross section view of the DFN counting assembly. The assembly is contained in a 55-gallon steel drum, 87 cm high and 57 cm in diameter. The drum contains about 150 kg of paraffin and rests on a square stainless steel plate on casters to achieve portability. An inner polyethylene wall 70 cm high with a 38-cm diameter circular acrylic bottom plate separates the outer shielding paraffin from the inner moderator paraffin. A cadmium sheet surrounds this cylinder on the side, bottom, and much of the top. (It should be

Figure 4-3

DFN COUNTING ASSEMBLY - CROSS SECTION



mentioned that the shielding paraffin and the moderating paraffin are the same material, but are differentiated by their different functions.) The inner structural materials for parts such as the sample tube, detector guides, and detector spacers, are made of acrylic, which is a good hydrogenous moderator. The assembly was constructed by putting the structural pieces in place, melting blocks of paraffin, and then pouring the paraffin, a kilogram or two at a time, around the pieces. Since the paraffin reduces in volume as it cools, it was found that the paraffin had to be carefully poured into place to avoid forming air gaps as it cooled, especially in places such as the underside of horizontal structural pieces.

The structural tubes are all acrylic tubes with $1/8$ inch (0.32 cm) wall thickness. The inner six detectors are all in tubes with inside diameter $2 \frac{1}{4}$ inches (5.72 cm). These tubes extend from the plate at the bottom of the moderator to above the upper surface of the shielding paraffin, which allows the detectors to be removed easily. A spacer plate $3 \frac{1}{2}$ inches above the bottom moderator plate supports the detector in the proper counting position. The remainder of the tube below the spacer plate contains moderating paraffin. Holes for the outer six detectors were drilled into the paraffin after it had solidified, which resulted in a smaller air gap between the detector wall and the moderator. The central sample tube is an acrylic tube with inside diameter of $1 \frac{1}{4}$ inches (3.12 cm), which

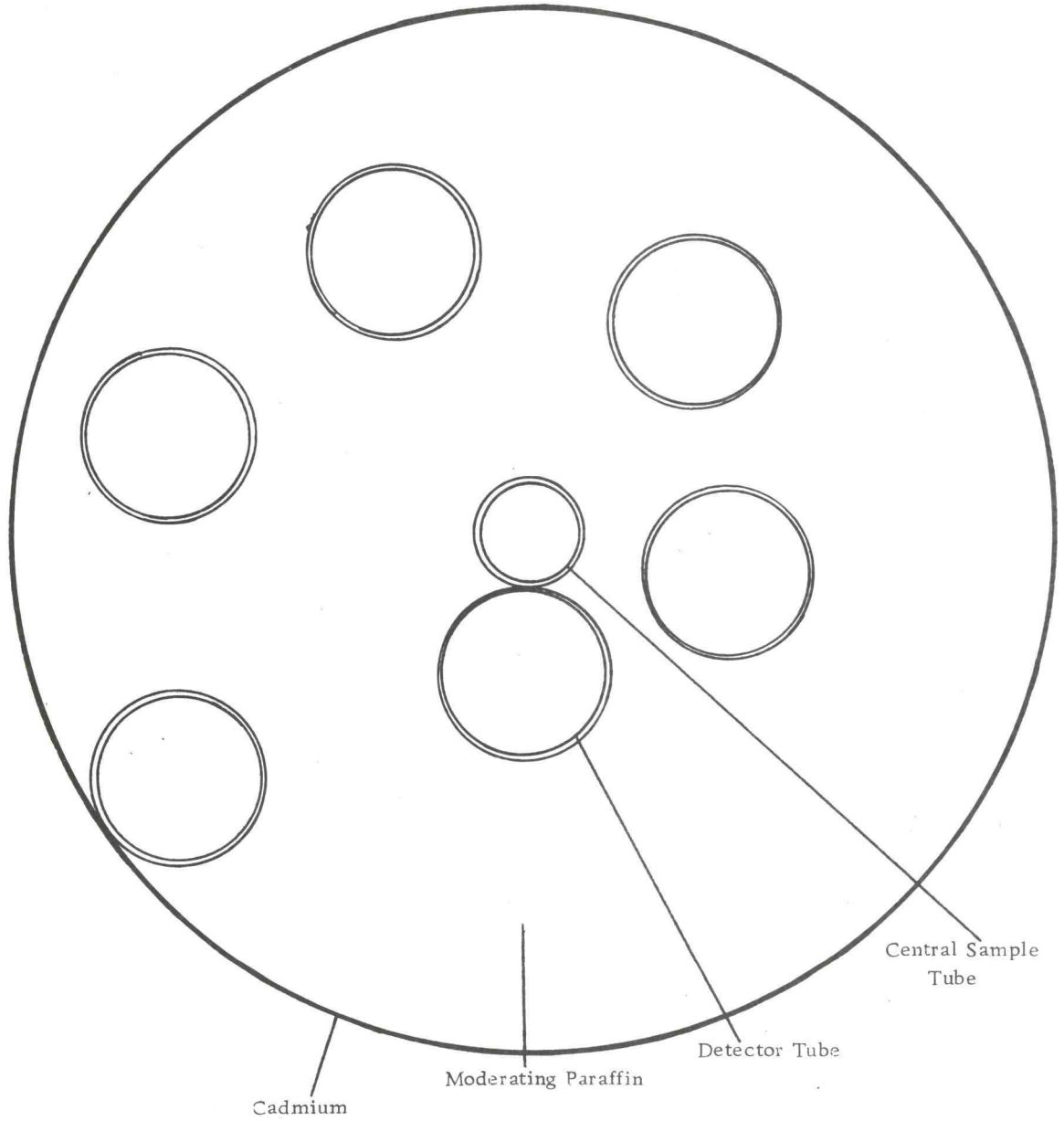
is positioned so that the center of the sample will lie in the horizontal plane which bisects the active volume of the detectors. A removable sample tube, with outside diameter of one inch (2.54 cm) and sealed at the bottom, extends above the electronic junction box above the detectors. During counting, the sample is located at the bottom of this tube, which is inside the central sample tube. After counting, the sample is quickly removed from the tube in order to measure its dose rate for health physics records.

Several DFN counting assemblies have a lead cylinder surrounding the counting position to reduce the gamma radiation field incident on the neutron detectors (31, 32). It was determined to be advantageous to omit the lead shielding in this system in order to increase the amount of moderator between the sample and the detectors. Thus the omission of lead allowed the detectors to be positioned closer to the sample in a region of higher neutron flux.

Positioning of the detectors was based on an experiment which varied the distance from sample to detector. The same moderating and shielding arrangement used in the final assembly was used for the test system, which is diagrammed in Figure 4-4. Six acrylic tubes were imbedded in the moderating paraffin at varying distances from the central sample tube. Five tubes were filled with paraffin plugs to provide moderating material in tubes not containing the detector. A single BF_3 detector was used, and the counts from a sample

Figure 4-4

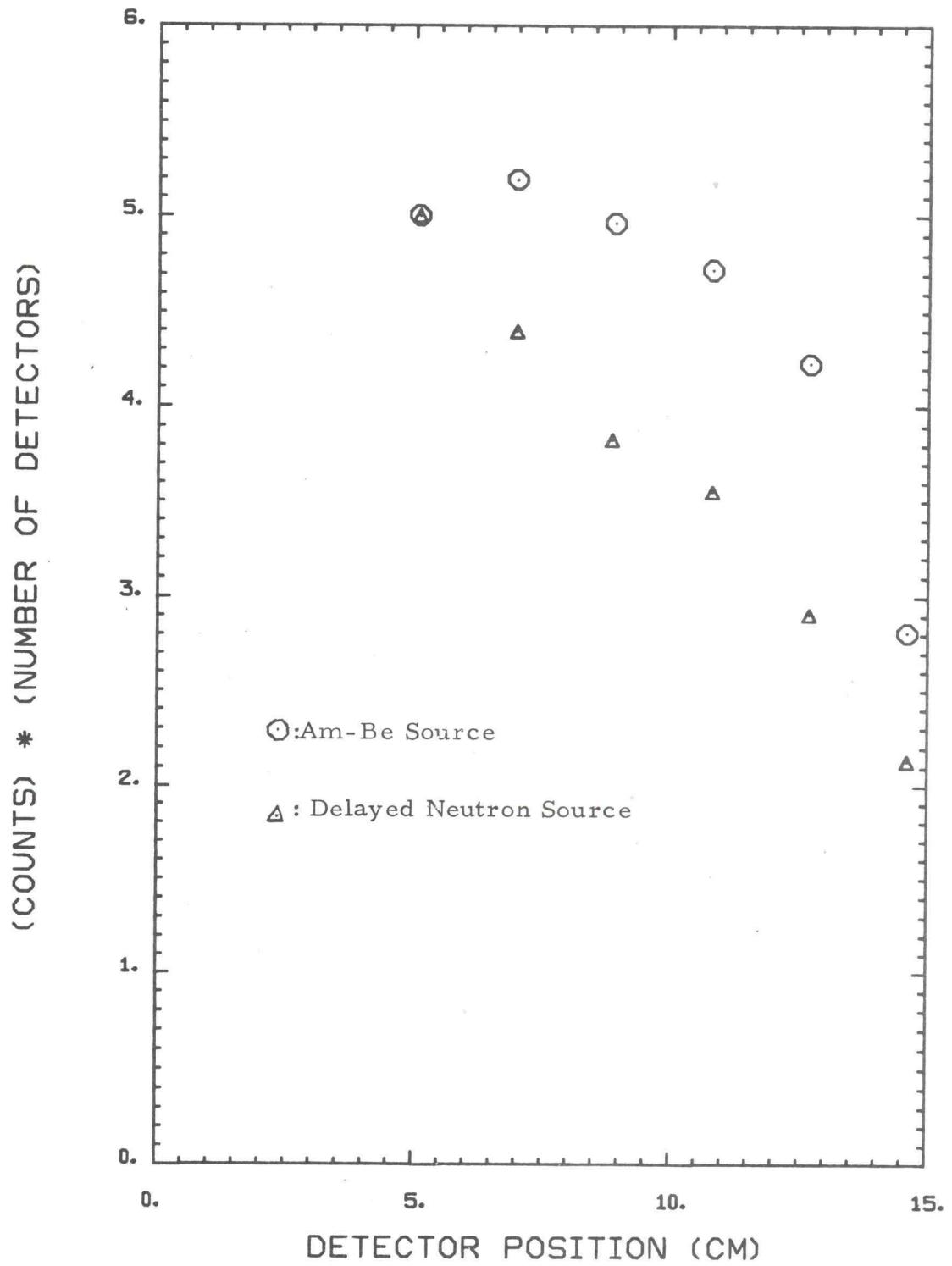
OVERHEAD VIEW OF THE DFN TEST ASSEMBLY



were recorded with the detector in each of the six positions. This was performed with an americium-beryllium neutron source and with a uranium delayed neutron source to get results for two different neutron energy distributions. For the delayed neutron source, a single uranium-containing sample was irradiated and counted for each trial. The results of this experiment are shown in Figure 4-5, which is a graph of CxN vs. sample-to-detector distance. CxN is the product of a normalized count (the count for a given detector position divided by the largest count due to the source) and the number of detectors which would fit in a ring of the given radius. The smallest sample-to-detector distance gave the highest count rate for a single detector. One of the curves shows a slight peak at 7 cm, however, since this is close to the smallest ring which will hold six detectors. With the detectors as close to the sample tube as possible, five detectors fit in the ring, but there are gaps between the tubes allowing neutrons to pass through undetected. Thus six detectors spaced in the smallest ring possible around the sample tube appears to be the optimum arrangement for six detectors.

The decision to use the smallest possible sample-to-detector distance was supported by a computer calculation. In this calculation, a one-dimensional computer code using multigroup diffusion theory calculated the radial neutron flux distribution in an assembly similar to the DFN counting assembly. The assembly was modelled

Figure 4-5
C*N VS DETECTOR POSITION



as having four regions of uniform material properties. The inner region was air, and this region also contained the fixed neutron source. The next region was water, with the same dimensions as the plastic and paraffin moderating region of the DFN assembly. It was followed by a cadmium region of appropriate thickness, which was followed by another water region, similar to the shielding paraffin. The calculation was performed using four neutron energy groups, and the neutrons were all emitted in the second group. The boundary conditions for the calculation were zero neutron current at the center, and zero incoming current at the outer boundary. The results of this calculation are presented in Figure 4-6, which is a plot of the radial distribution of the fast and thermal neutron fluxes in the assembly. The three fast group fluxes calculated by the computer code were collapsed into a single group flux. Although water was used as a moderator instead of paraffin, their moderating properties are similar enough that the flux distributions will be similar. The basic conclusion for both moderators is that the thermal neutron flux is highest in the center of the assembly and decreases rapidly with increasing radial distance. Thus a detector will be exposed to the highest possible neutron flux if it is positioned as close as possible to the sample.

An overhead view of the final DFN counting assembly is shown in Figure 4-7. The inner six detectors are placed at 60° intervals with their centers at a distance of 6.4 cm from the center of the

Figure 4-6
NEUTRON FLUX DISTRIBUTION
IN A WATER-MODERATED ASSEMBLY

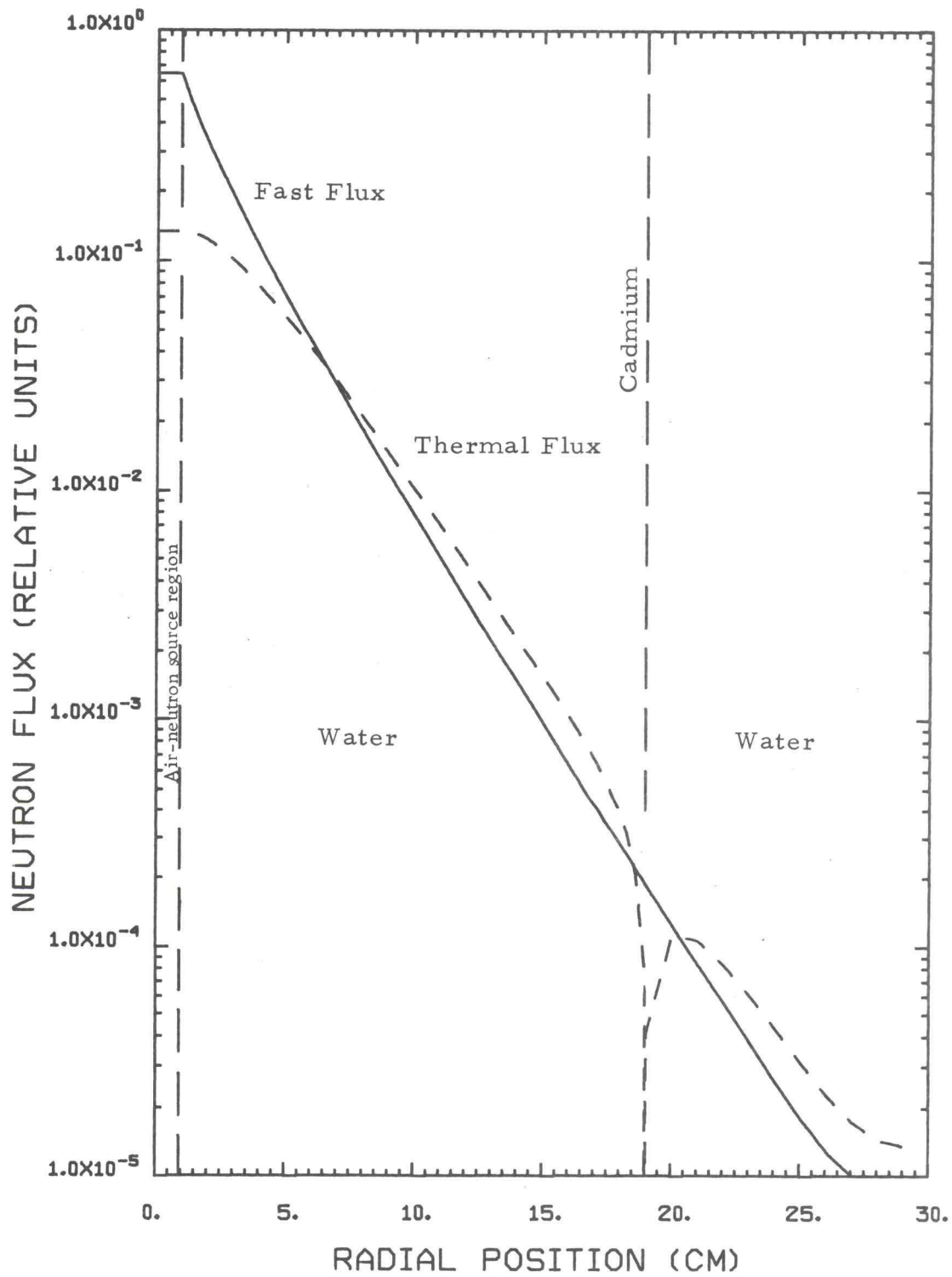
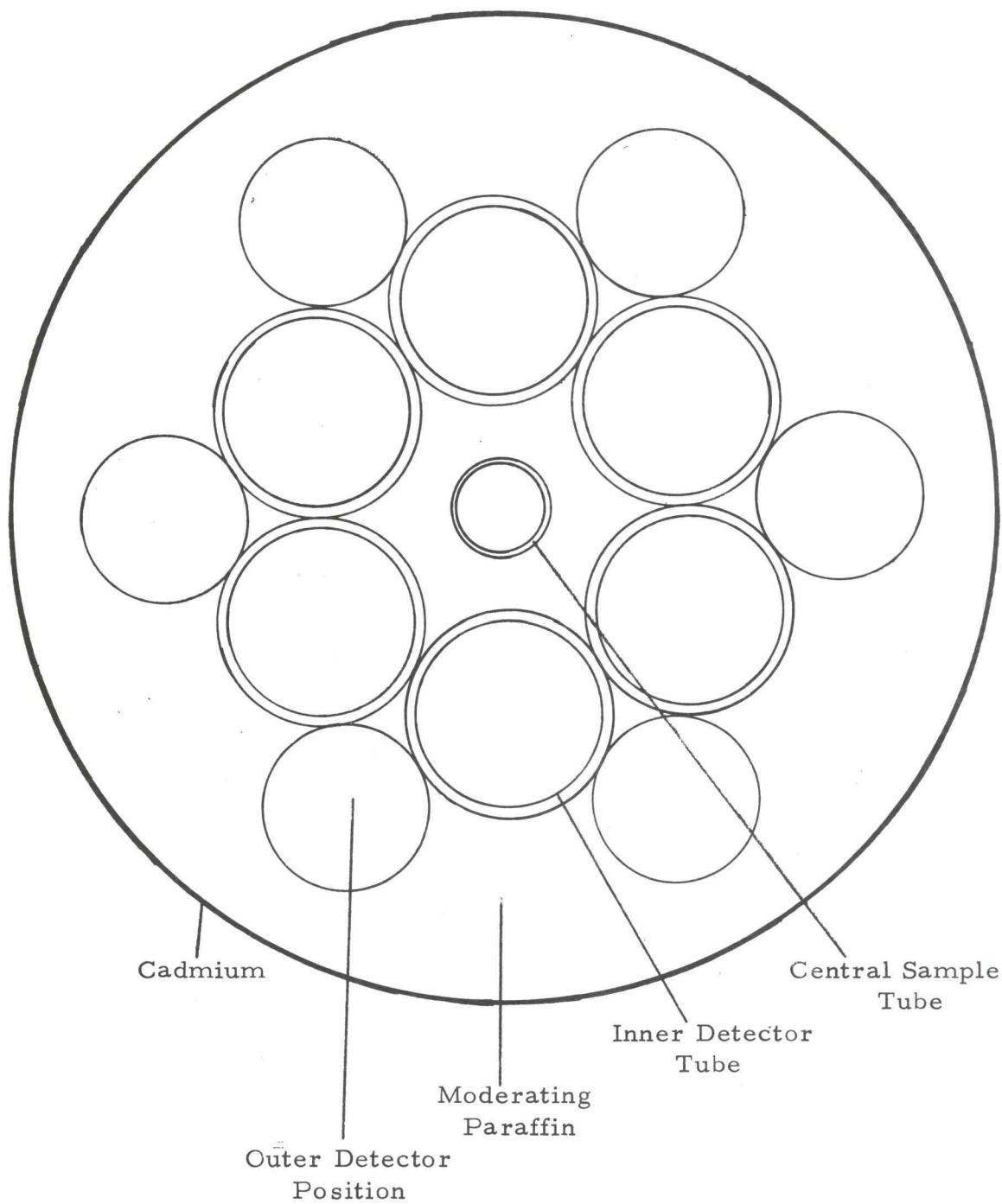


Figure 4-7

DFN COUNTING ASSEMBLY - OVERHEAD VIEW



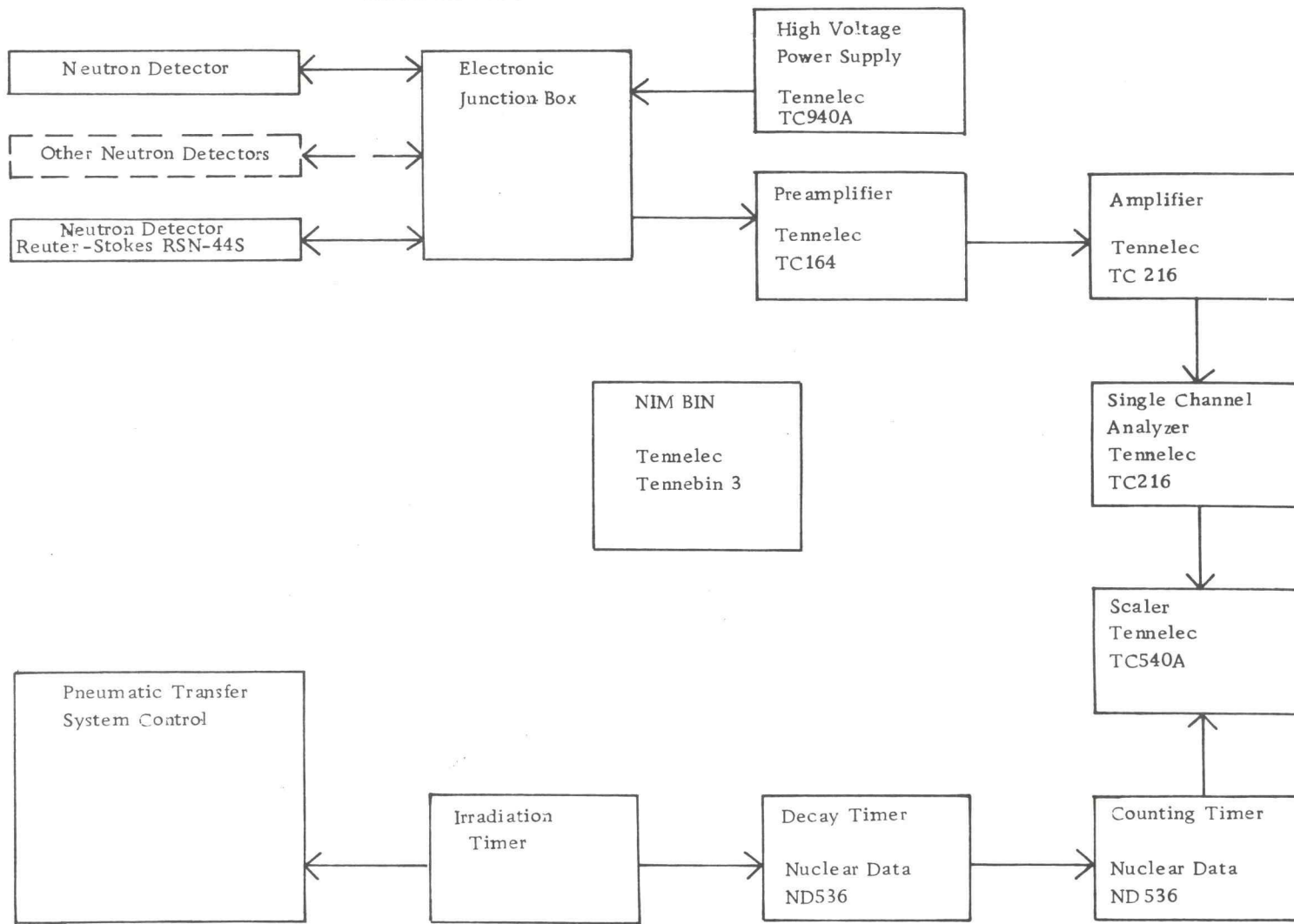
assembly. A neutron travelling outward radially from the sample position would have a smaller probability of being absorbed by a detector if it passed near the edge of a detector (or between two) than if it were incident along the diameter of a detector. Thus it was felt that counts could be increased if an additional ring of six detectors were placed outside the inner six, centered behind the gaps between two adjacent detectors. Six holes were drilled in the moderator at a radial distance of 11.7 cm from the center to hold six additional detectors. The addition of these six detectors resulted in a significantly higher count rate.

Figure 4-8 is a diagram showing the arrangement of the major components of the counting system. An electronic junction box is positioned directly above the counting assembly, and short (16.5 cm) cables from the 12 detectors are attached to connectors in the sides of the box. A cable from a high voltage supply in a NIM-bin leads into another connector in the box, as does a signal cable to the preamplifier. The high voltage signal is also routed from the single high voltage cable down the 12 detector cables. A switch is provided for each detector to switch it into or out of the electronic assembly, which allows counting with any combination of detectors. The signal from the preamplifier is routed through an amplifier/SCA to result in a number of counts recorded on the scaler.

Two electronic timers operate along with the irradiation timer

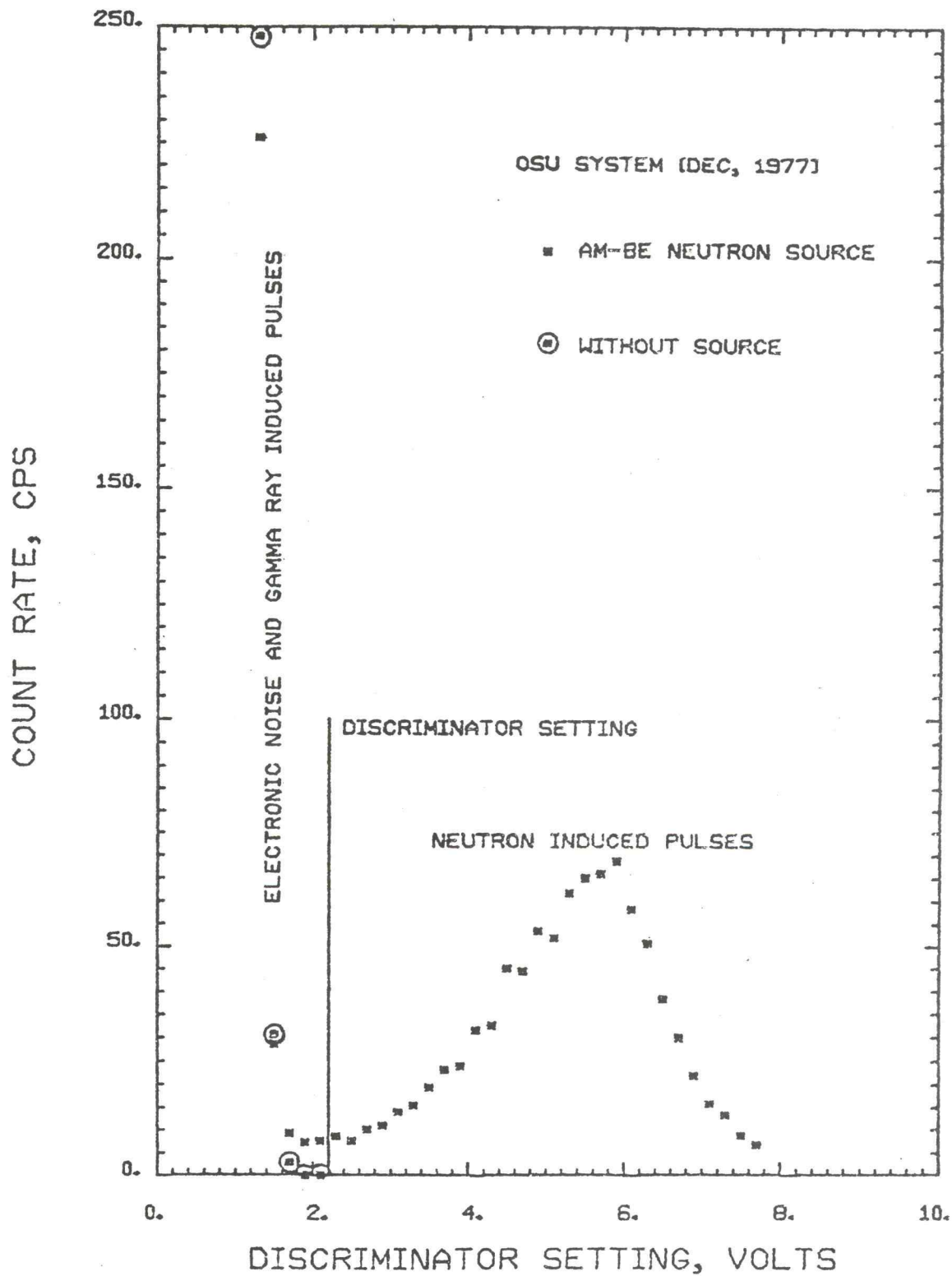
Figure 4-8

BLOCK DIAGRAM OF DFN ELECTRONICS



in the rabbit system to precisely control the various times in a sample analysis. The signal from the irradiation timer also starts the decay timer. When the decay timer switches off, it sends a signal to start the counting timer and open the gate on the scaler. When the counting timer switches off, it sends a signal to stop the scaler. After the scaler reading is manually recorded, a single reset button sets the scaler count back to zero and resets the delay and counting timers.

The preamplifier and amplifier perform the usual pulse-shaping and -amplifying functions. The single channel analyzer (SCA) performs the important function of ensuring that only pulses initiated by neutrons are routed to the scaler. The BF_3 detectors are somewhat sensitive to gamma radiation, but a gamma produces a much lower pulse height. Much electronic noise is also developed in the electronic circuit, and these noise-induced and gamma-induced pulses must be eliminated to properly record only neutron-induced pulses. Figure 4-9 shows the results of an experiment to determine the best SCA settings for discrimination. The SCA was set with a window width of 0.2 volts and stepped through the range of pulse heights from 0 to 10 volts. A ten second count was recorded for each pulse height setting, and two sets of measurements were made, one with a 98 mCi Am-Be source, and one with a 72 μCi ^{24}Na source. The ^{24}Na source was chosen because of the high energy gammas it emits (2754 and 1369

FIGURE 4-9 DISCRIMINATION AGAINST
GAMMA RAYS IN A DFN SYSTEM

keV), since the pulse heights are proportional to the energy of the gammas inducing them. These energies are higher than most gamma energies commonly encountered in DFN analyses; also a 72 μ Ci source is more intense than most of the samples routinely analyzed. In Figure 4-9 the count rate distributions for a ^{24}Na source and the Am-Be source are compared, and it is clear that above a setting of 2.2 volts electronic noise and gamma radiation do not produce a significant number of pulses. Nearly all of the neutron-induced pulses, however, do appear above the 2.2 volt setting. This experiment shows that the lower discriminator setting could be set a bit lower, at 2.0 or 1.8 volts. It was decided, however, that a conservative setting of 2.2 volts would eliminate the risk of including any pulses due to something other than neutrons in the gross count. The SCA window of 2.2 to 7.8 volts was adopted for this system. Two background counts of 1 1/2 hour duration confirmed this decision. In one count, the ^{24}Na source was in the assembly, and a count rate of 26.5 ± 0.5 counts per minute was recorded. In a similar count with no source near the assembly, the count rate was 25.4 ± 0.5 counts per minute. This slight difference in count rates cannot be considered a significant increase in the background count rate. Using the critical level criterion developed in Chapter V, the ^{24}Na source count does exceed the background count at the 84% confidence level, but does not exceed it at the 95% confidence level. Due to the variability in background

count rates introduced by the cosmic radiation contribution, it is justified to follow the 95% level and conclude that these two counts are not significantly different.

The BF_3 detectors used in the DFN assembly are model RSN-44S proportional counters, manufactured by Reuter-Stokes. The tubes are 5.08 cm (two inches) in diameter and 36 cm long, with the sensitive length equal to 31 cm. The walls are stainless steel, which has a slightly higher neutron absorption rate than the alternate aluminum wall, but it does not have the alpha-emitting contamination found in aluminum, which can be responsible for about one count per minute. The tubes are filled with BF_3 gas enriched to 96% ^{10}B at a gas pressure of 70 cm Hg. These detectors proved to be well matched, with similar operating characteristics. Using an Am-Be source, a voltage plateau measurement was performed for each detector individually. These measurements showed that a high voltage setting of 2800 volts was well within the operating plateau region of all detectors, justifying a single high voltage supply for all detectors. All detectors also had count rates within a few percent of each other, indicating that they are suited for operation in a single assembly.

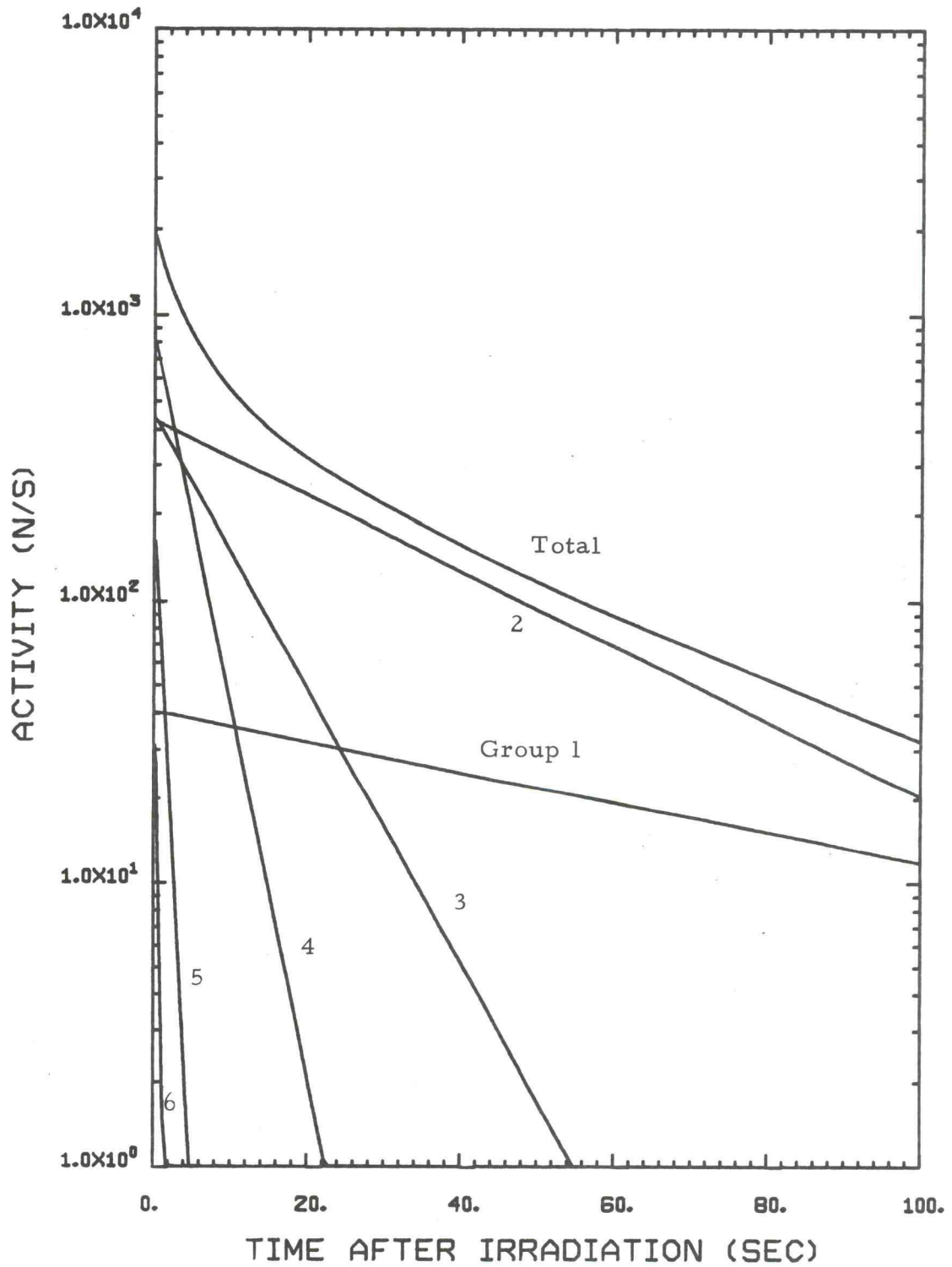
In Chapter III it was mentioned that exposing the sample to a high neutron fluence in a short time interval was advantageous for producing nuclides with short half lives, and thus reactor pulsing would be a good means of improving sensitivity. Unfortunately,

reactor pulsing poses a problem which makes it unsuitable for the routine analysis of a large set of samples. When the reactor is pulsed, the transient control rod is pneumatically forced out of the core, rapidly introducing a large amount of reactivity into the core. The rapid increase in neutron flux and power cause a rapid temperature rise in the fuel, and the negative thermal coefficient of reactivity rapidly decreases the flux and power. Reactor pulses are not exactly reproducible, due to the variations in the rate of control rod withdrawal and rates of temperature increase and heat conduction. Thus a set of reactor pulses would probably exhibit a fairly wide variation in neutron fluences. In order to use reactor pulsing to analyze a set of samples, the neutron fluence for each pulse would need to be measured. A small foil could be included in each polyvial, and the foils could be counted on a NaI or Ge(Li) detector to determine the number of neutrons irradiating each sample, but this would be a time-consuming procedure not suitable for a large number of samples. Thus it was decided that the OSTR would operate in the steady state mode for DFN analyses.

In determining the optimum cycle of irradiation, decay and counting times, it is useful to look at Figure 4-10, which is a graph showing the exponential decay characteristic of delayed neutron emission. For this graph, it was assumed that one microgram of ^{235}U was irradiated in a flux of 1×10^{11} n/cm²-s until all six delayed neutron

Figure 4-10

DECAY OF DELAYED NEUTRON ACTIVITIES

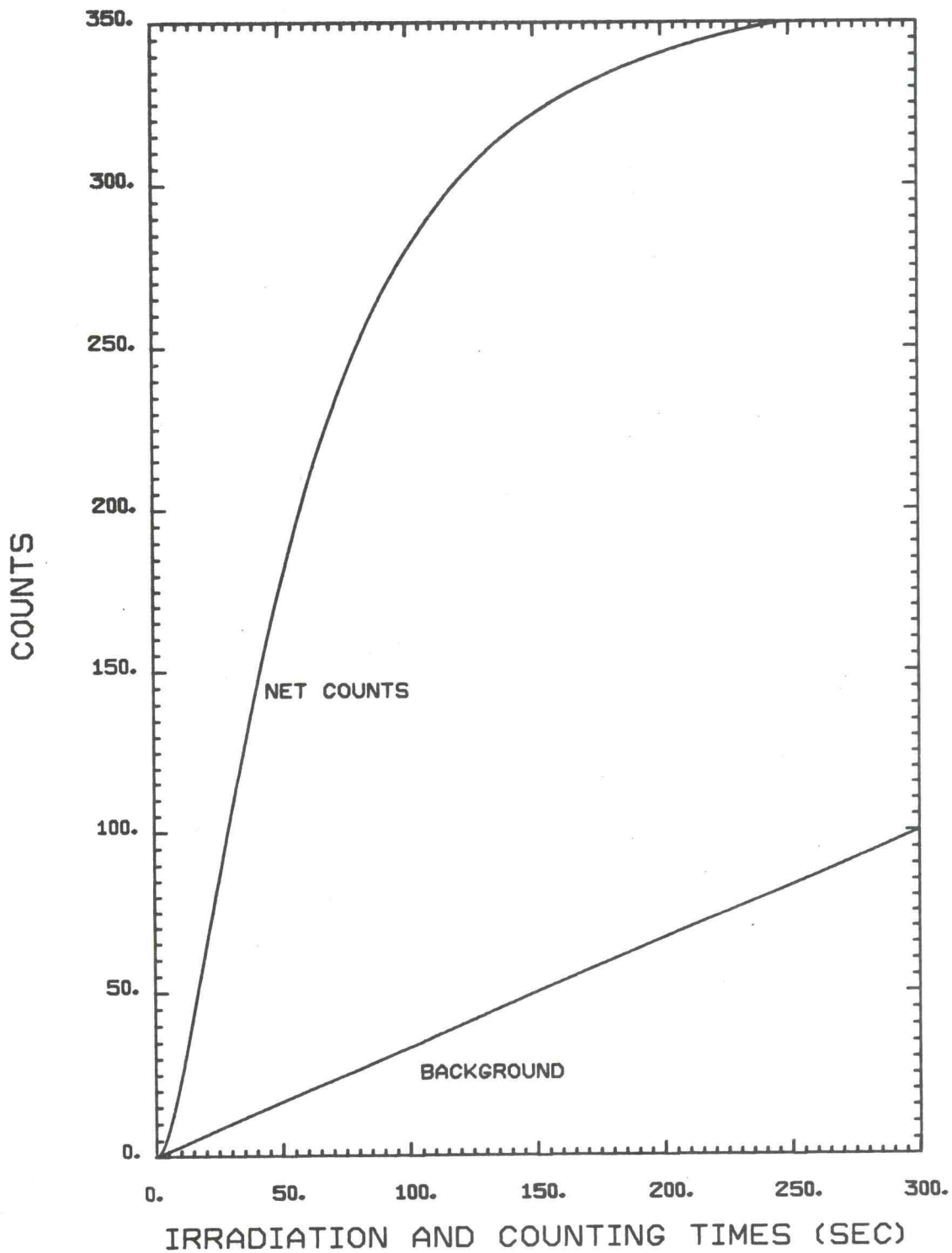


groups had reached their saturated activities. The irradiation time chosen for this calculation was 370 seconds, which would activate the first group (with the longest half life) to 99% of its saturated activity. The number of delayed neutrons emitted per second in each group was calculated for times between 0 and 100 seconds after irradiation and the activities of the six groups were summed to determine the total activity. The rapid decay in activity is quite apparent in this graph, which indicates that the largest number of net counts could be accumulated by making the decay period as short as possible. As mentioned earlier, in order to avoid high background counts from interferences such as contamination in the rabbit capsule, a decay period of no less than 20 seconds was found to be useful. Thus the 20 second decay period was adopted.

Figure 4-10 also shows that after about 80 seconds after irradiation the delayed neutron activity is quite low, less than 5% of the end-of-irradiation activity. This low activity brings into question the usefulness of prolonged counting times. A complicating factor here is that there is a continual accumulation of background counts, as illustrated in Figure 4-11. For this figure the net counts were calculated by the following formula:

$$C_{\text{net}} = \epsilon m \phi \frac{\bar{\sigma}_f N_{\text{av}} \nu}{A} \sum_{i=1}^6 \frac{\beta_i}{\lambda_i} (1 - e^{-\lambda_i t_0}) (e^{-\lambda_i t_1}) (1 - e^{-\lambda_i \Delta t}) \quad (4-1)$$

Figure 4-11

NET COUNTS AND BACKGROUND VS
COUNTING AND IRRADIATION TIMES

where:

$$C_{\text{net}} = \text{net counts}$$

$$\epsilon = \text{counting assembly efficiency} = 0.214$$

$$m = \text{mass of } ^{235}\text{U} = 2.75 \times 10^{-8} \text{ g}$$

$$\phi = \text{thermal neutron flux} = 1.7 \times 10^{12} \text{ n/cm}^2\text{-s}$$

$$\begin{aligned} \bar{\sigma}_f &= \text{thermal fission cross section for } ^{235}\text{U} = \frac{\sqrt{\pi}}{2} \cdot 582 \text{ b} \\ &= 516 \text{ b} \end{aligned}$$

$$N_{\text{Av}} = \text{Avagadro's number} = 6.02 \times 10^{23}$$

$$\nu = \text{average number of neutrons emitted per fission} = 2.418$$

$$A = \text{atomic mass of } ^{235}\text{U} = 235 \text{ g/mole}$$

$$\beta_i = \text{delayed group fractions, from Table 2-2}$$

$$\lambda_i = \text{delayed group decay constants, from Table 2-2}$$

$$t_0 = \text{irradiation time}$$

$$t_1 = \text{decay time} = 20 \text{ seconds}$$

$$\Delta t = \text{counting time.}$$

(This formula is derived in Appendix A.)

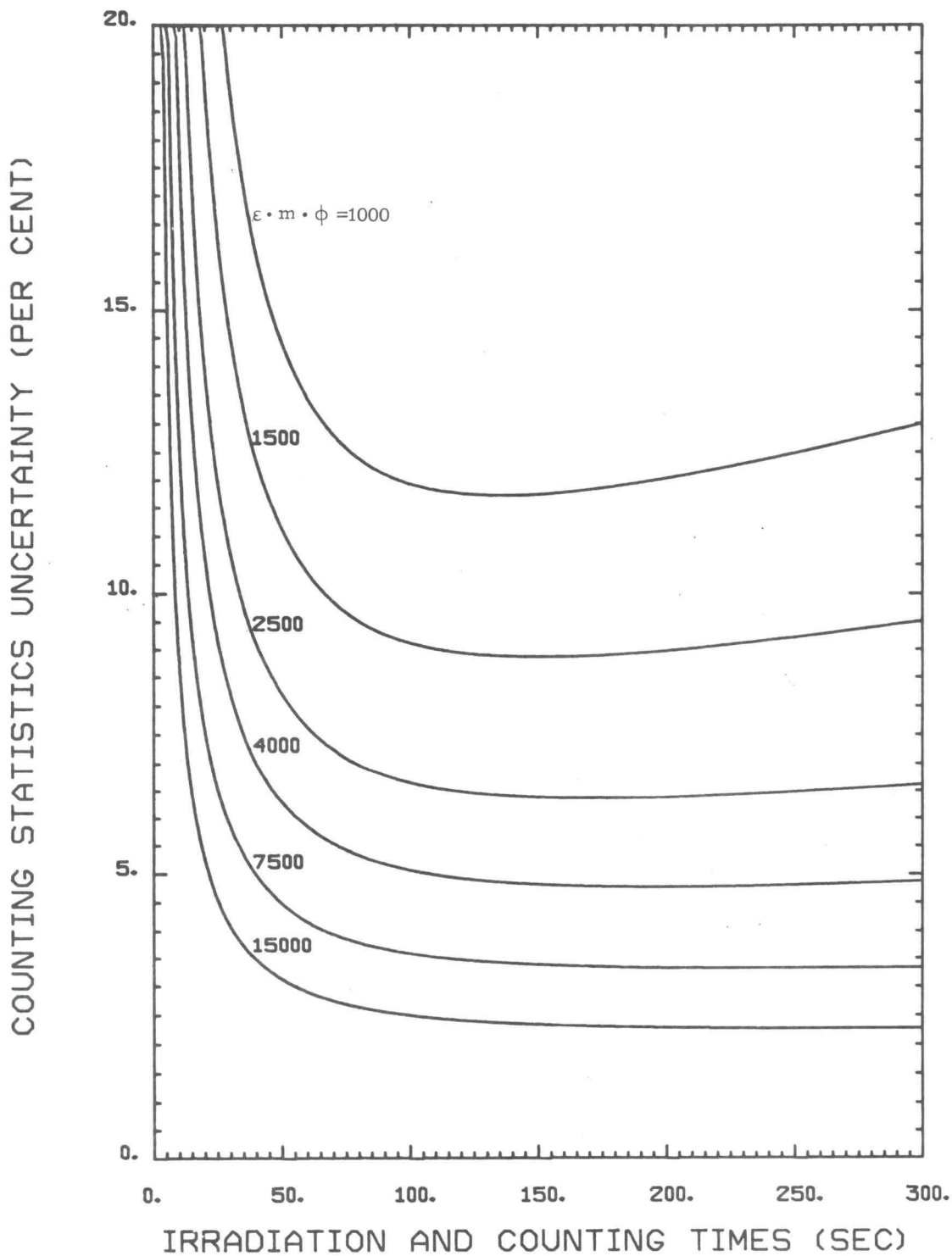
For these calculations, the irradiation and counting times were kept equal, which is an efficient method for the analysis of a large number of samples. The irradiation and counting times were varied from 0 to 300 seconds and the net counts calculated for each time. The background was assumed to be independent of the irradiation time, accumulating at a constant rate during the counting time interval.

For these calculations a background count rate of 20 counts per minute

was assumed, and the total background count was a product of the count time and the background rate. It is interesting to note that for count times from 0 to about 50 seconds the slope of the net count curve is very steep, indicating a rapid increase in net counts with increased t_0 and Δt . As these times become large, however, the slope decreases, suggesting an approach to an asymptotic value. An asymptotic value is indeed expected, corresponding to the $(1 - e^{-\lambda_i t})$ terms in the expression for C_{net} approaching 1. On the other hand, the background count increases at a constant rate, with the background counts a relatively low fraction of the net counts for times of about 50 seconds, but increasing to more than one fourth of the net counts at 300 seconds. A point is also reached at which the slope of the background curve exceeds the slope of the net counts curve, and above this point the background counts accumulate faster than the net counts. This time, of course, depends on the value of the background rate, which will vary somewhat. Above this point, increasing the counting time would actually increase the overall counting uncertainty due to this increase in background. This turning point suggests an optimum selection of counting and irradiation times.

Figure 4-12 further explores the search for the optimum set of times. For this graph the counting statistics uncertainty was calculated for various products of ϵ , m , and ϕ as a function of the counting and irradiation times, with a constant decay time of 20

Figure 4-12

UNCERTAINTY VS COUNTING AND
IRRADIATION TIMES

seconds. Since the net counts are actually found during a sample analysis by subtracting the background counts from the total counts, both uncertainties must be taken into account in calculating the uncertainty in the net counts. The absolute uncertainty for a given count, expressed as one standard deviation, is equal to the square root of the count, so that the absolute uncertainty in the net counts is given by:

$$\Delta C_{\text{net}} = \sqrt{(\Delta C_{\text{tot}})^2 + (\Delta C_{\text{BKGD}})^2} = \sqrt{(C_{\text{net}} + B_t \Delta t)^2 + (B_t \Delta t)^2}$$

since the total counts, $C_{\text{tot}} = C_{\text{net}} + B_t \Delta t$. The relative uncertainty, expressed as a percentage, is thus:

$$\delta C_{\text{net}} = \frac{\sqrt{C_{\text{net}} + 2 B_t \Delta t}}{C_{\text{tot}} - B_t \Delta t} \times 100\%$$

The upper curve on the graph is for $\epsilon \cdot m \cdot \phi = 1000$, which could correspond to a counting system efficiency of 21.4%, a thermal flux of 1.7×10^{12} n/cm²-s, and 2.75 nanograms of ²³⁵U. This would result in about 82 net counts with a 60s-20s-60s cycle, which is nearing the lower limit for a useful number of counts. For this case the graph does have a definite minimum, at times of 137 seconds; i. e., times greater than this would actually increase the measurement's uncertainty. It is interesting to note that for values of $\epsilon \cdot m \cdot \phi$ greater than

1000, the lines lie lower on the graph, as expected, but the minima for these curves occur for greater times. This can be explained by the fact that higher $\epsilon \cdot m \cdot \phi$ values result in greater precursor activities which require longer times of decay before they contribute a lower count rate than the background rate. Thus the minimum of the curve for each product of $\epsilon \cdot m \cdot \phi$ will lie at a different set of times, and the optimum time cycle cannot be based on this minimum if different count rates occur. Another problem with this criterion is that a count rate giving a reasonably low uncertainty will require very long times to reach the minimum.

Looking at the lower curve in Figure 4-12 we note that the curves become nearly horizontal with increasing times, and this feature will help make the final decision. The lower curve is for an $\epsilon \cdot m \cdot \phi$ of 15000, which would give about 1235 counts in a 60s-20s-60s cycle. This is a good counting rate for most analyses. Table 4-1 lists some revealing data from this calculation.

Table 4-1. Counts due to varying irradiation and counting times.

$t_0 = \Delta t$ (sec)	Net Counts	Background Counts	Uncertainty (%)
20	376	7	5.25
40	859	13	3.46
60	1235	20	2.89
90	1599	30	2.55
120	1807	40	2.40
300	2133	100	2.26

This table illustrates that as the time becomes longer, a further increase by any given amount has less effect on the uncertainty. For example, increasing the times from 40 to 60 seconds (by 50%) decreases the uncertainty by 0.57%, whereas an additional 50% increase, to 90 seconds, decreases the uncertainty by only 0.34%. Increasing the times from 60 seconds to 300 seconds will only decrease the uncertainty by a total of 0.63%, and this improvement in the sensitivity is not worth the undesirable aspects of increased times. In the analysis of a number of samples it is advantageous to keep the counting and irradiation times short, thus requiring a shorter total analysis time, or allowing a larger number of samples to be analyzed in a given experimental time period. Another disadvantage of a long irradiation time is the problem of increasing the total activity of the sample, which could pose a hazard to the experimenters who are exposed to the sample's radiation, or cause problems in handling the radioactive sample.

The final choice of count and irradiation times takes all these factors into account, but it must still be somewhat subjective. A set of samples to be analyzed will probably produce a range of count rates, and any one curve in Figure 4-12 would not be adequate to describe them all. The count and irradiation times need to be kept as low as possible, but the curves in Figure 4-12 have steep slopes below about 50 seconds, so the choice would need to be at least 50

seconds. On the other hand, above about 75 seconds the slopes are getting fairly flat, which means that the choice should not be as high as 75 seconds. The choice of 60 seconds has been made for the system being described, and this seems to be a reasonable balance of the various factors.

V. UNCERTAINTIES

Among the many factors which can affect the uncertainty in a DFN analysis, the count rate due to background is one of the easiest to measure, but certainly not the easiest to explain. The count rate due to background in the OSU DFN counting assembly is usually about 20 to 25 counts per minute, with no sample in the counting position. At power levels up to 100 kW, the background count rate appears to be independent of the reactor's operating power level, which would indicate that the neutrons escaping from the reactor do not produce more than a negligible count rate in the assembly. When the reactor is operating at its full power level of one megawatt, the background count rate does increase by a small amount, from 20.98 ± 0.14 counts per minute at zero power to 31.14 ± 0.51 cpm at 1 MW, in a measurement made in March, 1978.

One source of background counts could be radioactive contamination in the detector assembly. Any contamination outside the detector tube itself probably can be ignored, since any emitted alpha or beta particles would not penetrate through the moderator and detector wall, nearly all gammas are discriminated against, and it is highly unlikely that a neutron-emitting contaminant would be present. Information provided by the Reuter-Stokes Company, manufacturers of the BF_3 detectors, indicates that alpha-emitting contaminants in the

detector walls could provide a small background count rate, since pulses due to alphas are indistinguishable from pulses due to neutrons. The company states that the usual count rate is about two counts per minute in an aluminum-walled detector, and about one-tenth of that in a stainless-steel-walled detector of the size used in the OSU DFN assembly. This would account for about 2.4 cpm in the 12 detectors, which is about 10% of the background count rate.

One of the most important components of the background is probably due to cosmic radiation. Most of the primary particles in cosmic radiation are protons and nuclei of elements with atomic numbers up to $Z=26$, which have extremely high energies, usually around 10 GeV (although some may have energies as high as 10^{10} GeV). Most of these particles do not reach the ground, but interact with atoms high in the atmosphere to produce high energy particles such as muons, electrons, and photons. These secondary particles are very penetrating due to their high energy, and it seems probable that some could penetrate into the BF_3 detectors to create counts--perhaps above the SCA discriminator. In a study described by Hopper (58), however, it was determined that cosmic ray counts produced in a BF_3 detector were due to neutrons, another component of cosmic radiation. This study measured cosmic radiation at sea level with two different sets of detectors in a paraffin-moderated assembly. One set had detectors filled with BF_3 enriched to 96% ^{10}B , the other had 10% ^{10}B ,

and the counts recorded in the two sets of detectors were in proportion to the ^{10}B enrichment. Counts due to ionizing radiation can only affect the orbital electrons in the fill gas in the detectors, and thus should not vary with the ^{10}B enrichment. These detectors must have been counting neutrons, which interact only with the ^{10}B . A study done by Balestrini (54) also confirmed background counts due to cosmic rays. In this case, the external shielding for the DFN counting assembly was a deep pool of water. An experiment which varied the background count rate by varying the depth of the counting assembly's position beneath the water's surface showed that neutrons from the nearby reactor had no effect on the background at depths below about 20 cm, but the count rate continued to decrease as a function of depth, down to a depth of three meters. This decrease could be explained by highly penetrating radiation, such as cosmic radiation. The DFN counting assembly used at OSU has sufficient shielding around the moderator to keep the background counts due to external neutrons at an acceptably low level.

The discussion in Chapter IV indicated the important role of the system's background count rate in determining the counting uncertainty. The counting statistics uncertainty for a sample is a very important characteristic which needs to be further explored. Delayed neutron emission depends on the decay of precursor nuclides, and this radioactive decay follows the probabilistic laws of random events.

If the number of radioactive decays during a certain time interval were counted, and then a number of similar counts were made, one would find that the results for these trials would not all be identical. This lack of exact reproducibility would be expected to occur even if there were no error on the part of the experimenter or his equipment; it would be inherent in the random nature of radioactive decay. If an infinite number of identical counts could be made, one would find that the results would fit a normal distribution, and the mean value of this distribution would be the best definition of a "true mean count rate" for this radioactive sample. The width of a normal distribution can be described in terms of σ , the standard deviation. If a number of trials fits a normal distribution, then 68.3% of all these trials will have values which lie within 1σ of the mean, and 95.5% of the values will lie within 2σ of the mean. In an actual experiment, however, the experimenter may make only one measurement, and the set of expected results for this measurement will form a Poisson distribution. A characteristic feature of the Poisson distribution is that its variance, σ^2 (the square of the standard deviation), is equal to its mean. The probability of a certain value being observed in a Poisson-distributed set of expected results will approach that of a normal distribution as the value increases.

Thus if an experimenter makes a single measurement of an activity, this measured value will be his best estimate of the mean

value of the distribution. The square root of his measurement will be the best estimate of the standard deviation of the expected measured results. This would be reported as $x \pm \sqrt{x}$, where x is the measured value. The meaning of this is that there is a 68.3% probability that the difference between the measured value and the mean value for an infinite set of identical measurements will be less than σ , where $\sigma = \sqrt{x}$.

The standard deviation expressed as the square root of a count is the absolute counting statistics uncertainty, and the relative uncertainty is $\frac{\sqrt{x}}{x} = x^{-1/2}$. Both expressions are useful in determining how well a single measurement estimates the best possible value (the mean of an infinite set of measurements). Note that although σ increases as x increases, the ratio of σ to x (the relative uncertainty) decreases. An experimenter would thus use a long counting period to get a good estimate of a sample's activity, since the total number of counts would be large and the relative uncertainty would be small. As an example, a sample with a constant activity which yields one count per second may give 100 counts in a 100 second counting period; the standard deviation would be 10, and the relative uncertainty would be 0.10. A 10,000 second count, on the other hand, may give 10,000 counts, with a standard deviation of 100, and relative uncertainty of 0.01. For the short count the experimenter would report the count rate as 1.0 ± 0.1 c/s, but he could report 1.00 ± 0.01 c/s for the

longer count.

In delayed neutron counting, the counting statistics uncertainty often cannot be significantly decreased by longer counting periods, since the activity is rapidly decreasing. The uncertainty can still be kept to a minimum, however, by ensuring that a sufficiently large number of counts occur during the counting interval. This can be done by making the sample mass large, or by increasing the reactor power level (and thus the neutron flux). With a large number of counts, the background count makes a small contribution to the uncertainty, as shown in Chapter IV.

The experimenter has an opportunity to introduce an uncertainty into a DFN analysis during the preparation of the samples and standards. The goal of a DFN analysis of a sample is to determine the concentration of uranium in the sample, usually in terms of parts per million (ppm--equivalent to the number of micrograms of uranium in a gram of sample). This is found by comparing the results of a DFN count for the sample with the number of counts due to one or several standards, which contain known amounts of uranium. This comparison will give the mass of uranium in the sample, which can be converted to the concentration by dividing by the sample mass. Thus it is important that the sample mass be accurately determined before the irradiation. Most samples analyzed on the OSU DFN system have been prepared using a Mettler balance capable of giving

a mass measurement which is accurate to within ± 0.001 grams. Most of the samples analyzed have a mass of about one gram, so the weighing error would be about 0.1%. Other sample preparation errors could come from the possibility of analyzing a slightly different amount of sample than had been weighed. This could happen, for instance, if a small amount of sample were spilled out of the polyvial before heat sealing, or if some more of the sample would contaminate the outside of the polyvial after weighing. Under careful preparation procedures, it is unlikely that the analyzed mass could differ from the assumed mass by more than 0.001 grams, and the uncertainty involved in the sample preparation of a one-gram sample would be less than 0.14%.

Since a one-gram sample is usually only a small part of the material which is being analyzed, the experimenter must be very careful to ensure that he is analyzing a sample which is representative of the entire material. This may involve carefully homogenizing the material before selecting a sample, or perhaps taking several samples, each from a different part of the material, and reporting several results.

The accuracy of a DFN analysis depends on the quality of the standards being used to convert counts to uranium mass. Care must be taken to make sure that the standard contains as nearly as possible the assumed amount of uranium. This involves the same types of

uncertainty and error that occur in the sample preparation. For solid standards, powdered samples of uranium ore prepared by the USDOE New Brunswick Laboratory (NBL) were diluted to the proper concentrations. The dilutant was a powdered rock called serpentine, a mineral which naturally contains very low concentrations of uranium. (The amount of uranium contained in a one-gram sample of serpentine is low enough to give the same count as that obtained with no sample in the counting assembly, so the serpentine is used for a background measurement in each analysis.) The NBL ores used were:

<u>Code Number</u>	<u>Material</u>	<u>%U₃O₈</u>	<u>%U</u>	<u>%Th</u>
3B	Pitchblende	3.90±.01	3.31±.01	0
7A	Monazite Sand	0.35±.016	0.30±.01	8.5±.05

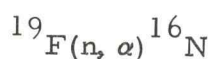
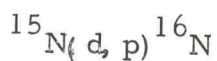
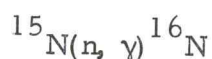
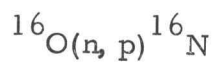
Most of the standards used were made from the 3B material, and the most commonly used standards had uranium concentrations as low as 1 ppm. Since the final concentration was a factor of 10^4 lower than the original concentration, several dilutions were necessary to obtain the final standard. For the lowest level standard, one gram of 3B was mixed with 31 grams of serpentine to form 3B/1000, one gram of 3B/1000 was mixed with nine grams of serpentine to form 3B/100, one gram of 3B/100 was added to nine grams of serpentine to form 3B/10, and one gram of 3B/10 was added to nine grams of serpentine to form 3B/1. Thus for 3B/1, the lowest concentration standard, the weighing process was performed eight times (twice per dilution), and the

total uncertainty for these weighings would be: $\sqrt{8 \times (.0014)^2} = .0040$, or .40%. In addition to weighing errors, these dilutions also presented the possibility of mixing errors. When one gram of 3B is added to 31 grams of powdered serpentine, the experimenter assumes that the concentration of any sample of the mixture is exactly 1/32 of the concentration of uranium in 3B. If the two materials were not mixed thoroughly, however, the selected sample could have come from a part of the mixture which had a concentration either much higher than, or much lower than, that which is assumed. It is very difficult to assign an uncertainty value which could be introduced by mixing, but it seems reasonable to assume that, using careful preparation procedures, this uncertainty is smaller than the other standard preparation uncertainties. Such an assumption appears reasonable, since the counts-vs.-concentration relationship is a good linear one (this will be discussed in Chapter VII). The confidence in the uranium concentration of the standards, then, can be expressed by an uncertainty of 0.47%, which takes into account the standard preparation errors and the uncertainty assigned by the New Brunswick Laboratory to the material from which the standards are made.

A DFN analysis can be subject to uncertainty due to interferences in the DFN counting system. These interferences are due to reactions which cause counts which are not due to delayed neutrons

from uranium in the sample. Other interferences could suppress valid counts. Interferences which could cause unwanted counts are electronic noise, gamma radiation, neutrons which are not delayed neutrons emitted by the sample, and the various components of background counts.

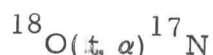
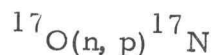
Interferences from electronic noise and nearly all gamma radiation is very effectively eliminated by the SCA discriminator settings, as discussed in Chapter IV, and since the background count rate is small and very nearly constant, compensation for it can be made very easily. There are, however, higher energy gammas which could cause some interfering counts, either directly by reactions in the detectors, or by (γ, n) reactions outside the detectors which result in neutrons that could cause counts. It was mentioned earlier that the SCA settings were determined with the help of a ^{24}Na source, which emits a 2754-keV gamma. There are very few nuclides which emit gammas with energies higher than this, but ^{16}N is a commonly produced nuclide which does. ^{16}N has a half life of 7.11 seconds and emits gammas with energies of 6.13 and 7.12 MeV. ^{16}N can be formed by any of the following reactions:



Whenever fluorine is present in a sample, much ^{16}N will be produced by (n, α) reactions, but F is not common in geological samples. The (d, p) reaction with ^{15}N would be important only when there is a large source of deuterons, and the (n, γ) reaction with ^{15}N is usually unimportant because of the low isotopic abundance of ^{15}N (0.36%), and its small cross section (0.04 mb). The (n, p) reaction with ^{16}O requires fast neutrons, but there is usually a large abundance of fast neutrons and oxygen in many DFN analyses. An experiment demonstrated that the polyethylene rabbit capsule is responsible for a high level of ^{16}N activity. After irradiation at one MW for one minute, the rabbit capsule was counted on a NaI detector and multichannel analyzer in the pulse height analysis mode. There were two distinct peaks, one in the 6 MeV region, and one in the 7 MeV region. It was difficult to assign a more precise energy to these peaks because they were very broad, due to the poor resolution of a NaI detector at high energies, but it was necessary to use the NaI rather than a Ge(Li) detector because of the poor efficiency of the Ge(Li) at high energies. A second rabbit was irradiated at one megawatt for one minute and again counted, this time in the multichannel scaling mode. The results of a 40 second count were analyzed by a computer program which determined the half life to be 7.14 seconds--very good confirmation of the presence of ^{16}N . Thus ^{16}N may be a source of counts in the BF_3 detectors when it is present, since the 6- and

7-MeV gammas may produce pulses high enough to be above the SCA setting.

Another nitrogen nuclide, ^{17}N , could also be responsible for unwanted counts. ^{17}N has a 4.16-second half life, and decays by either beta emission or neutron emission. Any neutrons emitted would be indistinguishable from a delayed fission neutron by the time they are moderated and reach the detector. ^{17}N could be formed by any of the following reactions:



The latter two reactions could occur in the presence of lithium, which undergoes a $^6\text{Li}(n, \alpha)t$ reaction, and the emitted tritons could initiate the ^{17}N -producing reactions. If lithium is not abundant in a sample, only the first reaction occurs. Another neutron-emitting nuclide, ^9Li , could also produce counts, but ^9Li must be formed by a $^9\text{Be}(n, p)^9\text{Li}$ reaction, and beryllium may not be common in samples. (If beryllium were present in a sample, either (γ, n) or (α, n) reactions with ^9Be would be more likely to cause unwanted counts than ^9Li .) ^9Li has a 0.17-second half life, which would be unlikely to affect most analyses.

In common analyses, ^{16}N , ^{17}N and ^9Li interferences are minimized by the twenty-second decay period between the end of

irradiation and the beginning of counting. Actually, 20 seconds is about three half lives of ^{16}N , and a large amount of ^{16}N could produce a significant number of counts after that. The polyethylene rabbit capsule contains a large quantity of oxygen, since it has a mass of about 17.5 grams, and the plastic is about 17% oxygen. A calculation, shown in detail in Appendix B, determines the activity at the end of irradiation to be 1.56×10^8 d/s, and during the counting interval (20 to 80 seconds after irradiation) 1.68×10^8 high energy gammas will be emitted by the rabbit capsule. These values seem high, since this rate of gamma emission would result in a higher dose rate than that normally measured, but the calculation does indicate the large number of high energy gammas emitted by ^{16}N . Thus the rabbit capsule could contribute a significant number of background counts even after 20 seconds of decay, which would raise the counting statistics uncertainty of a low-uranium-concentration analysis. If the sample is removed from the rabbit capsule before counting, the amount of ^{16}N and ^{17}N in the sample and polyvial is not enough to cause a large number of counts.

High energy gammas may also present a problem in the form of (γ , n) reactions. There are two nuclides which could emit neutrons when irradiated by gammas: ^9Be and ^2H . Both have threshold energies for the (γ , n) reactions: the gamma energy must be greater than 2.23 MeV for deuterium, and greater than 1.67 MeV for ^9Be . If either nuclide were present to a large extent in the moderator, a high flux of gammas with energies above the threshold could introduce

enough neutrons into the moderator to raise the number of counts in the detectors. It is unlikely that paraffin would contain much ^9Be , but there should be some ^2H present, since paraffin contains much hydrogen, and the natural isotopic abundance of deuterium in hydrogen is 0.015%. The effect of neutron-emitting nuclides in the moderator was investigated when the ^{24}Na source was counted. The 2754-keV gammas from ^{24}Na have energies higher than both thresholds, and a high intensity ^{24}Na source should produce a large number of neutrons if this type of interference is important. In Chapter IV, it was stated that this test resulted in no significant increase in the background count rate, and neutron-emitting nuclides in the moderator should not be a significant problem. A sample containing a large amount of deuterium or beryllium, however, could emit a significant number of interfering neutrons, and the experimenter must be aware of this potential problem.

The experimenter must also be aware of the possibility of unwanted counts from contaminants which are fissionable and emit delayed neutrons into the counting assembly. A laboratory used for DFN sample preparation may also be used for preparation of high-uranium concentration samples, and careful laboratory procedures should be followed to ensure that a sample is not accidentally contaminated with even trace amounts of high concentration uranium. The polyvials used are labelled "Lab Grade" and are high purity polyethylene; many analyses of empty polyvials have shown that they

do not contain enough contaminants to cause a count rate above the background. Similarly, careful procedures and much experience have given cause to believe that the rabbit capsules have never been a source of contamination by becoming contaminated and transferring the contamination to the outside of a sample's polyvial to produce unwanted counts.

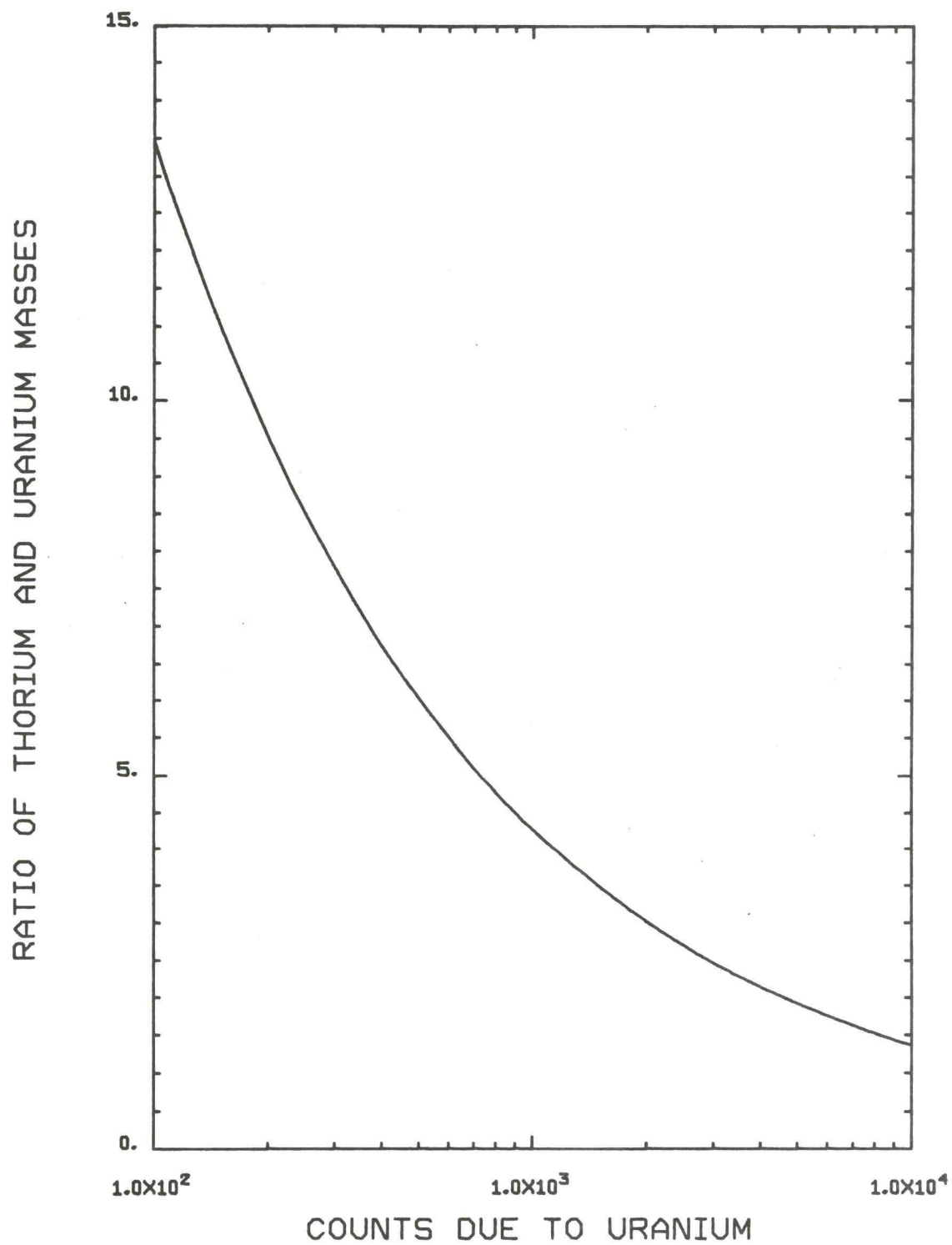
A type of contaminant could be present in the sample itself, if fissionable nuclides other than uranium were present in the sample, and the counts produced by these nuclides were assumed to be due to uranium. The only naturally occurring element which could cause this contamination is thorium: ^{232}Th can undergo fission due to fast neutrons. Since thorium will only undergo fast fission, and its fast fission cross section is quite low (about 0.1b from the fission threshold energy of about 1.4 MeV to 5 MeV), thorium would have to be in a concentration greater than uranium to affect the analysis.

An important concern which the experimenter needs to deal with is the amount of thorium a sample could contain which could significantly affect the uranium determination if no correction were made for it. The severity of the interference will, of course, depend on the amount of thorium in the sample, but it is useful to somewhat arbitrarily choose a critical level, L_C . For a given number of counts due to uranium, C_U , L_C will be the number of counts above C_U which must be observed so that C_T , the total number of counts,

can be considered to be significantly larger than C_U . The critical level is defined as the product of a one-sided confidence factor (for a normal distribution) and the standard deviation of the net count above C_U , i. e., $L_C = k\sigma_o$. (The variable k is defined so that $k = 1$ for an 84.2% confidence interval, $k = 2$ for a 95% confidence interval, $k = 3$ for 99%, etc.) Since $C_{net} = C_T - C_U$, $\sigma_o = \sqrt{\sigma_T^2 + \sigma_U^2}$. Since C_{net} is nearly zero, $C_T \doteq C_U$ and $\sigma_t \doteq \sigma_u$, so $\sigma_o = \sqrt{2}\sigma_u$ and $L_C = \sqrt{2}k\sigma_u$. For an 84.2% one sided confidence interval, $k = 1$, and $L_C = \sqrt{2}\sigma_u$. Thus an amount of thorium in a sample which will produce a number of counts less than L_C can be considered insignificant, since one can be 84.2% confident that the total number of counts will not be significantly greater than the number of counts due to uranium alone.

The effect of thorium contamination can be seen by calculating the ratio of the limiting thorium mass to the uranium mass which will produce a given number of counts. The limiting thorium mass is the mass of thorium which will produce L_C counts for the given C_U , and it can be considered to be the smallest mass of thorium which would cause a significant interference in a uranium determination. As C_U increases, L_C can be expected to increase, since σ_U will also increase, but L_C increases more slowly than C_U since it is proportional to $\sqrt{C_U}$. Thus as the uranium mass in a sample increases, the relative mass of thorium which causes an interference decreases. This effect is illustrated in Figure 5-1, a plot of

Figure 5-1

THORIUM-TO-URANIUM MASS RATIO
TO CAUSE INTERFERENCE

the Th/U mass ratio as a function of the number of counts. The ratio was found by the following formula: $\frac{L_C}{C_U} \times 95.16$, where 95.16 is the ratio of the uranium and thorium sensitivities. The ratio decreases from about 14.4 at $C_U = 100$ to 1.36 at $C_U = 10000$. At $C_U = 1000$, a typical number of counts, the concentration of thorium in a sample can be about 4.34 times the uranium concentration before it significantly affects the number of counts. As the number of counts increases above this, the relative uncertainty in the uranium count decreases and the determination becomes more sensitive to thorium concentrations at this ratio.

Thus the experimenter must be aware of the possibility of thorium contamination in his sample. If he has reason to suspect the presence of thorium in the sample, a correction can be made for the contamination by a cadmium-covered analysis. This type of analysis will be discussed in detail in Chapter VI. A more serious source of contamination could be presented by the presence of fissionable isotopes which are not naturally occurring. These are transuranic fissionable elements, some of which are also fissile (such as ^{239}Pu), and it would be very difficult to make a correction for more than one unknown fissionable contaminant.

Another type of interference could occur if a large amount of neutron absorbing material were in the sample. This could cause an unwanted decrease in counts due to absorption during irradiation

and during counting. In the irradiation, a sample which strongly absorbs neutrons could cause a decrease in counts by "self shadowing": decreasing the neutron flux at various points in the sample region and preventing fission from occurring at the expected rate. During the counting period, a highly absorptive sample could capture delayed neutrons, preventing them from resulting in counts. An obvious solution to the problem of absorptive interference is to make the sample and standard identical in their physical dimensions, densities and compositions. In this manner one can be certain that each point in a sample will be exposed to the same flux as the corresponding point in the standard, and a uranium atom will have the same probability of fissioning whether it is in any given position in the sample, or in the corresponding position in the standard. During the counting period a neutron emitted from a certain position in the sample will have the same probability of escaping absorption and resulting in a count as a neutron emitted from the corresponding position in the standard. Thus a sample and standard which are nearly identical physically will obey the same relationship between counts and mass of uranium present.

In actual practice it is not always possible to use standards which are physically identical to the samples, especially when analyzing a variety of types of samples. This problem can be alleviated by making the sample small, so that neutrons striking

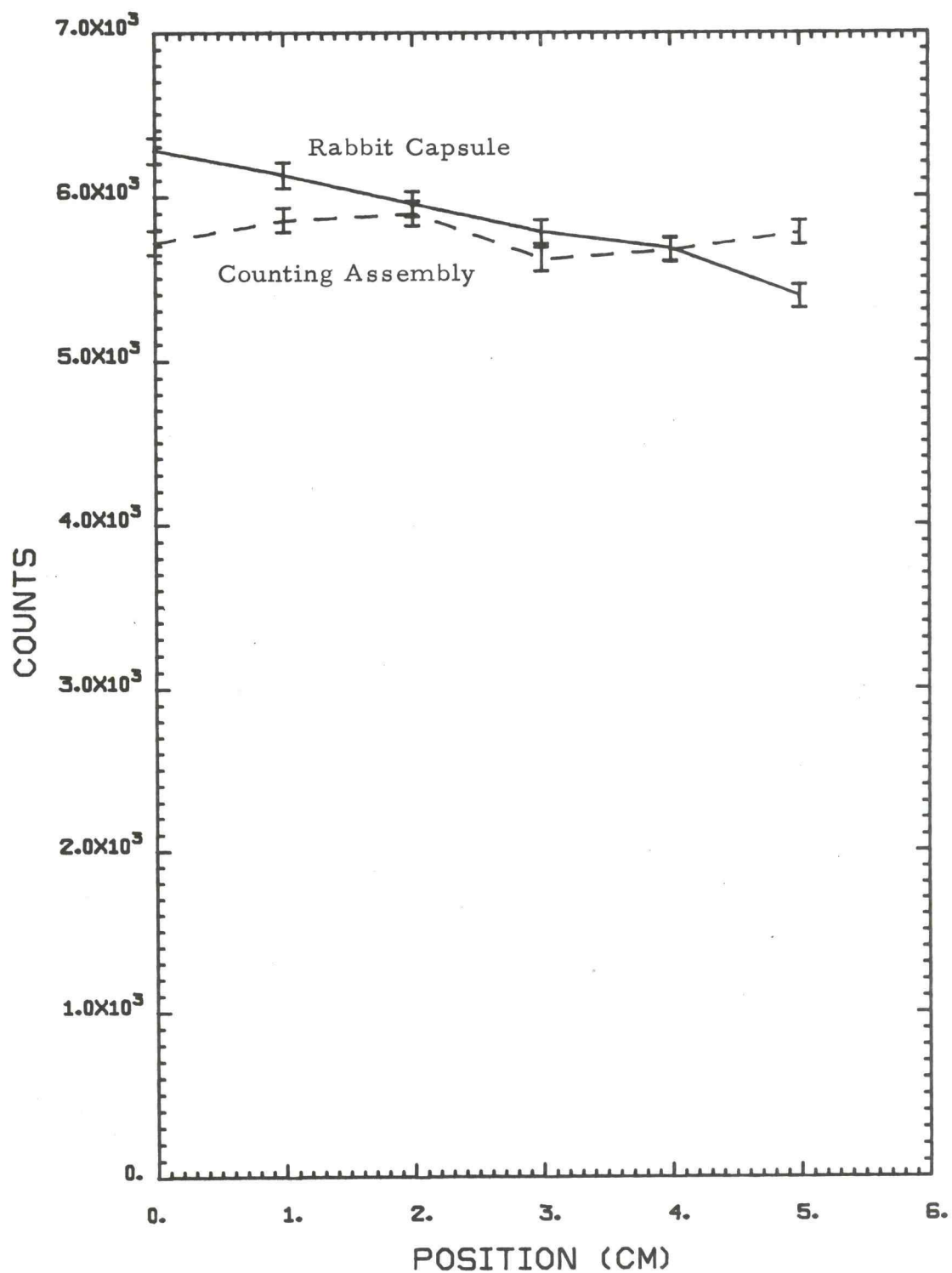
the central regions of the sample will not have penetrated through much material, and will have had a low probability of being absorbed. In a test of this effect, two samples were analyzed at 10 kW. One sample, with a mass of 1.105 g, was made from uranium ore diluted with serpentine, was sealed in a 2/5-dram polyvial, and contained 286.1 μg of uranium. The other sample, also of uranium ore and serpentine, was in a 2/27-dram polyvial, contained 284.9 μgU , and had a sample mass of 0.1899 g. The large sample resulted in 5799 counts, or 20.27 c/ μgU , while the small sample resulted in 5872 counts, or 20.61 c/ μgU . Since the smaller sample would have smaller absorption effects, the count rate should be larger for it than for the large sample, and here it was larger by 1.6%. Before drawing a conclusion it should be noted that the counting statistics uncertainty for each count was 1.3%, only slightly less than the difference between counts. An important conclusion which can be drawn from this experiment, however, is that a typical sample, packaged in a 2/5-dram vial, is small enough so that self shadowing is a minor effect. However, self shadowing could be a major effect if the sample contained a strong neutron absorber, such as boron or hafnium.

An important consideration for minimizing uncertainties in DFN analysis is positioning of the sample, both in the irradiation position and in the counting position. The variation of neutron flux

with position in the OSTR rabbit irradiation position was shown in Figure 4-2 where the flux was measured by gold foil activation. A variation of flux with position should produce a corresponding variation in the fission rate for a uranium sample and hence a variation in counts. An experiment was performed in which the irradiation position was varied by placing polyethylene spacers in the bottom of the rabbit capsule; the results are illustrated by the solid line in Figure 5-2. The position (in cm) is measured from the bottom of the rabbit capsule to the bottom of the outside polyvial. The line appears to have a nearly constant slope, decreasing with increasing position. The variation of counts with position is about 2.7%, very close to the 2.9% variation of flux with position which was previously determined.

Positioning of the sample in the counting assembly could also present some uncertainty if not kept constant. The sample tube in the counting assembly is centered parallel to the 12 detectors. The counting efficiency of the detector assembly is dependent on the total solid angle subtended by the detectors with respect to sample position. As the sample position moves up and down the sample tube, the solid angle changes, and the counting efficiency also changes. Thus a constant sample counting position must be maintained in order to maintain a constant sensitivity. The variation of counts with counting position is illustrated by the dashed line in Figure 5-2, which was

Figure 5-2

VARIATION OF POSITION IN RABBIT CAPSULE
AND IN COUNTING ASSEMBLY

obtained by varying the counting position by inserting spacers into the sample tube. A variation of position in the counting assembly did not produce an obvious trend in the variation of the counts, as was observed with the irradiation position variation. A horizontal line cannot be drawn through all the error bars, however, which would indicate that there could well be some variation in the number of counts if the counting position is varied. Thus the counting position, while not as critical as the irradiation position, should remain fixed for consistent results.

The uncertainty in a DFN analysis will be dependent upon the quality of the experimental equipment and the skill with which it is used. Modern electronic components for nuclear counting applications are quite stable, and components such as the high voltage supply, preamplifier, amplifier, SCA and scalar can be expected to introduce no more than insignificant uncertainties. The timers which control the irradiation, decay, and counting times can be very important, however. To see how errors in the timing can affect the count, a calculation can be made to find the percent difference between the counts due to a normal 60s-20s-60s cycle and a measurement with one of the times increased by an assumed error of 0.5 seconds. Using equation 4-1, an increase of 0.5 seconds in the irradiation time would cause a 0.32% increase in counts (assuming that the count rate is sufficiently high to neglect the background

counts). The same 0.32% increase in counts would be due to a 0.5 second increase in the counting time. An increase in the decay time of 0.5 seconds would cause a 1.59% decrease in the number of counts, however. Since such a variation in the cycle times from one analysis to the next could cause a variation in counts, it was considered important to minimize the variation by precisely controlling the decay and counting times with accurate electronic timers. When set to control a twenty-second decay time and a sixty-second count time, the uncertainties introduced by timing errors are negligible. The irradiation time is not as easy to precisely control, due to the automatic timing equipment used in the OSTR rabbit system. The automatic timer is also capable of giving a set of timing intervals which are nearly identical and introduce negligible uncertainty into a DFN analysis. Unfortunately the time interval controlled by the rabbit system automatic timer must be hand set on a dial and includes the transit time for the capsule's travel from the terminal to the reactor. Thus the consistency of the irradiation times for a set of samples depends on the consistency in the capsule transit times and on the consistency of the dial settings. These times should be nearly identical for identical samples, since the system pressure which propels the capsules is nearly constant. If the samples being analyzed have quite different weights, however, they require slightly different transit times, and a potential exists for added uncertainty due to

variations in irradiation times. In actual experience with the OSU DFN system, there have seldom been instances in which the transit time has varied by as much as a half second, which would mean that this uncertainty is seldom greater than 0.32%.

An important test for an analytical system is its reproducibility: how accurately it can reproduce the results of a given analysis. Since a DFN analysis is nondestructive, a sample can be analyzed repeatedly and the same results can be expected each time. The reproducibility of the DFN system was tested in three different ways: repeatedly analyzing a single sample at a constant neutron flux level, analyzing a single sample at several different flux levels, and repeatedly analyzing a single set of samples at the same flux level, but on different days.

In the first experiment, a sample with mass 0.158 g was made from serpentine and 237 micrograms of natural uranium. This sample was analyzed ten times at a reactor power level of 10 kW. At least five minutes after the start of any one cycle elapsed before the start of the next cycle, which ensured that the delayed neutron activity from any irradiation had approached zero before the next cycle's counting period began. The ten analyses yielded the following counts:

4912

4886

4917

4875

4970

5086

4992

4996

4869

5110

The mean value of the counts was 4961, with a standard deviation of 85.6, which is 1.73% of the mean. A count of 4961 has an associated counting statistics uncertainty of 1.42% (one standard deviation).

Thus we can conclude that, aside from the counting statistics uncertainty, any contributions to the variation in counts are minimal, amounting to an uncertainty of less than 1%.

The reproducibility of a sample analysis at different flux levels is important because it is often desirable to vary the neutron flux in the reactor during a series of analyses. To do so an experimenter must be confident that changing the flux by a certain multiplicative factor will change the counts per microgram uranium by the same factor, as predicted in equation 4-1. To test the relationship between counts and neutron flux, a 0.200 g sample containing 30.0 micrograms of uranium was irradiated at five different power levels. The results are summarized in Table 5-1, and shown graphically in

Figure 5-3. The graph in Figure 5-3 shows that the measured counts at the various power levels lie very near a straight line which has a slope of 0.992, as determined by a linear least squares fit to the data. This shows that the relationship between counts and reactor power level can be assumed to be linear. This conclusion can be supported by applying a power law fit to the data from this experiment, which results in the following relation:

$$C = 61.48P^{.9882}, \quad r^2 = 0.99992. \quad (5-1)$$

The exponent of P in this equation is 0.9882, which again shows a good approximation to a linear relation between counts and reactor power level. The coefficient of determination, r^2 , gives a measurement of the validity of the fit to the data: r^2 can vary between zero and one, with one being the value for a perfect fit to the data.

Table 5-1 further explores the power level-counts relationship by calculating the count to be expected at a given power level, using Equation 5-1, and finding the percent difference between the calculated and the observed counts. This difference can be compared to the counting statistics uncertainty for each count, and it appears that the uncertainty due to counting statistics can account for most of the observed variation.

Figure 5-3
COUNTS VS REACTOR POWER LEVEL
FOR A SINGLE SAMPLE

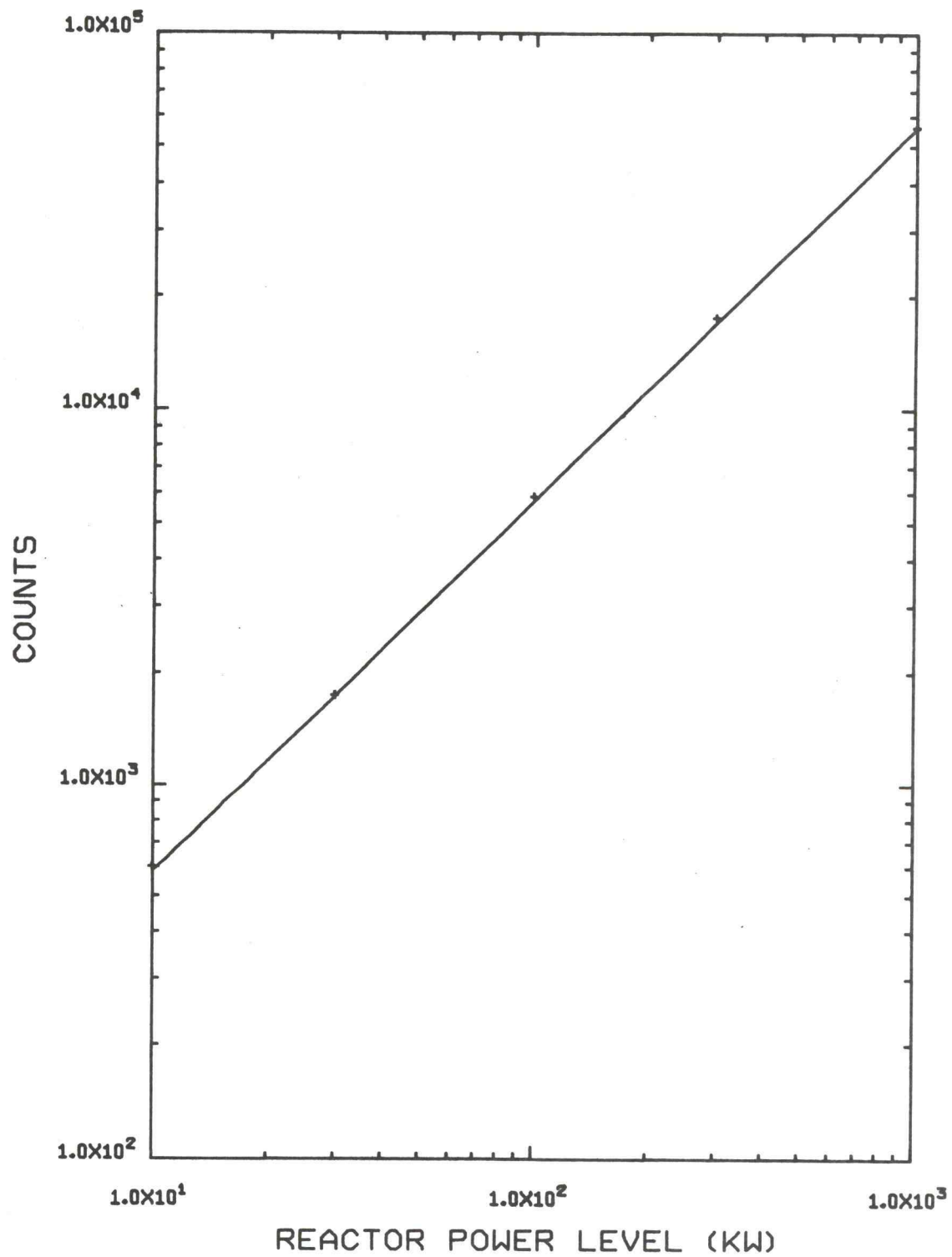


Table 5-1. Variation of counts with reactor power level.

Power Level (kW)	Recorded Counts C	Calculated Counts* C _{cal}	% Difference**	% Counting Statistics Uncertainty
10	600	598	0.28	4.1
30	1749	1772	1.31	2.4
100	5856	5823	0.56	1.3
300	17533	17246	1.64	0.76
1000	56011	56672	1.19	0.42

*From equation 5-1

**From $\frac{|C_{cal} - C|}{C} \times 100\%$

In the third reproducibility experiment the results of identical experiments on six different days were analyzed. There are several effects, which will be discussed shortly, which could cause results to vary from day to day, but would not affect the results of one analytical session. Most DFN analyses at OSU have been done on samples containing between one and five micrograms of uranium. These are irradiated at a reactor power level of 100 kW, and these are always analyzed by comparing them to the counts due to a set of standards made from NBL-3B. Table 5-2 tabulates the results of six sets of counts for the five standards. In each day's analysis, a calibration curve is determined by performing a linear least-squares fit to the data from the standards. Thus the curve relates the counts

Table 5-2. Uranium standards results.

Date	Counts due to Sample #NBL 3 B /					Total Counts	Slope of Calibration Curve (C/ μ gU)
	0	1	2	5	10		
8/26/77	27	268	633	1364	2795	5087	185.7
9/2/77	26	237	538	1370	2860	5031	192.5
9/8/77	26	233	549	1229	2795	4832	182.5
9/16/77	28	248	625	1303	2833	5037	188.2
10/19/77	20	276	578	1363	2845	5082	190.0
10/21/77	26	259	637	1382	2894	<u>5198</u>	<u>192.7</u>
					Mean:	5045 \pm 120	188.6 \pm 4.0

due to each standard with its uranium mass. The calibration curve is always linear, with a slope that can be identified as the system sensitivity, in counts per microgram of uranium. This relation can then be used to find the unknown uranium mass present in any sample that is analyzed by substituting the recorded counts into the calibration equation and solving for the mass. Table 5-2 shows the variation in calibration curve slopes: the six values have a mean value of 188.6 counts per microgram uranium, with a standard deviation of 2.1%. The contribution of the counting statistics uncertainty to this variation can be determined by finding the mean of the total counts for each set, 5045 counts, and noting that the counting statistics uncertainty due to these counts must be about 1.4%. This means that other sources of uncertainty must account for 1.6%, which is somewhat larger than the uncertainty identified for a single day's reproducibility experiment. Thus we conclude that there is a small day-to-day variation in the sensitivity, and for this reason a set of standards is counted with each day's set of sample analyses.

The major factors affecting DFN analysis on a day-to-day basis are concerned with the operating conditions of the reactor. The background count rate would also vary, but it is so much smaller than the number of counts observed in the experiment that it would be negligible. The most important feature of the reactor

operating condition, with respect to the DFN sensitivity, is the spatial flux distribution in the reactor core. The reactor operator judges the power level by reading the linear recorder, which records the signal from a compensated ion chamber positioned just outside the reactor core (located at the position marked "LIN" in Figure 4-1). When the linear recorder is calibrated, the heat generated by the core is measured at each of several different power levels, and the corresponding linear recorder reading is noted. Therefore when the operator adjusts the controls to set the reactor at a certain power level, he is basing the power level setting on a neutron flux measurement at the compensated ion chamber. If the spatial distribution of the neutron flux in the reactor core were always the same, then a given power level setting would always provide the same neutron flux to the rabbit position. If, however, the spatial flux distribution would vary, the flux at the rabbit position might not be identical for two identical power level settings.

One possible cause for a variation in the flux distribution could be shadowing of the compensated ion chamber by a neutron absorber in the lazy susan. The lazy susan is a rotating rack which can be loaded with samples for long term irradiations. It is located between the reactor core and the ion chamber and rotates around the core at one revolution per minute. If the rack were loaded with a number of samples which were strong neutron absorbers, the ion chamber

would be exposed to a lower flux than it would be if the rack were empty, and the operator would see a lower linear recorder reading than normal. He would then increase the power level, and positions inside the rabbit terminus would be exposed to a higher neutron flux than normal for that power level. Thus the DFN sensitivity would be varied.

Probably a more common cause for a variation in the flux profile would be a variation in the control rod positioning. The net reactivity of the reactor core decreases during the lifetime of the core due to a depletion of the fissile atoms and a buildup of fission product poisons. As the core loses total reactivity, the control rods need to be withdrawn further to give a critical configuration. This change in control rod positioning, and in fissile and absorptive material distribution, could cause an altered flux distribution. These changes occur over a long time span, however, and are probably not important. A more drastic need for a change in control rod positioning could be caused by a buildup of ^{135}Xe in the core. After a long reactor operation at high power, enough xenon could be present in the core to affect the reactivity of the core, requiring the control rods to be withdrawn further than normal. Thus the flux profile could again be altered.

Variations in the core's fission product inventory could affect the linear recorder reading by exposing the ion chamber to differing

gamma fluxes. The ion chamber is sensitive to gammas, but the gamma contribution to the ion chamber reading is normally nullified by proper adjustment of the compensating voltage. At higher neutron fluxes, the gamma contribution becomes less important with respect to the neutron contribution to the signal. However, if the compensating voltage were not accurately adjusted, the gamma contribution could have an effect on the signal to the linear recorder. In such a case, differing quantities of fission products in the core, due to variations in the recent operating history of the reactor, could cause varying gamma fluxes at the compensated ion chamber, and thus a distorted linear recorder trace. The effect could be a change in neutron flux at the rabbit position for a given reactor power level setting, and thus a change in the DFN sensitivity.

The gamma effect on DFN sensitivity is probably a minor effect, and there may be other minor effects, such as operator judgment in reading the linear recorder. The linear recorder trace does move slightly about an equilibrium position, and this oscillation increases in magnitude with increasing power level. Different reactor operators could make differing assumptions as to where the equilibrium position is located, and they make slightly different settings for a given power level. This should be a small effect, however, and should not make much difference in the DFN sensitivity.

VI. APPLICATIONS

As stated in Chapter I, the primary purpose for developing OSU's DFN system was the routine analysis of adsorber materials used in the extraction of uranium from seawater. Samples of each adsorber are analyzed before being exposed to seawater and then again after several different periods of exposure, ranging from one day to several weeks. The adsorber materials of interest usually have a uranium concentration varying from one to twenty parts per million, and the analyses are usually performed with a 60 second irradiation, 20 second decay, 60 second counting time cycle at 100 kW. The sample masses are typically one gram, and the delayed neutron counts therefore vary from about 200 to about 4000 counts. The counting statistic uncertainties vary from about 8% to under 2%, which is adequate for these samples. An 8% uncertainty seems high, but the samples with lower uranium concentrations are usually less interesting as adsorbers, and it is therefore less important to have low uncertainties in their measurements. The adsorption experiments themselves often vary with a number of factors, making an analytical uncertainty of several percent sufficient. It is always desirable to analyze the samples at the lowest possible reactor power level to minimize gamma activity produced by exposure to the neutron flux. In the case of samples exposed to seawater, this becomes especially

important, since the adsorber may pick up sodium and chlorine from the salt in the water, with both elements capable of yielding high gamma activities. In routine analyses the radioactivity of all samples are monitored immediately after counting, and the adsorber samples irradiated at 100 kW usually have a gamma activity of less than 1 R/hr when measured at the window of a "Cutie-Pie" monitor. This is an acceptably low activity, since the experimenters are exposed only briefly to the radioactive samples and at a larger distance. A calibration curve is made for each set of analyses by irradiating and counting a set of uranium ore standards, consisting of three or four one-gram samples containing from one to fifteen micrograms of uranium, plus one containing no uranium. A sample calibration curve is presented as Figure 7-1. Also in Table 7-1 is a listing of a representative selection of uranium adsorbers, and the results of their analyses.

The uranium adsorption studies also included some elution studies, in which a liquid solution was used to remove any uranium from an exposed adsorber. The elution was performed by putting an elutant solution in contact with a uranium-containing adsorber for a certain period of time, then decanting the elutant, and using distilled water to wash the remaining elutant off the adsorber. The effectiveness of an elutant was determined by a mass balance study represented by the following equation:

$$U_a = U'_a + U_e + U_w, \text{ where}$$

U_a = total amount of U on the adsorber before elution

U'_a = total amount of U on the adsorber after elution

U_e = total amount of U in the elutant after elution

U_w = total amount of U in the wash after elution.

This mass balance equation assumes that the concentration of uranium in the wash and elutant before elution was zero. This assumption was verified by measuring samples from each before the elution. Samples representing each of the four terms in the equation were then analyzed to find their uranium concentrations, and the total uranium masses for each were found by multiplying by the total mass of each uranium-containing material. It was difficult to obtain better than an approximate agreement in the mass balance, due to experimental difficulties in accurately collecting all the wash water or ensuring a uniform contact with all parts of the adsorber. The interesting point of the elution study was the successful application of the DFN technique to the analysis of uranium in a liquid sample. Some representative results of these studies are shown in Table 7-1.

The DFN technique has also been successfully used to analyze the concentration of uranium in porcelain dentures (56). The manufacturers of porcelain dentures add a small amount of uranium to the teeth to imitate the fluorescence of natural teeth (59). The uranium concentrations are required to be below a limit of 500 ppm U set by

the U. S. Nuclear Regulatory Commission. The DFN analysis of a set of 14 teeth identified the average concentration as 224 ppm U, well under the limit. The analysis also included a tooth made from acrylic which was shown to contain no measurable uranium. The analysis of these samples was performed at a power level of 10 kW, which resulted in a sufficiently high number of counts for each sample. The results of these analyses are presented in Table 7-2.

Another study measured the uranium concentrations in products which contained phosphates. Much of the phosphate used in products such as detergent and fertilizer comes from large mineral deposits in Florida which often contain significant amounts of uranium. Several studies (60, 61) have investigated the feasibility of extracting the uranium as a by-product of the phosphate mining; some work has been done on a limited basis. If the uranium is not extracted, however, there is a possibility of it appearing in the final product. At OSU, many different types and varieties of fertilizers and detergents were analyzed and found to have a wide variation in uranium concentrations. Some of the samples had uranium concentrations low enough to produce no more than background levels, while some samples had as much as 60 ppm U. Due to the wide variation in uranium concentrations, the samples were usually analyzed at 100 kW, which was acceptable since it did not result in excessive gamma and beta activity. Some representative phosphate analyses are presented in Table 7-3.

DFN analysis is well-suited to the measurement of geological samples, both uranium ores and ordinary soils. A soil sample taken

from the OSU campus in Corvallis, was found by DFN analysis to have a uranium concentration of 3.36 ppm, which is somewhat higher than the average concentration of uranium in the earth's crust, 2 ppm (62). Another soil sample, taken near John Day in Eastern Oregon, contained only 1.59 ppm U. A possible reason for the difference in uranium concentrations in the two soils could be due to the nature of the soils. The soil in the region near John Day is made from fractured lava and ash. Any rainfall quickly washes through the soil to springs or deep wells. In this situation uranium is leached out of the soil and carried away. In the Corvallis area, however, water is retained in the soil and does not flush through it quickly. This would be less efficient for transporting uranium, and could account for the higher concentration in the Corvallis soil. Several samples of the mineral pegmatite were analyzed. This pegmatite, taken from a mine in South Dakota, was being mined for its high concentration of tantalum. It was also found to contain several hundred ppm U. Results of these geological sample analyses are presented in Table 7-5. The analysis of uranium concentrations in ore material is a very easy task, due to the high concentrations of uranium present, and can be performed at 10 kW or even 1 kW. Some typical results are listed in Table 7-4.

All of the applications which have been discussed have used a single irradiation and counting period, but the sensitivity of a DFN

system can be improved by multiple cycling of irradiation, decay, and counting periods. The details of multiple cycling and a discussion of its effectiveness are presented in Chapter VIII.

A DFN system which uses a reactor as the neutron source is of course limited to analyses which can be performed in the reactor building. Some versatility can be obtained by using a more portable source of neutrons, such as a neutron generator or a ^{252}Cf source. In Chapter III a borehole logging technique for analyzing uranium boreholes which used a 14-MeV pulsed neutron generator was described (37). DFN systems have also used ^{252}Cf sources successfully (34, 36).

A possible application of DFN analysis is the in-situ measurement of uranium concentrations in ore samples. A geologist could use a mobile DFN system, consisting of a moderated ^{252}Cf irradiation facility, a rabbit system, and counting assembly, all mounted in a small truck or van and trailer. The system could be operated at a site where uranium surveys are being performed to provide immediate and invaluable feedback of the quality of the ore. Such a system would have a much lower neutron flux than a reactor could provide. The thermal flux at an irradiation position due to a 10-mg ^{252}Cf source would be about $2 \times 10^8 \text{ n/cm}^2\text{-s}$, a factor of about 10^5 less than the OSTR thermal flux. To compensate for the lower neutron flux, larger samples (up to 25 grams) could be analyzed,

multiple cycling could be incorporated, and more-sensitive ^3He detectors could be substituted for the BF_3 detectors. The sensitivity of such a system can be inferred from the sensitivity of the OSU DFN system, using the ratio of neutron fluxes and detector sensitivities. For a 25-gram sample, five cycles per sample, 60-second, 20-second, 60-second, 5-second cycling times, and a background count of 20 counts per minute, the system sensitivity would be about seven counts per ppm U, which would be useful for samples with uranium concentrations greater than about 4 ppm. This sensitivity would be sufficient for any significant uranium-bearing material.

DFN analysis could also be used for the determination of the ratios of uranium isotopes in samples containing no other fissionable material. For an isotopic discrimination, two measurements are needed, one in which the sample is enclosed in a cadmium capsule during irradiation, and one with the sample bare. The difference between the bare count and the cadmium-covered count is the number of counts which are due to ^{235}U fission only, since ^{238}U does not undergo thermal fission. By comparing this count to a calibration curve made from a set of ^{235}U standards, the mass of this isotope in the sample can be determined. Fission of ^{235}U does make a contribution to the cadmium-covered counts, since σ_f for ^{235}U is about 100 b from the cadmium cutoff energy (about 0.5 eV) to about 1.5 eV.

Thus the ^{235}U contribution must be subtracted from the cadmium-covered counts to obtain a number of counts due only to ^{238}U . The ^{235}U contribution can be expressed as:

$$C_{25} = (C_b - C_{\text{Cd}})K, \text{ where } K = \frac{\phi_f \cdot \sigma_{f-f}}{\phi_{\text{th}} \cdot \sigma_{f-\text{th}}} \quad (6-1)$$

In this expression:

C_{25} = cadmium-covered counts due to ^{235}U

C_b = total bare counts

C_{Cd} = total cadmium-covered counts

σ_{f-f} = fast fission cross section for ^{235}U

$\sigma_{f-\text{th}}$ = thermal fission cross section for ^{235}U

ϕ_f = fast neutron flux

ϕ_{th} = thermal neutron flux

The number of counts due to ^{238}U can then be compared to a calibration curve obtained from a set of ^{238}U standards to determine the mass of ^{238}U in the sample. The ^{235}U enrichment is then found as the ratio of the mass of ^{235}U to the total mass of uranium in the sample. For best results the total amount of uranium in the sample should be high enough to ensure a large number of counts due to ^{238}U .

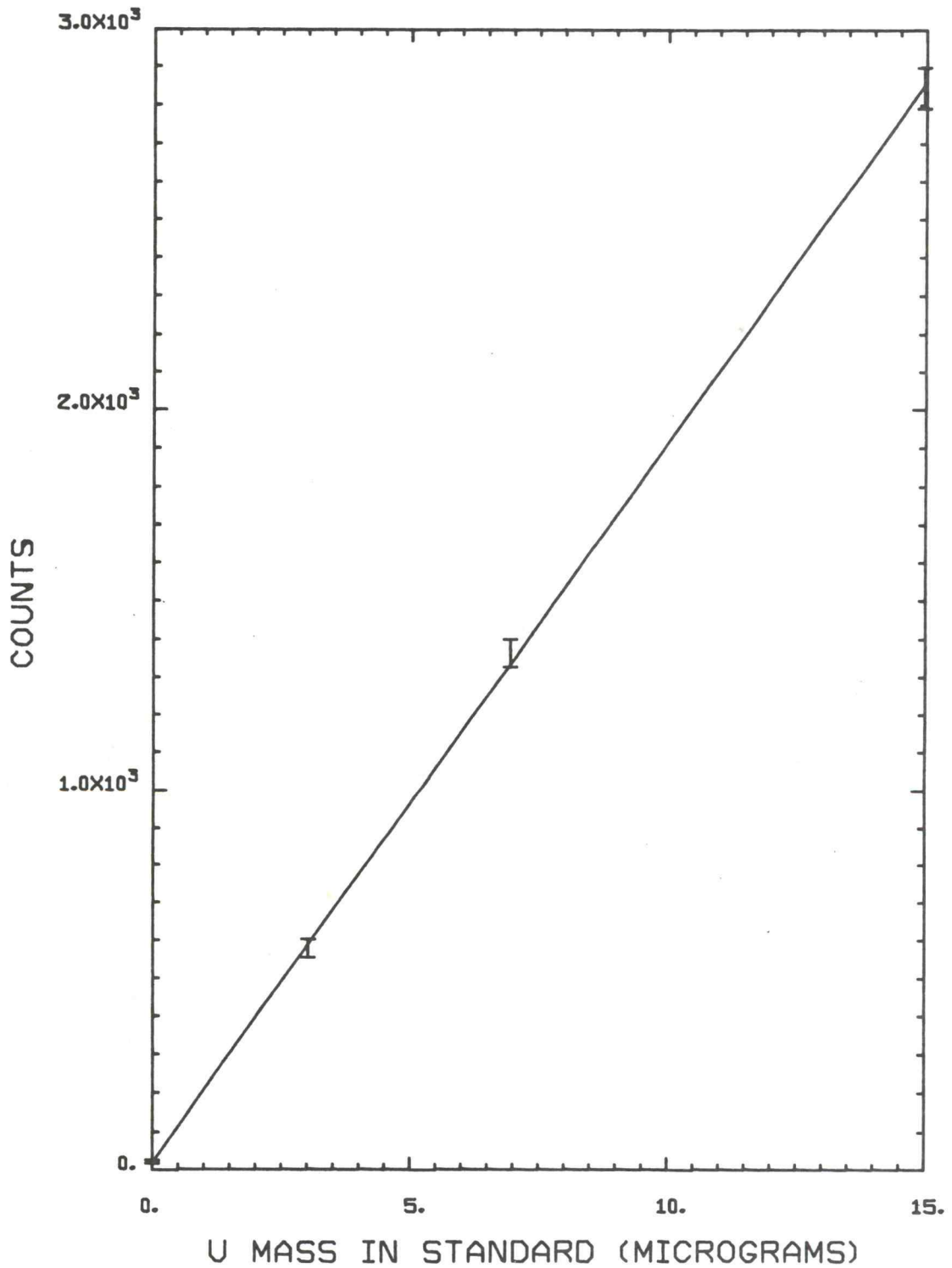
Bare and cadmium-covered analyses can also be used to measure both thorium and natural uranium in a single sample. Again, only the ^{235}U present can undergo thermal fission, so the uranium mass can be determined by comparing $C_b - C_{\text{Cd}}$ to a calibration

curve obtained from the analysis of natural uranium standards. A similar natural uranium calibration curve can be obtained for cadmium-covered counts, and the sensitivity obtained from this curve can be used to determine how many cadmium-covered counts result from uranium. Subtracting this uranium contribution from the cadmium-covered counts leaves counts due only to thorium; these counts can be compared to a thorium calibration curve (obtained using thorium standards) to find the thorium concentration in the sample. In actual practice, three sets of standards would not be needed for each set of analyses, since the ratio of the sensitivities for thorium, cadmium-covered uranium, and bare uranium counts should be quite constant. Thus one set of standards could be analyzed, and the sensitivities for the other two found by multiplying the measured sensitivity by the appropriate ratio.

VII. RESULTS

Figure 7-1 is a graph of the calibration curve for the October 19, 1977 DFN analysis (the data for this curve were presented in Table 5-2). The irradiation was performed at a reactor power of 100 kW with irradiation, decay, and counting times of 60 seconds, 20 seconds, and 60 seconds. Each of the points on the graph corresponds to a standard, the horizontal axis indicating the mass of uranium in the standard and the vertical axis the number of counts produced by each. The error bar for each point indicates the counting statistics uncertainty. The straight line is the graph of the calibration equation, $C = 189.4 m + 20$, where C is the total number of counts produced by m micrograms of uranium. This value was found by using a linear least-squares fit formula modified so that the equation passes through the point $C = 20$, $m = 0$ (20 counts were produced by the zero-uranium-mass standard). It has been found to be desirable to make this modification to the least squares fit because it gives better results for finding the uranium mass of a sample which produces a low number of counts, while having practically no effect on a sample producing a higher number of counts. It will be noted that the lowest concentration standard was omitted from this curve, since it was determined that it produced a consistently low number of counts, which indicates that the assumed value for the uranium content is suspect.

Figure 7-1

URANIUM CALIBRATION CURVE
FOR 100 KW

The sensitivity of the DFN system can be expressed as the slope of the calibration equation. Physically, this is equivalent to the ratio of the net counts produced by a sample (total counts minus background counts) to the mass of uranium in the sample. Knowing the sensitivity of the DFN system, the efficiency of the counting assembly can also be calculated. From Equation 4-1,

$$\epsilon = C_N \left[m \phi \frac{\nu \bar{\sigma}_f N_{av}}{A} \sum_{i=1}^6 \frac{\beta_i}{\lambda_i} (1 - e^{-\lambda_i t_0}) e^{-\lambda_i t_1} (1 - e^{-\lambda_i \Delta t}) \right]^{-1} \quad (7-1)$$

Since fission in uranium is dominated by thermal fission of ^{235}U , ϕ_{th} and $\bar{\sigma}_f$ are used for thermal fission of ^{235}U . The λ_i and β_i values are taken from Table 2-2, and $\nu = 2.418$.

The average sensitivity at 100 kW, as discussed in Chapter V, was 188.6 c/ μgU , so 188.6 was the value used for C_N , corresponding to a value for m of 7.2×10^{-9} g, the mass of ^{235}U in one microgram of natural uranium. The thermal flux, $\phi_{th} = 1.7 \times 10^{12}$ n/cm²-s, and $\bar{\sigma}_f = \frac{\sqrt{\pi}}{2} \cdot 582$ b. These values result in an efficiency of 21.4% for a 60 second irradiation, 20 second decay, and 60 second counting cycle.

Another important characteristic of a counting system is the minimum level of detection, which is the smallest mass which one can be reasonably confident of detecting. "Reasonably confident" is a subjective phrase which may become more meaningful by using

the critical level, L_C , which was discussed in Chapter V. The critical level can be defined in terms of the background count and its standard deviation, C_B and σ_B , in place of C_u and σ_u . Thus $L_C = k\sigma_B$. Any count greater than $C_B + L_C$ can be considered to be greater than background.

The detection limit, L_D , is defined as the number of counts which one can be "reasonably confident" is greater than L_C . L_D can be found by the following formula, derived in Appendix C:

$$L_D = 2L_C + k^2 = 2\sqrt{2} k\sigma_B + k^2.$$

If an 84.2% confidence interval is used, then $k = 1$, $L_C = \sqrt{2}\sigma_B$, and $L_D = 1 + 2\sqrt{2}\sigma_B$. For a DFN system operating with a background count of 31.1 counts (the typical background count at 1 MW), $L_D = 17$ counts. This means that the minimum level of detection for the OSU DFN system is $\frac{17 \text{ counts}}{1886 \text{ c}/\mu\text{gU}} = 0.0090 \mu\text{gU}$, or nine nanograms of uranium, at 1 MW.

The wide variety of applications of DFN uranium analysis was discussed in Chapter VI. Tables 7-1 through 7-5 list the results of many of these analyses. Since June, 1976 more than 1900 samples have been analyzed at OSU by DFN counting. During this time, two different counting assemblies were used. The original one, using 14 BF_3 detectors, was "inherited" from a previous project, and it was used until the current system, described in Chapter IV, became

Table 7-1. Seawater-uranium adsorbers.

Sample	Sample Mass (g)	Date Analyzed	Reactor Power	System Sensitivity (C/ μ gU)	Counts	μ gU	ppmU
Chitosan, S. E. *	2.355	5/26/77	100 kW	67.8	116	1.48	0.63
Crab Shell, S. E.	4.085	10/7/76	1 MW	662.5	3626	5.35	1.31
Cellulose, S. E.	1.020	10/7/76	1 MW	662.5	271	0.28	0.28
Ti(OH) ₄ , S. E.	0.904	9/29/76	100 kW	66.97	1667	24.62	27.23
Peat Moss, S. E.	1.440	11/10/76	100 kW	60.80	239	2.32	1.61
Diatomaceous Earth	0.433	8/26/77	100 kW	185.7	248	1.13	2.61
Diatomaceous Earth, S. E.	0.974	8/26/77	100 kW	185.7	493	2.45	2.52
Zeolite, S. E.	2.253	11/8/77	100 kW	182.5	311	1.56	0.69
Elutant	2.101	6/7/77	1 MW	689.1	1125	1.58	0.75
Elution Study: Wash Water	2.156	6/7/77	1 MW	689.1	126	0.132	0.061

*:S. E.: Seawater Exposed

Table 7-2. Porcelain dentures.

Sample	Sample Mass (g)	Date Analyzed	Reactor Power	System Sensitivity (C/ μ g U)	Counts	μ g U	ppm U
1	0.481	11/18/76	10 kW	6.90	779	110	229
2	0.660	11/18/76	10 kW	6.90	1017	144	219
3	0.366	11/18/76	10 kW	6.90	583	81.6	223
4	0.318	11/18/76	10 kW	6.90	508	70.7	222
5	0.347	11/18/76	10 kW	6.90	559	78.1	225
6	0.290	11/18/76	10 kW	6.90	479	66.5	229
7	0.296	11/18/76	10 kW	6.90	447	61.9	209
8	0.292	11/18/76	10 kW	6.90	451	62.4	214
9	0.272	11/18/76	10 kW	6.90	425	58.7	217
10	0.339	11/18/76	10 kW	6.90	583	81.6	240
11	0.314	11/18/76	10 kW	6.90	518	72.2	230
12	0.395	11/18/76	10 kW	6.90	657	92.3	234
13	0.675	11/18/76	10 kW	6.90	1075	153	227
14	0.485	11/18/76	10 kW	6.90	767	108	223

Table 7-3. Phosphates.

Sample	Sample Mass (g)	Date Analyzed	Reactor Power	System Sensitivity (C/ug U)	Counts	ug U	ppm U	% P ₂ O ₅
<u>Detergents:</u>								
Cold Power Detergent	0.840	1/13/77	1 MW	642.2	79	0.200	0.238	?
Calgonite Dishwasher Soap	1.776	1/13/77	1 MW	642.2	132	0.283	0.159	?
Amway Laundry Detergent	2.214	1/13/77	1 MW	642.2	114	0.255	0.115	8.7
Amway Dishwasher Detergent	2.005	1/13/77	1 MW	642.2	6932	10.87	5.42	15.1
<u>Fertilizers:</u>								
Ammonium Phosphate Sulfate	6.498	1/13/77	1 MW	642.2	250,556	382.5	58.9	20
Monoammonium Phosphate	6.773	1/13/77	100 kW	64.86	24,852	379.3	56.0	55
Diammonium Phosphate	5.797	1/13/77	100 kW	64.86	22,955	350.1	60.4	46
Ammonium Phosphate (Elephant Brand)	4.697	1/13/77	100 kW	64.86	6386	94.6	20.1	20
Osmocote	6.937	1/13/77	100 kW	64.86	421	2.66	0.38	6
Miller's Liquid Plant Food	2.848	1/13/77	100 kW	64.86	607	5.53	1.94	8

Table 7-4. Uranium ore samples.

Sample	Sample Mass (g)	Date Analyzed	Reactor Power	System Sensitivity (C/ μ gU)	Counts	μ gU	ppm U
B26	1.193	3/11/77	10 kW	6.784	17505	2584	2167
B27	1.087	3/11/77	10 kW	6.784	18373	2712	2495
B28	1.126	3/11/77	10 kW	6.784	18049	2664	2366
B29	1.257	3/11/77	10 kW	6.784	15863	2343	1864
B30	1.257	3/11/77	10 kW	6.784	15716	2321	1846
B31	1.240	3/11/77	10 kW	6.784	16573	2447	1974
C25	1.010	3/11/77	10 kW	6.784	21140	3118	3087
C26	1.002	3/11/77	10 kW	6.784	24550	3619	3613
C27	0.998	3/11/77	10 kW	6.784	22720	3350	3356
C28	1.019	3/11/77	10 kW	6.784	24517	3614	3547
C29	0.979	3/11/77	10 kW	6.784	3451	520	531

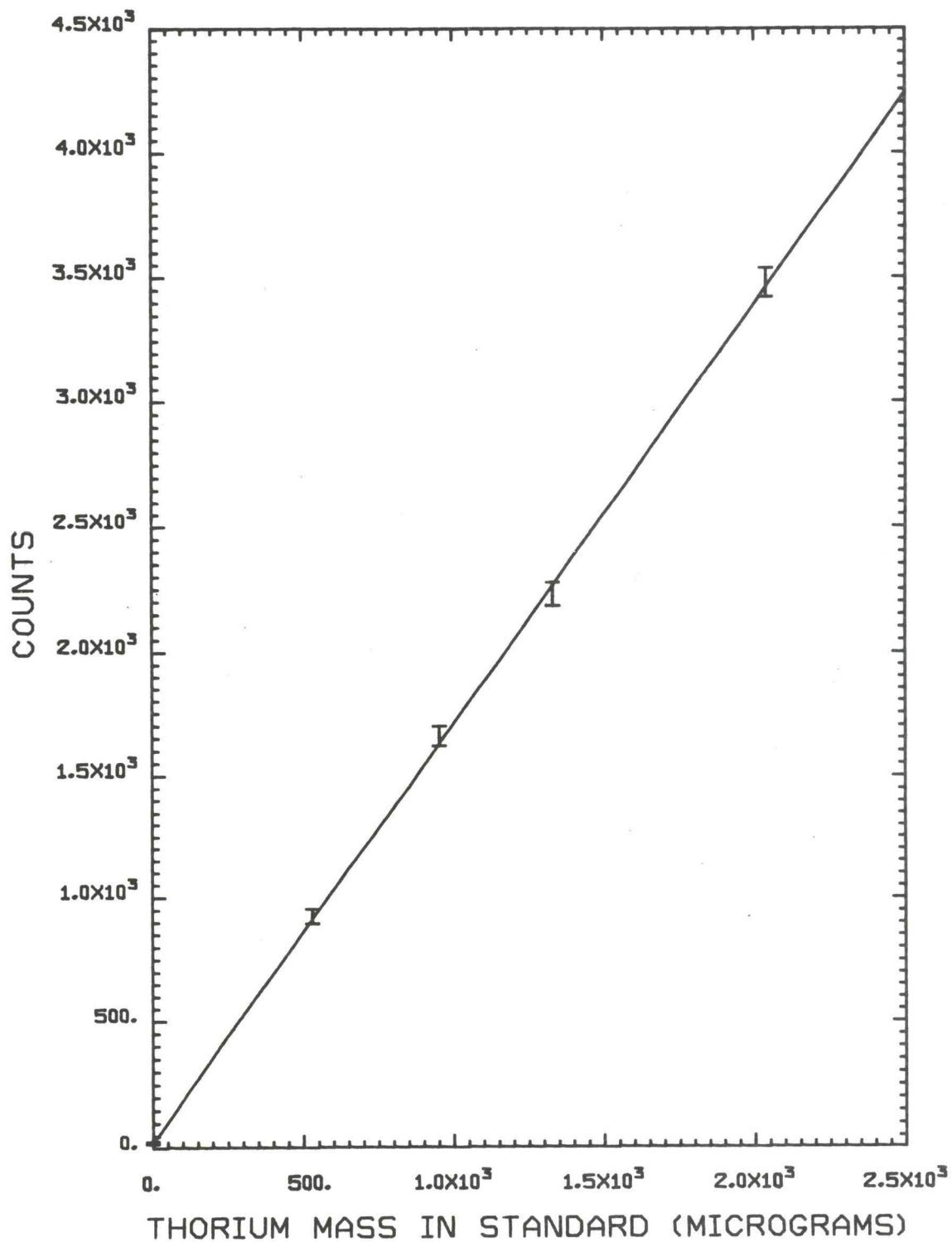
Table 7-5. Miscellaneous geological samples.

Sample	Sample Mass (g)	Date Analyzed	Reactor Power	System Sensitivity (C/ μ gU)	Counts	μ gU	ppm U
Corvallis Soil	7.863	10/1/76	100 kW	52.99	18179	26.42	3.360
John Day Soil	1.203	12/8/77	100 kW	202.2	407	1.909	1.587
Zircon Sand	3.425	11/10/76	100 kW	60.8	63710	1046	305.4
Pegmatite	0.4093	5/10/78	10 kW	18.56	1752	93.48	228.4
Pegmatite	0.5278	5/10/78	10 kW	18.56	1590	84.75	160.6
Pegmatite	0.3555	5/10/78	10 kW	18.56	1535	81.79	230.1
Pegmatite	0.1605	5/10/78	10 kW	18.56	2604	139.4	868.4

operable in June, 1977. The current assembly has an efficiency which is greater than the efficiency of the original assembly by a factor of about three and has a smaller background count rate. In the tables of results, many of the samples were analyzed with system sensitivities corresponding to about 670 c/ μ gU at 1 MW; these were analyzed using the original system. Those analyzed with system sensitivities corresponding to about 1880 c/ μ gU at 1 MW were analyzed with the current counting assembly.

Figure 7-2 is a calibration curve for a DFN analysis of thorium, performed on April 24, 1978. The standards were made from pure ThO_2 powder diluted with powdered serpentine to give thorium concentrations varying from 2317 to 9265 ppm. About 200 mg of each was packaged in a 2/27-dram polyvial, heat sealed, and placed in a 2/5-dram vial, which was also heat sealed. The irradiations were performed in cadmium capsules at 100 kW, and the number of counts ranged from 926 to 3478. The straight line on the graph is a linear least-squares fit, which resulted in the calibration equation: $C = 1.688 m_{\text{Th}} + 21$; $r^2 = 0.9991$, where m_{Th} is the thorium mass in the sample in micrograms. Subsequent thorium analyses have shown that a more typical thorium sensitivity at 100 kW is 2.101 c/ μ gTh. This compares to a uranium sensitivity of 185.6 c/ μ gU observed on the same day. Thus the DFN sensitivity for thorium is 1.13% of the sensitivity for uranium.

Figure 7-2
THORIUM CALIBRATION CURVE
FOR 100 KW



In a preliminary study of uranium enrichment determinations, the ratio of cadmium-covered counts to bare counts minus cadmium-covered counts at a given power level for natural uranium was determined to be 6.3%. The correction factor, K in Equation 6-1, was found by the analysis of a set of standards made by mixing known amounts of natural and depleted uranium. The samples were prepared so that they all contained the same amount of ^{238}U , but had differing amounts of ^{235}U . Thus a linear least-squares fit to the data for the cadmium-covered counts gave an equation for a line whose slope was the sensitivity value for cadmium-covered counts due to ^{235}U . The ratio of this value to the slope of the ^{235}U calibration curve (using the difference between the bare and cadmium-covered counts) is equal to K. The value for K was determined to be 0.036. The evaluation of these two factors was a good indication that uranium enrichment determinations can be successfully performed by DFN analysis.

VIII. IMPROVEMENTS

When the current DFN counting assembly was constructed, several changes in design were made which greatly improved the sensitivity over that of the old system. The major improvement was repositioning the detectors to take advantage of the higher neutron flux at smaller radial distances from the sample. For two concentric rings of detectors, the current positioning scheme is believed to be the best possible. A thermal neutron incident normally to the wall of a BF_3 detector such as the one described in Chapter IV will have a 32% probability of being absorbed by a ^{10}B atom in the detector. This assumes that the neutron traverses a distance through the fill gas equal to one detector diameter. One diameter is the mean chord length for an infinitely long cylinder, and this absorption value is only slightly larger than the actual value for a detector of finite length, when the length is much larger than the source-to-detector distance. Any neutron which is travelling near the edge of a detector in the inner ring will probably strike an outer detector near its center. Thus a reasonable estimate is that more than 50% of the neutrons emitted by the source in directions which will pass through the detectors will be absorbed in the two rings of detectors. An additional detector outside these two rings will subtend a smaller solid angle than one in the inner ring, be in a region of smaller neutron flux (even assuming no detectors between it and the sample),

and would still be no greater than 32% efficient in absorbing the neutrons which do strike it. Thus an additional ring of detectors would cause an increase in counts, but the increase is probably not worth the added cost.

Another important improvement in the new system compared to the old one is improved shielding to decrease the background count rate. The new assembly has a sheet of cadmium surrounding the counting chamber vertical walls and bottom surface, and paraffin outside the cadmium, as did the old one, but the new system also has shielding on the top surface, with the exception of holes for the detector and central sample tube. Considering that much of the background count rate is due to cosmic radiation, the shielding on top should be quite effective in reducing the background. Another improvement may be made by making removable plugs to put in the holes above the detectors. These plugs could have a bottom surface of cadmium, with paraffin above it, and the only gap would be a small hole for the signal cable to pass through. This added shielding could make a small decrease in the background rate, which would be beneficial for samples requiring lower detection limits than those being analyzed currently.

A possible improvement which could be made over the present design is an increased effort to avoid gaps in the moderator between the sample and the detectors. There is a small possibility that voids

may have been introduced in the paraffin region during the pouring of the molten wax, but the procedure may have been careful enough to avoid it. A more important place for increasing the amount of moderator is in the detector tube region. The inner six detectors were positioned inside lucite tubes with inner diameters of 5.72 cm. Since the outside diameter of the detector is 5.08 cm, there is a 0.32-cm air gap around the tube. The outer detectors were not placed in plastic tubes, but were placed in holes drilled directly into the paraffin. This method resulted in a smaller air gap, but it could still be improved upon. It was very difficult to drill the holes in a perfect vertical line, and some air gaps did result due to the slight curvature of the holes. An improved drilling technique which ensured straighter holes, or closer tolerances in the plastic tubes, could increase the amount of moderating material.

Another opportunity for increasing the moderator is in the design of the sample tube. Presently the removable tube has an outside diameter of 2.54 cm, and it fits in a tube with inside diameter of 3.18 cm, resulting in a 0.32-cm air gap. This could be replaced by a single central tube with one inch (2.54 cm) outside diameter, if a different method of retrieving the sample from the counting chamber were used. If increased moderating material were placed at both the detector wall and the central sample tube, this could add about 0.64 cm of moderating material in the central region. This may seem minor,

but these changes would increase the moderator thickness to 2.92 cm, which is an increase of more than 25%. The increased ability to thermalize neutrons can only result in greater sensitivity.

One way to improve the efficiency of the counting system is the repositioning of the detectors to more closely approximate a 4π solid angle subtended by the detectors. An "ideal" arrangement would be a spherical detector with the sample inserted into the center. Working with cylindrical detectors, however, requires their arrangement in a ring, which leaves a circular opening at the top and bottom through which neutrons can escape without being detected unless scattered back toward a detector. It may be advantageous to insert several detectors horizontally at the bottom and at the top to close these circular openings. Positioning the detectors at the top would be difficult, since signal cables coming from the vertical detectors would interfere with the placement of the horizontal detectors, and a gap would need to be provided for the central sample tube. Placement of the detectors below the vertical ones would also be difficult due to the large distance between the detectors and the preamplifier. Keeping the signal cables between the detectors and preamplifier as short as possible is crucial in minimizing electronic noise. If a practical method of positioning the horizontal detectors were found, however, they could significantly improve the sensitivity.

The system efficiency could also be improved by the substitution

of ^3He detectors for the BF_3 detectors. Reuter-Stokes, which manufactures both types of detectors, quotes a sensitivity of 28 cps when exposed to a thermal neutron flux of $1 \text{ n/cm}^2\text{-s}$ for the BF_3 detector described in Chapter IV. The sensitivity for an equivalent ^3He with shorter active length (only 20.3 cm) is $40 \text{ cps/n/cm}^2\text{-s}$. Correcting for the differences in length yields a neutron counting efficiency for the ^3He detector that is 2.2 times greater than the efficiency for the equivalent BF_3 . Thus replacing the BF_3 detectors by a set of ^3He detectors could improve the sensitivity by a factor of 2.2.

Another major improvement could be achieved in DFN sensitivity by the multiple cycling of samples. Under most counting conditions the repetition of a given counting cycle will result in a decrease in the uncertainty of the measurement. There are limits, however, to the effectiveness of multiple cycling, since the total number of background counts is also increasing. Care must be taken to choose the optimum cycling conditions. The following equation predicts the total number of counts in a sample analysis using multiple cycling:

$$C_T = \epsilon m \phi \frac{\bar{\sigma}_f N_{av} v}{A} \sum_{i=1}^6 \frac{\beta_i}{\lambda_i} (1 - e^{-\lambda_i t_0}) e^{-\lambda_i t_1} (1 - e^{-\lambda_i \Delta t}) U_i + NB \Delta t, \quad (8-1)$$

where

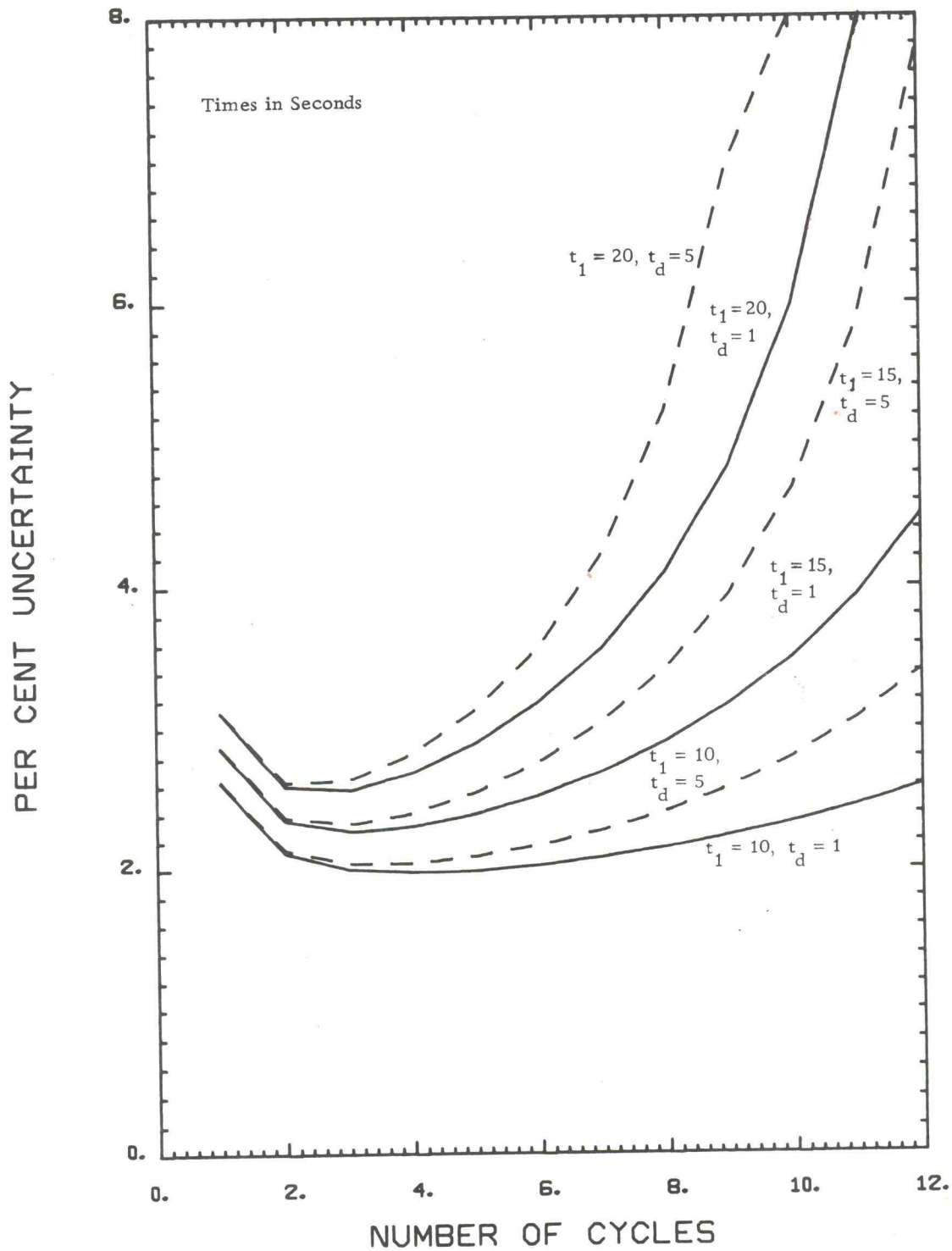
$$U_i = [N - (N+1) e^{-\lambda_i T} + e^{-(N+1)\lambda_i T}] / (1 - e^{-\lambda_i T})^2$$

All terminology is the same as in Equation 4-1, with the addition of T , which is the total time per cycle; N , the number of cycles; and B , the background count rate. Equation 8-1 is derived in Appendix A. Since C_T is proportional to N , the number of counts from a sample can be increased by increasing the number of cycles, limited only by the point where the exhaustion of uranium atoms by fission and absorption becomes noticeable. No realistic analysis could ever include that many cycles, but an analysis could be limited by the total time to be spent on the analysis of each sample. A given time limitation is related to an optimum choice of cycling times and number of cycles, as illustrated in Figure 8-1.

In Figure 8-1 the relative counting statistics uncertainty is plotted as a function of the number of cycles, for different combinations of decay and delay times. The decay time is still the time between the end of irradiation and the beginning of counting, while the delay time is the time between the end of one count and the beginning of irradiation for the next cycle. The delay time takes into account the time needed to transfer the sample from the counting position to the irradiation position. The uncertainty values in Figure 8-1 were calculated using Equation 8-1, assuming a constant background of 20 counts per minute, equal irradiation and counting times, and a combination of values for ϵ , m and ϕ which would give about 730 net counts for a 60s-20s-60s single cycle. The total time for the

Figure 8-1

UNCERTAINTY VS NUMBER OF CYCLES
FOR A 300 SECOND TOTAL EXPERIMENT



analysis of one sample was assumed to be 300 seconds, the decay time for each curve on the graph was either 10, 15, or 20 seconds, and the delay time either one or five seconds. The upper curve, with $t_1 = 20$ s and $t_d = 5$ s (t_d is the delay time), would correspond to the limitations of the present OSU DFN system, since the rabbit transit time is about five seconds, and the decay time is usually 20 seconds to allow interferences to decay. Note that for this line the minimum occurs at two cycles, since for more cycles than that the relative uncertainty actually increases. For such large decay and delay times, as the number of cycles is increased, the delay and decay times take up a larger percentage of the total experiment time, giving less actual time for irradiation and counting (for example, at $N = 12$, there is the absurd situation where delay and decay times occupy the total experiment). It should be noticed that, as t_1 and t_d decrease, the curves in Figure 8-1 go lower, and the minimum values occur at larger values of N . Thus any system which takes advantage of multiple cycling will need to use shorter decay and delay times than 20 seconds and five seconds. The delay times can be decreased by installing a rabbit system with higher transit speeds, or perhaps shorter transit distances. To allow for shorter delay times, the sample will need to remain in the rabbit capsule. This and the need to decrease decay times will necessitate solving the problems of interferences from ^{16}N and ^{17}N . A lead shield between the sample

and detectors may help, and electronic discrimination may also be able to decrease the number of high energy gammas causing interference counts. If these problems could be solved and the decay time reduced to a value approaching the transit time, multiple cycling could definitely be used to improve the DFN system sensitivity.

BIBLIOGRAPHY

1. "Neutron Cross Sections, " USAEC Report BNL-325, Third Edition (1973).
2. G. R. Keepin, "Physics of Delayed Neutrons- Recent Experimental Results, " Nuclear Technology, 13, 53-58 (1972).
3. G. R. Keepin, Physics of Nuclear Kinetics, Addison-Wesley, Reading, Mass. (1965).
4. W. R. Sloan and G. L. Woodruff, "Delayed Neutron Energy Spectra, " Transactions of the American Nuclear Society, 15, 942-943 (1972).
5. R. Batchelor and H. R. McK. Hyder, "The Energy of Delayed Neutrons from Fission, " Journal of Nuclear Energy, 3, 7-17 (1956).
6. J. J. Duderstadt and L. J. Hamilton, Nuclear Reactor Analysis, John Wiley and Sons, New York (1976).
7. E. B. Sandell, Colorimetric Determination of Trace Metals, Ch. XLVII, Interscience Publishers, Inc., New York, Third Edition (1959).
8. C. J. Rodden, ed., Analytical Chemistry of the Manhattan Project, McGraw-Hill, New York (1950).
9. F. S. Grimaldi, I. May, M. H. Fletcher and J. Titcomb, "Summary of Methods of Analysis for the Determination of Uranium and Thorium, " U.S. Geological Survey Bulletin, 1006, 1-9 (1954).
10. F. S. Grimaldi and H. Levine, "The Visual Fluorimetric Determination of Uranium in Low-Grade Ores, " U.S. Geological Survey Bulletin, 1006, 43-48 (1954).
11. G. R. Price, R. J. Ferretti and S. Schwartz, "Fluorophotometric Determination of Uranium, " Analytical Chemistry, 25, 322-331 (1953).
12. F. A. Centanni, A. M. Ross and M. A. DeSesa, "Fluorometric Determination of Uranium, " Analytical Chemistry, 28, 1651-1657 (1956).

13. G. W. C. Milner, J. D. Wilson, G. A. Barnett and A. A. Smales, "The Determination of Uranium in Sea Water by Pulse Polarography, " Journal of Electroanalytical Chemistry, 2, 25-38 (1961).
14. E. Rona, L. O. Gilpatrick and L. M. Jeffrey, "Uranium Determination in Sea Water, " Transactions, American Geophysical Union, 37, 697-701 (1956).
15. M. G. Inghram, "Trace Element Determination by the Mass Spectrometer, " Journal of Physical Chemistry, 57, 809-814 (1953).
16. A. von Baeckmann, "Determination of Actinide Elements by X-Ray Analysis, " Analytical Chemistry of Nuclear Fuels, Proceedings of a Panel, Vienna, IAEA, Vienna, 33-44 (1972).
17. L. S. Birks and E. J. Brooks, "Analysis of Uranium Solutions by X-Ray Fluorescence, " Analytical Chemistry, 23, 707-709 (1951).
18. R. D. Cherry, "The Determination of Thorium and Uranium in Geological Samples by an Alpha Counting Technique, " Geochimica et Cosmochimica Acta, 27, 183-189 (1963).
19. M. Koide, E. D. Goldberg, "Uranium-234/Uranium-238 Ratios in Sea Water, " Progress in Oceanography, 3 ed. M. Sears, Pergamon Press, Oxford, England, 173-177 (1965).
20. R. H. Augustson and T. D. Reilly, "Fundamentals of Passive Nondestructive Assay of Fissionable Material, " USAEC Report LA-5651-M (1974).
21. L. A. Kull and R. O. Ginaven, "Guidelines for Gamma-Ray Spectroscopy of ^{235}U Enrichment, " USAEC Report BNL-50414 (1974).
22. K. K. Bertine, L. H. Chan and K. K. Turekian, " Uranium Determinations in Deep-Sea Sediments and Natural Waters using Fission Tracks, " Geochimica et Cosmochimica Acta, 34, 641-648 (1970).
23. T. Hashimoto, "Determination of the Uranium Content in Sea Water by a Fission Track Method with Condensed Aqueous Solution, " Analytica Chimica Acta, 56, 347-354 (1971).

24. A. A. Smales, "The Determination of Small Quantities of Uranium in Rocks and Minerals by Radioactivation," Analyst, 77, 778-789 (1952).
25. H. Wakita, H. Nagasawa, S. Uyeda and H. Kuno, "Uranium and Thorium Contents in Ultrabasic Rocks," Earth and Planetary Science Letters, 2, 377-381 (1967).
26. G. L. Bate and J. R. Huizenga, "Abundances of Ruthenium, Osmium and Uranium in Some Cosmic and Terrestrial Sources," Geochimica et Cosmochimica Acta, 27, 345-360 (1963).
27. A. O. Brunfelt and E. Steinnes, "Instrumental Activation Analysis of Silicate Rocks with Epithermal Neutrons," Analytica Chimica Acta, 48, 13-24 (1969).
28. E. Steinnes and D. Brune, "Determination of Uranium in Rocks by Instrumental Activation-Analysis Using Epithermal Neutrons," Talanta, 16, 1326-1329 (1969).
29. M. W. Echo and E. H. Turk, "Quantitative Determination of U-235 by Delayed Neutron Counting," USAEC Report PTR-143 (1957).
30. S. Amiel, "Analytical Applications of Delayed Neutron Emission in Fissionable Elements," Analytical Chemistry, 34, 1683-1692 (1962).
31. F. F. Dyer, J. F. Emery, G. W. Leddicotte, "A Comprehensive Study of the Neutron Activation Analysis of Uranium by Delayed Neutron Counting," USAEC Report ORNL-3342 (1962).
32. R. W. Jewell, W. John and D. H. White, "A High Efficiency Graphite-Moderated Neutron Counter," Nuclear Instruments and Methods, 63, 185-188 (1968).
33. H. R. Lukens and V. P. Guinn, "Assay of Uranium and Thorium Based upon Reactor Pulse Activation and Delayed Neutrons," Transactions of the American Nuclear Society, 12, 45 (1969).
34. K. W. MacMurdo and W. W. Bowman, "Assay of Fissile Materials by a Cyclic Method of Neutron Activation and Delayed Neutron Counting," Nuclear Instruments and Methods, 141, 299-306 (1977).

35. R. C. Hagenauer, C. L. Zyskowski and L. C. Nelson, Jr., "Determination of Uranium-235 by a Delayed Neutron Counting Technique, " USAEC Report NBL-267, 51-55 (1973).
36. "²⁵²Cf-Based Borehole Logging System for In-Situ Assaying of Uranium Ore, " Californium-252 Progress, No. 21, 17 (1976).
37. W. W. Givens, W. R. Mills, C. L. Dennis and R. L. Caldwell, "Uranium Assay Logging Using a Pulsed 14-MeV Neutron Source and Detection of Delayed Fission Neutrons, " Geophysics, 41, 468-490 (1976).
38. S. Amiel, J. Gilat and D. Heymann, "Uranium Content of Chondrites by Thermal Neutron Activation and Delayed Neutron Counting, " Geochimica et Cosmochimica Acta, 31, 1499-1503 (1967).
39. W. H. Davies and R. F. Coleman, "The Determination of Traces of Uranium by Delayed Neutron Emission, " UKAEA Report AWRE 0-88/64 (1964).
40. N. H. Gale, "Development of Delayed Neutron Technique as Rapid and Precise Method for Determination of Uranium and Thorium at Trace Levels in Rocks and Minerals, with Applications to Isotope Geochronology, " Radioactive Dating and Methods of Low-Level Counting, IAEA, Vienna, 431-452 (1967).
41. H. H. Kramer, V. J. Molinski and H. W. Nass, "Urinalysis for Uranium-235 and Uranium-238 by Neutron Activation Analysis, " Health Physics, 13 27-30 (1967).
42. H. W. Nass, "Diversified Instrumental Nuclear Analysis Methods Using a Reactor, " Proceedings of the Third International Conference on Modern Trends in Activation Analysis, NBS Spec. Pub. 312, Vol. 1, 563-573 (1969).
43. H. W. Nass, "Delayed Neutron Analysis Method - Analysis of 235-Uranium and 238-Uranium in Varying Enrichments of 235-Uranium, " Tech. Memo. SFRC-78, Union Carbide Corp., Tuxedo, N. Y. (1971).
44. J. L. Brownlee, Jr., "The Detection and Determination of Fissionable Species by Neutron Activation-Delayed Neutron Counting, " Proceedings of the Third International Conference

on Modern Trends in Activation Analysis, NBS Spec. Pub. 312, Vol. 1, 495-500 (1969).

45. D. Ostle, R. F. Coleman and T. K. Ball, "Neutron Activation Analysis as an Aid to Geochemical Prospecting for Uranium," Uranium Prospecting Handbook, Proceedings of a NATO-sponsored Advanced Study Institute on Methods of Prospecting for Uranium Minerals, London, 95-109 (1971).
46. Z. Randa, J. Benada, J. Kuncir, M. Vobecky and J. Frana, "Radioanalytical Methods for the Non-Destructive Analysis of Lunar Samples" Journal of Radioanalytical Chemistry, 11, 305-337 (1976).
47. R. C. Hagenauer, C. L. Zyskowski and L. C. Nelson, Jr., "A Volume-Dependent Count Correction Factor for the Delayed Neutron Analysis of Uranium-235," USAEC Report NBL-277, 31-37 (1976).
48. H. R. Lukens, D. M. Fleishman and R. L. Bramblett, "Determination of ^{235}U in Highly Enriched Reactor Fuel Sticks," Journal of Radioanalytical Chemistry, 16, 97-104 (1973).
49. D. M. Bibby, R. P. Chaix and A. H. Andeweg, "The Determination of Uranium and Thorium by the Use of Delayed Neutrons," National Institute for Metallurgy Report No. 1625, South Africa (1974).
50. G. L. Cumming, "Determination of Uranium and Thorium in Meteorites by the Delayed Neutron Method," Chemical Geology, 13, 257-267 (1974).
51. C. Lee, H. J. Kim and H. I. Bak, "Simultaneous Analysis of Uranium and Thorium by the Delayed Fission Neutron Counting Method," Journal of the Korean Nuclear Society, 6, 80-88 (1974).
52. G. R. Reddy and M. SankarDas, "Analysis of Uranium by Delayed Neutron Counting Method," Indian Journal of Chemistry, 12, 405-409 (1974).
53. P. Hiismaki, V. Pitkanen, R. Rosenberg and A. Sorsa, "An Automatic Device for Large Scale Analysis of Uranium in Rocks and Sediments," Nuclex 75, Colloquium C, Series 2, Basel, Switzerland (1975).

54. S. J. Balestrini, J. P. Balagna and H. O. Menlove, "Two Specialized Delayed-Neutron Detector Designs for Assays of Fissionable Elements in Water and Sediment Samples," Nuclear Instruments and Methods, 136, 521-524 (1976).
55. R. J. N. Brits and M. C. B. Smit, "Determination of Uranium in Natural Water by Preconcentration on Anion-Exchange Resin and Delayed Neutron Counting," Analytical Chemistry, 49, 67-69 (1977).
56. S. E. Binney and R. I. Scherpelz, "Technique for Rapid Analysis of Uranium in Porcelain Dentures," Health Physics, 33, 341-343 (1977).
57. S. E. Binney and R. I. Scherpelz, "A Review of the Delayed Fission Neutron Technique," in press, Nuclear Instruments and Methods.
58. V. D. Hopper, Cosmic Radiation and High Energy Interactions, Prentice-Hall, Inc., Englewood Cliffs, N.J. (1964).
59. D. L. Thompson, "Uranium in Dental Porcelain," HEW Publication (FDA) 76-8061 (1976).
60. K. K. Dar, "Prospects of Using Indian Phosphorites as a Source of Uranium," Report CONF-681088-7, 351-359 (1970).
61. A. Deleon, M. Lazarevic, "Possibilities for Recovery of Uranium as a By-Product in the Production of Phosphate Fertilizers and Tripolyphosphate," Recovery of Uranium, IAEA, Vienna, 351-361 (1971).
62. "Survey of Energy Resources," World Energy Conference, London, 1974, McGregor and Werner, Inc., Washington, D. C., 193 (1974).

APPENDICES

Appendix A. Total Counts for a DFN Measurement

The net number of counts C_{net} obtained from a fissionable sample is given by

$$C_{\text{net}} = \epsilon \int_{t_1}^{t_2} A(t) dt \quad (\text{A-1})$$

where ϵ is the efficiency of the delayed neutron counting system, $A(t)$ is the delayed neutron activity, in delayed neutrons per second, of the sample at time t after removal from the neutron flux, and t_1 and t_2 are the start count and stop count times, also measured from the end of irradiation.

The activity $A(t)$ is given by

$$A(t) = \sum_{i=1}^6 A_{0i} e^{-\lambda_i t} \quad (\text{A-2})$$

where A_{0i} is the activity for delayed neutron group i at the end of irradiation, $\lambda_i = \ln 2 / t_{\frac{1}{2}i}$ is the decay constant corresponding to the half life $t_{\frac{1}{2}i}$ for group i , and the summation is over the six delayed neutron groups. The value of A_{0i} is given by

$$A_{0i} = \beta_i \nu \Sigma_f \phi V (1 - e^{-\lambda_i t_0}),$$

where $\nu\Sigma_f\phi V$ is the total number of fission neutrons emitted by a sample of macroscopic fission cross section Σ_f , volume V , and average neutron emission of ν neutrons per fission, when exposed to a neutron flux ϕ . The term β_i is the fraction of delayed neutrons emitted in group i and t_0 is the irradiation time. If Equation (A-2) and (A-3) are substituted into Equation (A-1), the result is

$$C_{\text{net}} = \epsilon\nu\Sigma_f\phi V \sum_{i=1}^6 [\beta_i(1-e^{-\lambda_i t_0})(e^{-\lambda_i t_1})(1-e^{-\lambda_i \Delta t})/\lambda_i] \quad (\text{A-4})$$

where the counting time $\Delta t = t_2 - t_1$. The factor $\nu\Sigma_f V$ can be evaluated as

$$\nu\Sigma_f V = \nu N_{\text{Av}} \bar{\sigma}_f m/A \quad (\text{A-5})$$

where N_{Av} is Avogadro's number, and m and A are the mass and atomic mass number of the fissionable nuclide. The net counts (Equation 4-1 in the text) is then given by

$$C_{\text{net}} = (\epsilon\nu m N_{\text{Av}} \bar{\sigma}_f \phi/A) \sum_{i=1}^6 [(\beta_i/\lambda_i) (1-e^{-\lambda_i t_0})(e^{-\lambda_i \Delta t_1})(1-e^{-\lambda_i \Delta t})]. \quad (\text{A-6})$$

The expression for the total counts from a sample undergoing N cycles using the DFN technique is best illustrated by reference to Table A-1 for a single half life (for simplicity), where the following notation is used:

A_s = Saturated activity of the sample [$A_s = \beta^v N_A \bar{\sigma}_f m \phi / A$
from Equations (A-3) and (A-5)]

$$S_0 = 1 - e^{-\lambda t_0}$$

$$S_1 = e^{-\lambda t_1}$$

$$S_2 = 1 - e^{-\lambda \Delta t}$$

$$S_3^* = e^{-\lambda (T - t_0)}$$

$$S_3 = e^{-\lambda T} = S_3^* (1 - S_0)$$

For the first cycle, the activity at the end of irradiation is determined by Equation (A-3) and the expression for the net counts for the first cycle is Equation (A-1). The value in the last column of Table A-1, the activity at the end of the cycle, is merely the activity at the end of irradiation times a decay factor for the balance of the cycle time. For subsequent cycles, the activity at the end of irradiation is the previous cycle's activity at the end of cycle times the decay term during irradiation plus the same activity term as for the first cycle (sample burnup is negligible). The total net counts C_{net} obtained in N cycles is the sum of the expressions in column 3 of Table A-1, namely

$$C_{\text{net}} = (\epsilon A_s S_0 S_1 S_2 / \lambda) [NS_3^0 + (N-1)S_3^1 + (N-2)S_3^2 + (N-3)S_3^3 + \dots + 2S_3^{N-2} + S_3^{N-1}]$$

$$= (\epsilon A_s S_0 S_1 S_2 / \lambda) \sum_{j=0}^{N-1} (N-j) S_3^j \quad (\text{A-7})$$

Table A-1. Buildup of Counts as Function of Cycle Time

Cycle Number j	Activity at End of Irradiation j	Net Counts from Cycle j	Activity at End of Cycle j
1	$A_s S_o$	$\epsilon A_s S_o S_1 S_2 / \lambda$	$A_s S_o S_3^*$
2	$A_s S_o S_3^* (1 - S_o) + A_s S_o$ $= A_s S_o (1 + S_3)$	$\epsilon A_s S_o (1 + S_3) S_1 S_2 / \lambda$	$A_s S_o (1 + S_3) S_3^*$
3	$A_s S_o (1 + S_3) S_3^* (1 - S_o) + A_s S_o$ $= A_s S_o (1 + S_3 + S_3^2)$	$\epsilon A_s S_o (1 + S_3 + S_3^2) S_1 S_2 / \lambda$	$A_s S_o (1 + S_3 + S_3^2) S_3^*$
4	$A_s S_o (1 + S_3 + S_3^2) S_3^* (1 - S_o) + A_s S_o$ $= A_s S_o (1 + S_3 + S_3^2 + S_3^3)$	$\epsilon A_s S_o (1 + S_3 + S_3^2 + S_3^3) S_1 S_2 / \lambda$	$A_s S_o (1 + S_3 + S_3^2 + S_3^3) S_3^*$
n	$A_s S_o (1 + S_3 + S_3^2 + S_3^3 + \dots + S_3^{n-1})$	$\epsilon A_s S_o (1 + S_3 + S_3^2 + S_3^3 + \dots + S_3^{n-1}) S_1 S_2 / \lambda$	$A_s S_o (1 + S_3 + S_3^2 + S_3^3 + \dots + S_3^{n-1}) S_3^*$

Equation A-7 is an arithmetic-geometric series, for which the summation term can be expressed as

$$\begin{aligned} \sum_{j=0}^{N-1} (N-j)S_3^j &= \frac{N(1-S_3^N)}{1-S_3} - \frac{S_3[1-NS_3^{N-1} + (N-1)S_3^N]}{(1-S_3)^2} \\ &= \frac{N - (N+1)S_3 + S_3^{N+1}}{(1-S_3)^2} \end{aligned} \quad (\text{A-8})$$

Now C_{net} can be expressed as

$$C_{\text{net}} = \frac{(\epsilon A_s S_0 S_1 S_2 / \lambda) [N - (N+1)S_3 + S_3^{N+1}]}{(1-S_3)^2} \quad (\text{A-9})$$

Equation (A-9) represents the total net counts for a single delayed neutron group. If Equation (A-9) is now summed over the six delayed neutron groups, the total net counts from all delayed neutron groups is given by

$$C_{\text{net}} = \sum_{i=1}^6 C_{\text{net}_i} = \epsilon A_s \sum_{i=1}^6 (S_{0_i} S_{1_i} S_{2_i} / \lambda_i) [N - (N+1)S_{3_i} + S_{3_i}^{N+1}] / (1-S_{3_i})^2 \quad (\text{A-10})$$

The number of counts due to background in one cycle is $B\Delta t$, where B is the background count rate, so the total number of background counts is equal to $NB\Delta t$. Substitution for the expressions A_s , S_0 , S_{1_i} , S_{2_i} , and S_{3_i} and use of the fact that

$$C_T = C_{\text{net}} + NB\Delta t,$$

where C_T is the total number of counts during the net counting times, results in the expression (Equation 8-1 in text):

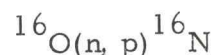
$$C_T = (\epsilon v m N_{Av} \bar{\sigma}_f \phi / A) \sum_{i=1}^6 (\beta_i / \lambda_i) (1 - e^{-\lambda_i t_0}) (e^{-\lambda_i t_1}) (1 - e^{-\lambda_i \Delta t}).$$

$$[N - (N+1)(e^{-\lambda_i T}) + e^{-(N+1)\lambda_i T}] / (1 - e^{-\lambda_i T})^2 + NB\Delta t$$

(The derivations of Equation 4-1 and 8-1 are taken from an article by S. E. Binney and R. I. Scherpelz which will soon be published in the journal Nuclear Instruments and Methods (57).)

Appendix B. The Production of ^{16}N in a Rabbit Capsule

To calculate the amount of ^{16}N produced in a rabbit capsule at a reactor power level of 1 MW, assume that all ^{16}N is produced by the reaction:



which has a microscopic cross section that can be approximated by a constant value, $\sigma = 40$ mb, above a threshold energy of 9 MeV.

The activity at the end of irradiation can be expressed as:

$$A_o = \phi \Sigma V (1 - e^{-\lambda t_o}),$$

where ϕ is the neutron flux with neutron energies above 9 MeV, Σ is the macroscopic cross section for the sample, V is the volume of the sample and t_o is the irradiation time. The decay constant,

$$\lambda = \frac{\ln 2}{7.11 \text{ s}} = 0.0975 \text{ s}^{-1}.$$

$$\begin{aligned} \Sigma V &= \frac{\sigma N_{\text{Av}} \rho V}{A} = \frac{\sigma N_{\text{Av}}^m}{A} = \frac{(0.04 \times 10^{-24})(6.02 \times 10^{23})(2.968)}{15.9994} \\ &= 0.00447 \text{ cm}^2 \end{aligned}$$

where m is found from the mass of the rabbit capsule, 17.5 g, and the abundance of ^{16}O in it, 17%.

It is assumed that ϕ can be found as the product of the fast flux in the rabbit position and the fraction of a prompt fission neutron spectrum with energies above 9 MeV. This assumption is based on

no moderation of the prompt fission neutrons with energies above 9 MeV. This approximation is not unreasonable, since the mean free path of a 9MeV neutron in water is about 14 cm, which is larger than the distance between the rabbit position and the nearest fuel rod. Thus

$$\phi = 7.5 \times 10^{12} \int_9^{\infty} \chi(E) dE$$

The expression used for $\chi(E)$ is an empirically fitted equation:

$$\chi(E) = 0.770 E^{\frac{1}{2}} e^{-0.776 E},$$

where E is the neutron energy in MeV. The integration was performed using a power series expansion of the exponential term, integrating each term of the series, and summing the integral.

This resulted in:

$$\int_9^{\infty} \chi(E) dE = 0.00469.$$

Thus $\phi = 3.51 \times 10^{10}$ n/cm²-s.

Thus, for a 60 second irradiation period:

$$A_0 = 3.51 \times 10^{10} \times 0.0047 [1 - \exp(-0.0975 \cdot 60)]$$

$$A_0 = 1.56 \times 10^8 \text{ dps.}$$

To find the number of high-energy gammas emitted during the count time interval, the activity is integrated from 20 seconds to 80 seconds after the end of irradiation, and multiplied by the sum of f_1 and f_2 , the fraction of disintegrations which produce each of the gammas:

$$\begin{aligned}
N_{\gamma} &= (f_1 + f_2) \int_{20}^{80} A(t) dt = (f_1 + f_2) \int_{20}^{80} A_o e^{-\lambda t} dt \\
&= (f_1 + f_2) \left(\frac{-A_o}{\lambda} \right) [e^{-80 \cdot \lambda} - e^{-20 \cdot \lambda}] \\
&= (0.69 + 0.05) \left(\frac{-1.56 \times 10^8}{0.0975} \right) [e^{-80 \cdot 0.0975} - e^{-20 \cdot 0.0975}] \\
N_{\gamma} &= 1.68 \times 10^8 \text{ gammas.}
\end{aligned}$$

Appendix C. Derivation of the Detection Limit

The detection limit, L_D , is the minimum count level which can be used for the determination of activities. Since k is the confidence factor for L_D being greater than L_C ,

$$L_D = L_C + k\sigma_D. \quad (C-1)$$

following the same argument used in Chapter V for L_C .

If a net number of counts, C_D , is equal to the detection limit,

$$L_D = C_D = C_t - C_b, \quad (C-2)$$

where C_t is the total number of counts within an associated

$$\sigma_t = \sqrt{C_t},$$

and C_b is the number of background counts with

$$\sigma_b = \sqrt{C_b}.$$

Thus

$$\begin{aligned} \sigma_D^2 &= \sigma_t^2 + \sigma_b^2 \\ &= C_t + C_b \\ &= (C_D + C_b) + C_b \\ \sigma_D^2 &= L_D + 2C_b. \end{aligned} \quad (C-3)$$

From C-1:

$$\begin{aligned} \sigma_D &= (L_D - L_C)/k \\ \sigma_D^2 &= (L_D^2 - 2L_C L_D + L_C^2)/k^2. \end{aligned} \quad (C-4)$$

Equating C-3 and C-4:

$$\begin{aligned} (L_D^2 - 2L_C L_D + L_C^2)/k^2 &= L_D + 2C_b \\ (L_D^2 - 2L_C L_D + L_C^2)/k^2 &= L_D + 2\sigma_b^2. \end{aligned} \quad (C-5)$$

From the definition of the critical level

$$L_C = \sqrt{2} k \sigma_b \quad (C-6)$$

$$L_C^2 = 2k^2 \sigma_b^2$$

$$2\sigma_b^2 = L_C^2/k^2. \quad (C-7)$$

Substituting C-7 into C-5:

$$(L_D^2 - 2L_C L_D + L_C^2)/k^2 = L_D + L_C^2/k^2,$$

Subtracting L_C^2/k^2 from both sides and rearranging:

$$L_D^2 - 2L_C L_D - k^2 L_D = 0.$$

By factoring out L_D and rearranging:

$$L_D = 2L_C + k^2 \quad (C-8)$$

Finally, substituting C-6 into C-8 gives:

$$L_D = 2\sqrt{2}k\sigma_b + k^2.$$